USGS
science for a changing world

Prepared in cooperation with the U.S. Environmental Protection Agency

Transport and Deposition of Asbestos-Rich Sediment in the Sumas River, Whatcom County, Washington

Scientific Investigations Report 2015–5177

U.S. Department of the Interior
U.S. Geological Survey

Cover: Photograph showing Swift Creek downstream of Oat Coles Road near Nooksack, Washington, October 31, 2012. Photograph by Christopher Magirl, U.S. Geological Survey.

Transport and Deposition of Asbestos-Rich Sediment in the Sumas River, Whatcom County, Washington

By Christopher A. Curran, Scott W. Anderson, Jack E. Barbash, Christopher S. Magirl, Stephen E. Cox, Katherine K. Norton, Andrew S. Gendaszek, Andrew R. Spanjer, and James R. Foreman

Prepared in cooperation with the U.S. Environmental Protection Agency

Scientific Investigations Report 2015–5177

U.S. Department of the Interior
U.S. Geological Survey

U.S. Department of the Interior
SALLY JEWELL, Secretary

U.S. Geological Survey
Suzette M. Kimball, Director

U.S. Geological Survey, Reston, Virginia: 2016

For more information on the USGS—the Federal source for science about the Earth, its natural and living resources, natural hazards, and the environment—visit http://www.usgs.gov or call 1–888–ASK–USGS.

For an overview of USGS information products, including maps, imagery, and publications, visit http://www.usgs.gov/pubprod/.

Suggested citation:
Curran, C.A., Anderson, S.W., Barbash, J.E., Magirl, C.S., Cox, S.E., Norton, K.K., Gendaszek, A.S., Spanjer, A.R., and Foreman, J.R., 2016, Transport and deposition of asbestos-rich sediment in the Sumas River, Whatcom County, Washington: U.S. Geological Survey Scientific Investigations Report 2015–5177, 51 p., http://dx.doi.org/10.3133/sir20155177.

ISSN 2328-0328 (online)

Contents

Contents

Figures

Figures—Continued

Figures—Continued

Tables

Conversion Factors

International System of Units to Inch/Pound

Multiply	By	To obtain
	Length	
centimeter (cm)	0.3937	inch (in.)
micron (µm)	0.00003937	inch (in.)
millimeter (mm)	0.03937	inch (in.)
meter (m)	3.281	foot (ft)
kilometer (km)	0.6214	mile (mi)
	Area	
square kilometer (km^2)	247.1	acre
square kilometer (km^2)	0.3861	square mile (mi^2)
	Volume	
liter (L)	0.2642	gallon (gal)
cubic centimeter (cm^3)	0.06102	cubic inch (in^3)
cubic meter (m^3/yr)	35.31	cubic foot per year (ft^3/yr)
cubic meter (m^3)	0.0008107	acre-foot (acre-ft)
	Flow rate	
meter per second (m/s)	3.281	foot per second (ft/s)
cubic meter per second (m^3/s)	35.31	cubic foot per second (ft^3/s)
	Mass	
gram (g)	0.03527	ounce, avoirdupois (oz)
tonne (t)	1.102	ton, short (2,000 lb)
tonnes per day (t/d)	1.102	ton per day (ton/d)
tonnes per day per square kilometer [(t/d)/km^2]	2.8547	ton per day per square mile [(ton/d)/mi^2]
tonnes per year (t/yr)	1.102	ton per year (ton/yr)
tonnes per square kilometer per year [(ton/km^2)/yr]	2.854	ton per square mile per year [(ton/ mi^2)yr]
	Density	
gram per cubic centimeter (g/cm^3)	62.4220	pound per cubic foot (lb/ft^3)

Temperature in degrees Celsius (°C) may be converted to degrees Fahrenheit (°F) as

$$°F = (1.8 \times °C) + 32.$$

Datums

Vertical coordinate information is referenced to the North American Vertical Datum of 1988 (NAVD 88).

Horizontal coordinate information is referenced to the North American Datum of 1983 (NAD 83).

Elevation, as used in this report, refers to distance above the vertical datum.

Supplemental Information

Specific conductance is given in microsiemens per centimeter at 25 degrees Celsius (µS/cm at 25 °C).

Concentrations of suspended sediments in water are given in either milligrams per liter (mg/L) or grams per liter (g/L).

Abbreviations

ADCP	acoustic Doppler current profiler
ANOVA	analysis of variance
bcf	bias correction factor
CI	confidence interval
CVO	USGS Cascades Volcano Observatory
EC	Environment Canada
EPA	U.S. Environmental Protection Agency
EWI	equal-width increment method of sampling
FBU	Formazin Backscatter Unit
FNU	Formazin Nephelometric Unit
lidar	light detection and ranging
MSPE	model standard percentage error
NIOSH	National Institute of Occupational Safety and Health
NOM	natural organic matter
NWIS	National Water Information System
PLM	polarized light microscopy
PI	prediction interval
RKM	river kilometer
SSC	suspended-sediment concentration
SSL	suspended-sediment load
TEM	transmission electron microscopy
USGS	U.S. Geological Survey
WY	water year (October 1 through September 30)
XRD	x-ray diffraction spectroscopy

Transport and Deposition of Asbestos-Rich Sediment in the Sumas River, Whatcom County, Washington

By Christopher A. Curran, Scott W. Anderson, Jack E. Barbash, Christopher S. Magirl, Stephen E. Cox, Katherine K. Norton, Andrew S. Gendaszek, Andrew R. Spanjer, and James R. Foreman

Abstract

Heavy sediment loads in the Sumas River of Whatcom County, Washington, increase seasonal turbidity and cause locally acute sedimentation. Most sediment in the Sumas River is derived from a deep-seated landslide of serpentinite that is located on Sumas Mountain and drained by Swift Creek, a tributary to the Sumas River. This mafic sediment contains high amounts of naturally occurring asbestiform chrysotile. A known human-health hazard, asbestiform chrysotile comprises 0.25–37 percent, by mass, of the total suspended sediment sampled from the Sumas River as part of this study, which included part of water year 2011 and all of water years 2012 and 2013. The suspended-sediment load in the Sumas River at South Pass Road, 0.6 kilometers (km) downstream of the confluence with Swift Creek, was 22,000 tonnes (t) in water year 2012 and 49,000 t in water year 2013. The suspended-sediment load at Telegraph Road, 18.8 km downstream of the Swift Creek confluence, was 22,000 t in water year 2012 and 27,000 t in water year 2013. Although hydrologic conditions during the study were wetter than normal overall, the 2-year flood peak was only modestly exceeded in water years 2011 and 2013; runoff-driven geomorphic disturbance to the watershed, which might have involved mass wasting from the landslide, seemed unexceptional. In water year 2012, flood peaks were modest, and the annual streamflow was normal. The fact that suspended-sediment loads in water year 2012 were equivalent at sites 0.6 and 18.8 km downstream of the sediment source indicates that the conservation of suspended-sediment load can occur under normal hydrologic conditions. The substantial decrease in suspended-sediment load in the downstream direction in water year 2013 was attributed to either sedimentation in the intervening river reach, transfer to bedload as an alternate mode of sediment transport, or both.

The sediment in the Sumas River is distinct from sediment in most other river systems because of the large percentage of asbestiform chrysotile in suspension. The suspended sediment carried by the Sumas River consists of three major components: (1) a relatively dense, largely non-flocculated material that settles rapidly out of suspension; (2) a lighter component containing relatively high proportions of flocculated material, much of it composed of asbestiform chrysotile; and (3) individual chrysotile fibers that are too small to flocculate or settle out, and remain in suspension as wash load (these fibers are on the order of microns in length and tenths of microns in diameter). Whereas the bulk density of the first (heaviest) component of suspended sediment was between 1.5 and 1.6 grams per cubic centimeter (g/cm^3), the bulk density of the flocculated material was an order of magnitude lower (0.16 g/cm^3), even after 24 hours of settling. Soon after immersion in water, the fresh chrysotile fibers derived from the Swift Creek landslide seem to flocculate readily into large bundles, or **floccules**, that exhibit settling velocities characteristic of coarse silts and fine sands (30 and 250 micrometers). In quiescent water within this river system, the floccules settle out quickly, but still leave between 2.4 and 19.5 million chrysotile fibers per liter in the clear overlying water. Consistent with the results from previous laboratory research, the amounts of asbestiform chrysotile in the water column in Swift Creek, as well as in the Sumas River close to and downstream of its confluence with Swift Creek, were determined to be directly correlated with pH. This observation offers a possible alternative to either turbidity or suspended-sediment concentration as a surrogate for the concentration of fresh asbestiform chrysotile in suspension.

Continued movement and associated erosion of the landslide through mass wasting and runoff will maintain large sediment loads in Swift Creek and in the Sumas River for the foreseeable future. Given the present channel morphology of the river system, aggradation (that is, sediment accumulation) in Swift Creek and the Sumas River are also likely to continue.

Introduction

A 0.55-square-kilometer (km^2), deep-seated landslide (or **earthflow**, to use the Varnes [1978] classification) of serpentinite from Sumas Mountain, in eastern Whatcom County, Washington, feeds a surplus of sediment to Swift Creek, its alluvial fan, and the Sumas River. The Sumas River is an underfit stream that flows north to the Fraser River in British Columbia, Canada (fig. 1). Because of the resulting oversupply of sediment relative to the sediment-transport capacity of both Swift Creek and the Sumas River, aggradation (that is, sediment accumulation) is widespread throughout both channels, leading to a propensity for flooding. During large floods, flood-plain inundation can be extensive in this system, resulting in the deposition of Sumas River sediment on riparian areas, agricultural fields, and residential properties (Whatcom County, 2012).

Aggradation of coarse-grained sediment (sand and gravel) in Swift Creek on its alluvial fan just west of Sumas Mountain (fig. 1) has prompted dredging for flood control and, at times in the past, commercial uses (Wroble, 2009; Whatcom County, 2012). A total sediment load of 94,000 cubic meters per year (m^3/yr) was estimated in Swift Creek in the 1970s (Converse Davis Dixon Associates, 1976), and recent estimates of total sediment load contributed by Swift Creek were 23,000–94,000 m^3/yr (30,000–120,000 yd^3/yr) (Van Gosen, 2010; Whatcom County, 2012). The annual sediment load is highly variable and depends on hydrology and landslide dynamics. Linneman and others (2009), for example, reported varying rates of landslide movement both between years and within the flood seasons (typically between October and March); they observed an increase in landslide movement rates in the late winter after seasonal rainfall led to saturation and enhanced movement. Debris flows from the landslide are common (Kerr Wood Leidal Associates, Limited, 2005; Bayer and Linneman, 2010; Whatcom County, 2012), and episodically delivers large volumes of sediment to the alluvial fan reach of Swift Creek during the flood season. Even in the absence of debris flows, the suspended-sediment loads in Swift Creek and the Sumas River are heavy during much of the flood season, when rainfall-driven runoff causes rapid increases in streamflow.

Sediment from the landslide is predominantly disaggregated and weathered serpentinite, primarily serpentine minerals, with various associated minerals, including chlorite, illite, hydrotalcite, lizardite, and chrysotile (Bayer and Linneman, 2010; Van Gosen, 2010). The chrysotile, although naturally occurring, creates the potential for asbestos exposure and increased health risks for residents living near the flood plain, where fluvial deposits of chrysotile can desiccate and become airborne (Wroble, 2009). In addition to chrysotile, sediment from Swift Creek contains concentrations greater than ambient levels of other potentially harmful materials such as the metals cadmium, cobalt, manganese, and nickel, all of which may inhibit aqueous biotic productivity and vegetation growth in the flood plain (Schreier, 1987; Whatcom County, 2012).

Although the landslide has been active since the early 20th century, recent analysis of the sediment revealed its high chrysotile content (Wroble, 2009) and led resource managers to treat the sediment in the system with caution. As remediation options that would mitigate effects from the asbestos-laden sediment from the landslide are considered, scientific information on the physical characteristics related to the underlying hydrology, sediment-transport potential, and geomorphology of the Sumas River system is required. The U.S. Environmental Protection Agency requested that the U.S. Geological Survey (USGS) study the hydrology and geomorphology of the Sumas River and Swift Creek to assist decision-makers from agencies managing sediment, flood risks, and health risks in the Sumas River watershed.

Purpose and Scope

This report documents a multi-faceted study of the Sumas River system in Whatcom County that was done to quantify fluvial sediment loads, assess the transport potential of fine-grained fluvial sediment, determine the characteristic settling velocity of the chrysotile derived from the Swift Creek landslide (also referred to as the Sumas Mountain landslide), and improve understanding of the concentration and distribution of suspended chrysotile in the Sumas River system. The study incorporated new hydrologic and sediment data from the Sumas River and Swift Creek, previous data and insight from published literature, and principles of sediment transfer and geomorphology from rivers in other locations.

Objectives of the study included:

1. Continuous recording of streamflow and suspended-sediment concentration and computation of suspended-sediment load at multiple locations along the main stem of the Sumas River from upstream of its confluence with Swift Creek to the Canadian border in water years[1] 2011–13;
2. Analysis of the relation between particle suspension and deposition as a function of flow velocity;
3. Quantification of the chrysotile content of suspended sediments in the river; and
4. Interpretation of the underlying hydrologic and geomorphologic processes that control the movement, distribution, and concentrations of chrysotile along the Sumas River corridor.

Study Area

The study area for this investigation was the area of the Sumas River watershed that is in the Fraser Lowland of Washington State (fig. 1).

[1]A water year is the period from October 1 of any given year to September 30 of the following year. Water year is used almost exclusively throughout this report. To reduce confusion between calendar years and water years in this report, all reference to years and periods is to water years unless specifically referred to as calendar year.

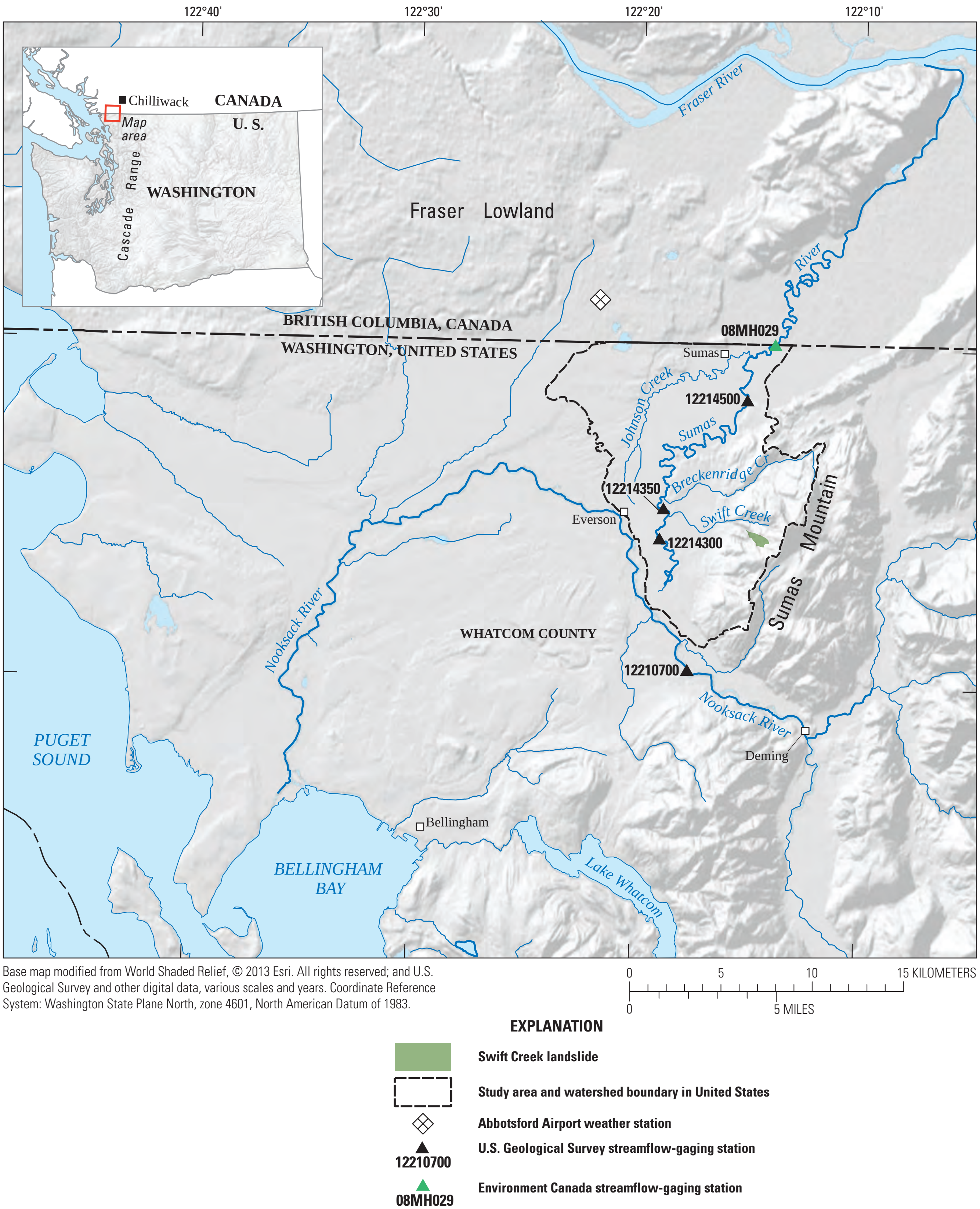

Base map modified from World Shaded Relief, © 2013 Esri. All rights reserved; and U.S. Geological Survey and other digital data, various scales and years. Coordinate Reference System: Washington State Plane North, zone 4601, North American Datum of 1983.

Figure 1. Location of study area and study sites in the Sumas River watershed and surrounding area, Whatcom County, Washington, United States, and southern British Columbia, Canada.

Geology, Geomorphology, and Sediment Transport

The Fraser Lowland is geologically young and shaped by Pleistocene glaciation and multiple advances of the Cordilleran ice sheet from British Columbia (Easterbrook, 1963; Armstrong and others, 1965; Clague, 1986; Booth, 1994; Kovanen and Slaymaker, 2015). During the Vashon Stade of the Fraser Glaciation, which ended about 13,500 years ago, ice sheets as thick as 2,000 m (Kovanen and Easterbrook, 2001) covered the entire Sumas River watershed. Glacial ice permanently retreated from the Sumas River Valley following the Sumas Stade about 11,000 years ago (Easterbrook, 1963; Armstrong and others, 1965), leaving behind a complex assemblage of glacial features, relic outwash channels, and lakes (Kovanen and Slaymaker, 2015).

In the past 10,000 years, during the Holocene Epoch, the Fraser River to the north and the Nooksack River to the south reworked the broad glacial plain of the Fraser Lowland, forming flood-plain terraces and alluvial corridors (Clague, 1986; Kovanen and Slaymaker, 2015). The region west of Sumas Mountain, near the cities of Nooksack, Everson, and Sumas (fig. 2), was shaped by the Nooksack River (Collins and Montgomery, 2011), which drains 1,500 km^2 of the Cascade Range near Deming, forming a broad alluvial fan caused by the heavy sediment load in the river (Czuba and others, 2011). At times during the Holocene, the Nooksack River flowed north toward the Fraser River (Pittman and others, 2003), forming a 2–4-km wide flood plain from Everson to the International Boundary, now occupied by the Sumas River. In the late Holocene, the Nooksack River avulsed to its current course down a relic outwash channel toward Puget Sound at Bellingham Bay (Pittman and others, 2003; Collins and Montgomery, 2011).

The Swift Creek landslide on Sumas Mountain, which is the source of much of the sediment in the Sumas River, has been geologically active for hundreds of years. The landslide became remobilized in the 1930s or 1940s during a period of increased precipitation (Kerr Wood Leidal Associates, Limited, 2005; Whatcom County, 2012). The landslide consists primarily of Jurassic-age serpentinite rock overlain by the Huntingdon conglomerate (Converse Davis Dixon Associates, 1976; Dragovich and others, 1997; Bayer and Linneman, 2010). The landslide is deep-seated, with rotational and translational blocks (Converse Davis Dixon Associates, 1976; Kerr Wood Leidal Associates, Limited, 2005; Whatcom County, 2012) contributing to slow but consistent downslope movement of 4–5 m/yr. The greatest rates of movement occur in the wetter months, with increased saturation from prolonged rainfall (McKenzie-Johnson, 2004; Linneman and others, 2009; Bayer and Linneman, 2010). Heavy precipitation on the surface of the landslide, or pooling and subsequent outburst flooding from within the landslide, spawn debris flows that episodically release large volumes of sediment to Swift Creek and the downstream fluvial system. The estimated volume of the largest known debris flow, which occurred in 1971, was 120,000 m^3 (Converse Davis Dixon Associates, 1976; Kerr Wood Leidal Associates, Limited, 2005; Whatcom County, 2012). Smaller debris flows occur periodically (Bayer and Linneman, 2010).

The Sumas River drains the western slopes of Sumas Mountain (elevation 1,039 m) and the agricultural areas of the Fraser Lowland in Whatcom County, and flows north into Canada near the city of Sumas (fig. 2). The region is a productive agricultural area because of its rich alluvial sediments, high rainfall, and temperate climate. The Sumas River is a tributary of the Fraser River, which drains an area of 220,000 km^2 in British Columbia. For this study, a stationing system was established in which locations along the river were identified by their distance upstream of the International Boundary and denoted by river kilometer (RKM). Thus, RKM 0.0 represents the Sumas River at the International Boundary (fig. 2), and Swift Creek enters the Sumas River at RKM 24.8. The Sumas River flows within the larger floodplain of the Nooksack River (fig. 2) and is considered to be an underfit stream, in that it flows through a flood plain established by a larger river (Knighton, 1998). The Sumas River drops slightly in elevation from Swift Creek to the International Boundary of the United States and Canada (fig. 3). At the International Boundary, the Sumas River has a drainage area of 139 km^2, with a relatively moderate (0.01 percent) slope (U.S. Geological Survey, 2014a, 2014b). At its confluence with Swift Creek, the Sumas River has a slope of about 0.1 percent (U.S. Geological Survey, 2014a).

Upstream of its confluence with the Sumas River, Swift Creek rises steeply toward Sumas Mountain and the landslide (fig. 3) and the catchment area is 9.4 km^2 (U.S. Geological Survey, 2014b). During periods of heavy precipitation, Swift Creek is laden with sediment derived from the landslide, giving the water an appearance that has been described as resembling “stirred yogurt” (Bayer and Linneman, 2010). Heavier sediment, including sand and gravel, travels predominantly as bedload, the coarsest particles settling out of suspension on the alluvial fan of Swift Creek before reaching the main stem of the Sumas River (Whatcom County, 2012). Smaller sediment in Swift Creek and the main stem of the Sumas River moves predominantly in suspension and consists of sands that quickly fall out of suspension when flow velocity decreases. A finer component of sediment that includes silts and clays also settles more slowly. This finer sediment contains asbestiform chrysotile, which forms bundles, or floccules, that are visible to the naked eye. In sections of the stream where flow velocity is low, the suspended sediment and river water behave much like a two-phase system, with floccules flowing along the bottom and clear water flowing near the top. The flow behavior is reminiscent of miso soup. In a glass sample bottle, the interface between the flocculated sediment and overlying clearer water is well defined and descends with time as flocculated sediment settles (fig. 4). The flocculated phase of the suspended sediment in Swift Creek is readily transported and has been observed at downstream locations in the main stem of the Sumas River and in water samples collected from the river.

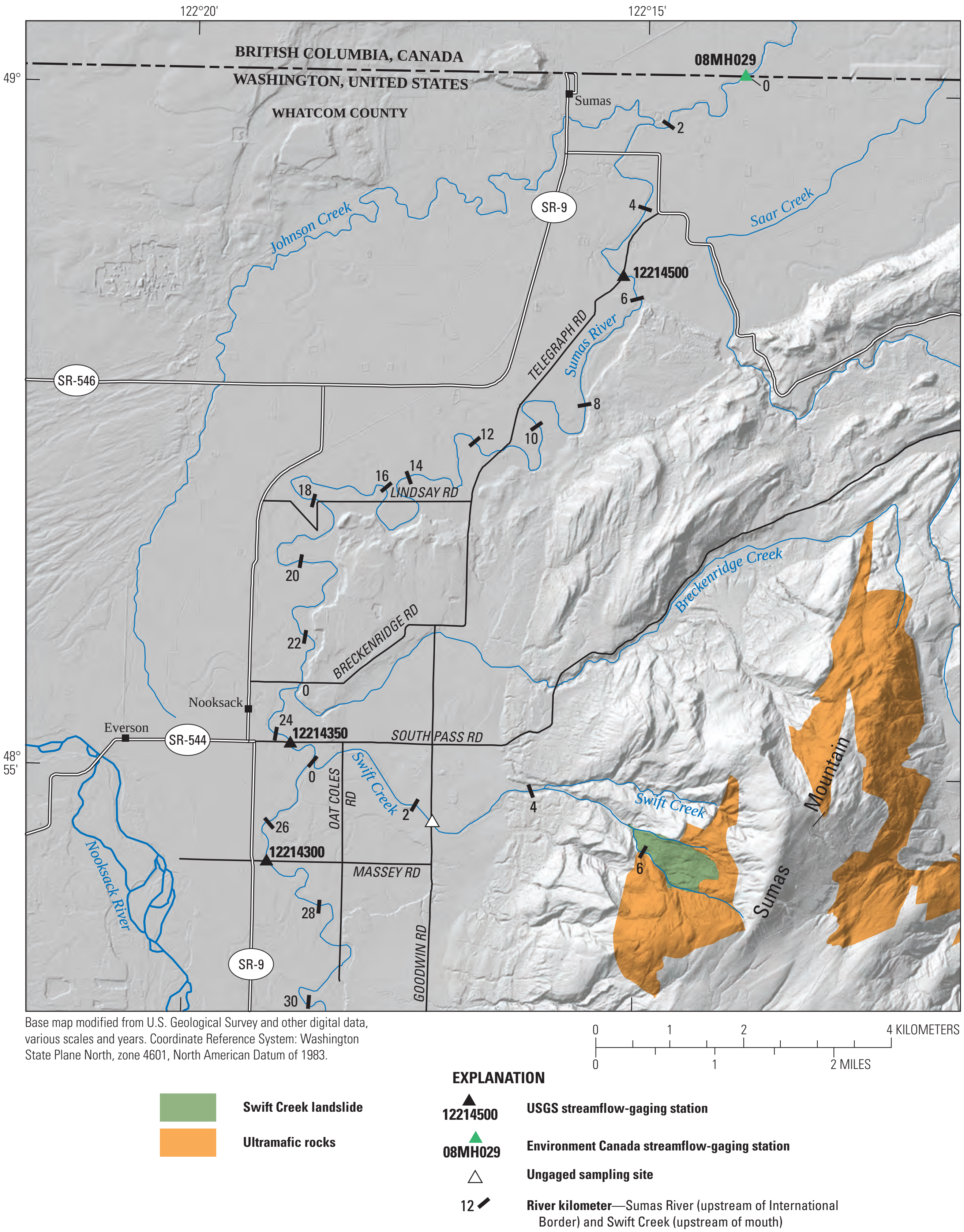

Figure 2. Locations of streamflow-gaging stations on the Sumas River operated by the U.S. Geological Survey (USGS) during water years 2011–13 and Swift Creek, the Swift Creek landslide (also referred to as the Sumas Mountain landslide), and Sumas Mountain in Whatcom County, Washington.

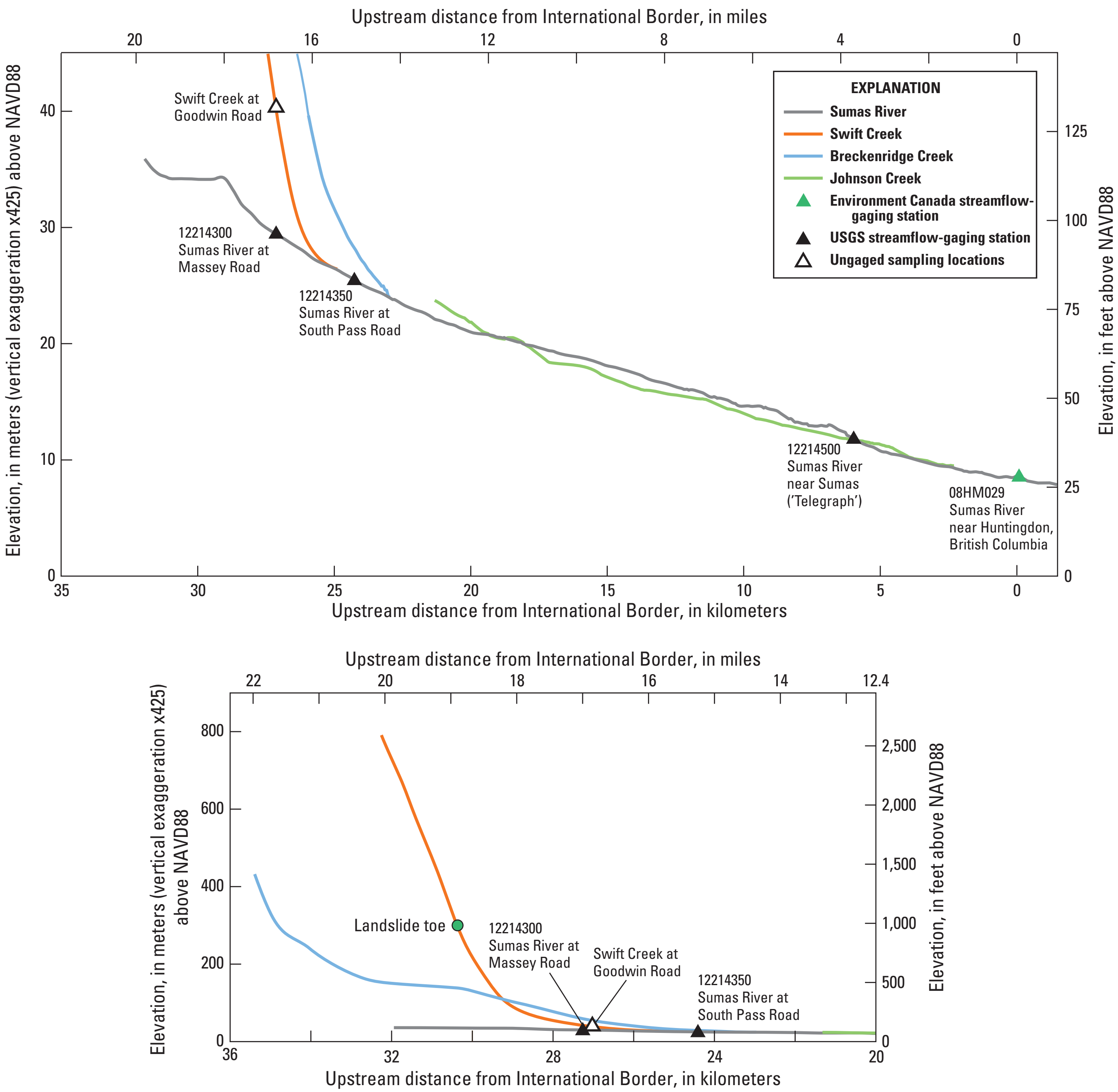

Figure 3. Longitudinal elevation profiles of the Sumas River and tributaries, including Swift Creek, which drains the area of a landslide on the western slope of Sumas Mountain in Whatcom County, Washington. NAVD88, North American Vertical Datum of 1988.

Figure 4. Sediment sample collected from Swift Creek near the toe of the Swift Creek landslide, Whatcom County, Washington. Note the distinct interface between the upper phase of clearer water and the flocculated phase that settles with time. Photograph by Christopher Magirl, U.S. Geological Survey, October 31, 2012.

Hydrology

The hydrology of the Sumas River is governed by the maritime climate of the Pacific Northwest, which is predominated by cool, wet winters with little snow in the lowlands and warm, dry summers. Streamflow is seasonal, with high flows typically occurring between December and February as the result of orographic precipitation from frontal systems. The largest floods typically result from the landfall of warm, narrow plumes of tropical moisture that often are referred to as "atmospheric rivers" (Neiman and others, 2011). Because of the relatively low elevation of the Sumas River watershed and its maritime climate, runoff is dominated by the magnitude and timing of rainfall rather than by spring snowmelt, which contributes relatively little runoff. Mean annual precipitation derived from measurements made between 1945 and 2013 at the Abbottsford Airport weather station in British Columbia, in the northwestern part of the Sumas River watershed (figs. 1 and 5) is 1,540 mm (Environment Canada [EC], 2013a). On average, the most precipitation occurs in November (222 mm) and the least occurs in July (43.4 mm).

Since 1952, EC has operated streamflow-gaging station (08MH029) on the Sumas River near Huntingdon, British Columbia (Environment Canada, 2013b), hereinafter referred to as "Huntingdon." Although the record is not complete, Huntingdon provides the longest streamflow history available for the Sumas River (56 years; 1953–68, 1970–71, 1973–94, 1996, and 1999–2013). Periods with missing or incomplete data occurred when the gaging station was operated seasonally, or not at all. The mean annual streamflow for the period of record at Huntingdon is 3.37 m^3/s (119 ft^3/s), and the long-term seasonal pattern of flow is evident in the hydrograph of mean monthly streamflow (fig. 5).

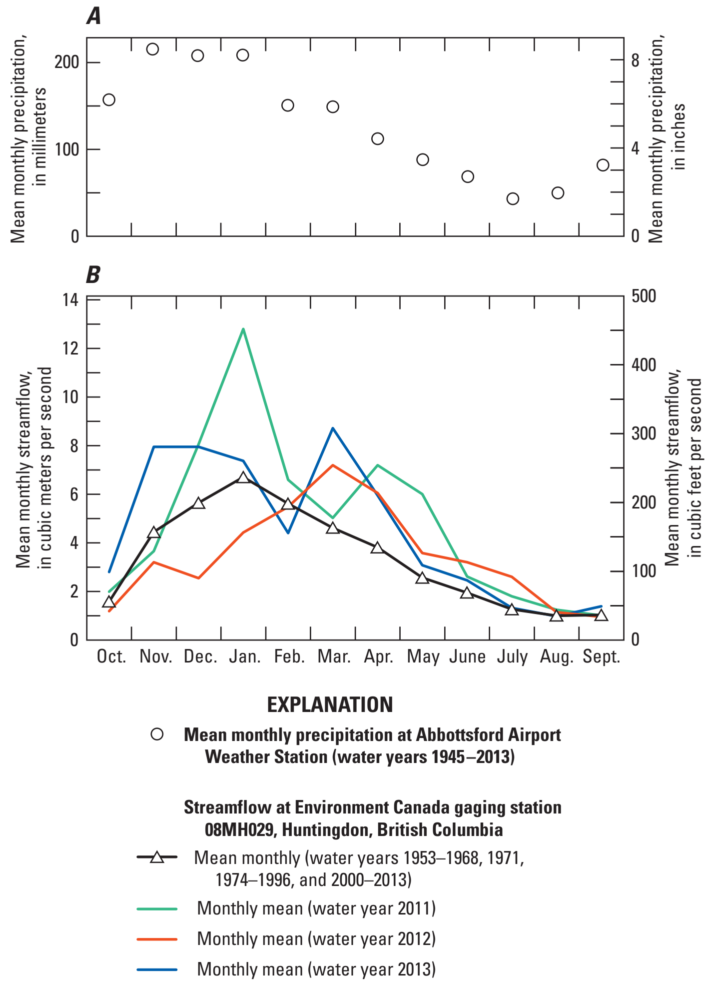

Figure 5. Mean monthly precipitation based on 69 years of precipitation record (1945–2013) at Abottsford Airport weather station (*A*), and mean monthly streamflow based on 56 years of streamflow record (1953–68, 1970–71, 1973–94, 1996, and 1999–2013) and monthly mean streamflow for water years 2011–13 at Sumas River at Huntingdon (*B*), British Columbia, Canada. Streamflow-gaging station operated by Environment Canada.

Annual mean streamflow at Huntingdon during the study period was 43 percent greater than normal in 2011 (4.84 m^3/s [171 ft^3/s]), 3 percent greater than normal in 2012 (3.48 m^3/s [123 ft^3/s]), and 34 percent greater than normal in 2013 (4.53 m^3/s [160 ft^3/s]). Monthly mean streamflows at Huntingdon in 2011 and 2013 generally were higher than normal throughout the year, whereas in 2012, monthly mean streamflows were lower than normal from November through February and higher than normal from March through July (fig. 5). A flood-frequency analysis of peak streamflow at Huntingdon using the USGS software PEAKFQ (Veilleux and others, 2014) indicates that the 2-year recurrence interval of 27.0 m^3/s (953 ft^3/s) for streamflow (that is, the peak flow that, on average, has a 50 percent chance of being equaled or exceeded in any year) was exceeded twice during 2011–13; on these occasions, peak streamflow was 29.0 m^3/s (1,020 ft^3/s) on January 14, 2011 and 28.0 m^3/s (989 ft^3/s) on January 10, 2013.

Suspended-Sediment Concentration and Load

The oversupply of sediment in Swift Creek poses challenges to conventional stream-gaging methods and to the long-term operation of in-stream sensors (Paul Pittman, Geomorphologist, Element Solutions, oral commun., 2011; Clement, 2014). Thus, to determine the amount of suspended sediment conveyed by Swift Creek to the Sumas River, an indirect approach for monitoring streamflow and suspended sediment was used that included the installation of streamflow-gaging stations on the Sumas River upstream and downstream of its confluence with Swift Creek. Three USGS streamflow-gaging stations were installed:

1. Sumas River at Massey Road near Nooksack (12214300, hereinafter referred to as “Massey”), 2.3 km upstream of the Swift River confluence at RKM 27.1;

2. Sumas River at South Pass Road at Nooksack (12214350, hereinafter referred to as “South Pass”), 0.6 km downstream of the Swift River confluence at RKM 24.3; and

3. Sumas River near Sumas (12214500, located at Telegraph Road and hereinafter referred to as “Telegraph”), 18.8 km downstream of the confluence at RKM 6.0.

Data from the streamflow-gaging stations at Massey and South Pass allowed a mass-balance calculation of streamflow and suspended sediment delivered by Swift Creek to the Sumas River, and data from the downstream Telegraph gaging station provided an understanding of the timing of sediment transport to the International Boundary (fig. 2).

Methods for Determining Suspended-Sediment Load

Determining the mass-flux of suspended sediment in a stream or river, sometimes referred to as suspended-sediment discharge, but referred to herein as suspended-sediment load (SSL), requires concurrent measurements of both streamflow and suspended-sediment concentration (SSC). Guy (1970) provided the following equation for calculating suspended-sediment load:

$$L_s = Q \times C_s \times k \,, \qquad (1)$$

where,

L_s is SSL in tonnes per day;
Q is streamflow in cubic meters per second;
C_s is SSC in milligrams per liter; and
k is an International System of Units conversion equal to 0.0864 t-L-s/m^3-mg-day (0.0027 tons-L/ft^3-mg-day when Q is expressed in cubic feet per second and assumes a specific gravity of 2.65 for sediment [Porterfield, 1972]).

Streamflow

At each of the three USGS streamflow-gaging stations (fig. 6), a non-contact, radar-based water-level sensor (WaterLOG® H-3613i™) was used to measure stage to within 6 mm. The use of non-contact water-level sensors was appropriate because of the high sediment load of the Sumas River and potential problems (such as sensor burial, sensor exposure during low flows, or sensor damage during high flows) were avoided. An independent wire-weight gage at each site was used to manually measure water levels during routine site visits and to provide verification of stage-sensor readings. A data-collection platform (WaterLOG® H-500XL™) was used at each gaging station to query sensors at 15-minute intervals, store data, and provide hourly transmissions of data by satellite telemetry to the USGS Automated Data Processing System. Eight to 10 measurements of streamflow per year were made over a range of streamflows at each of the 3 gaging stations using either acoustic Doppler current profilers (ADCP) or Price mechanical current meters (AA or Pygmy type), following standardized USGS methods for each instrument (Rantz and others, 1982; Mueller and others, 2013). The continuous 15-minute record of stage at each gaging station was used to compute streamflow using standard USGS stage-discharge methods (Rantz and others, 1982). All streamflow data collected during this study are available online through the USGS National Water Information System (NWIS) website (http://waterdata.usgs.gov/wa/nwis/sw).

Figure 6. U.S. Geological Survey streamflow-gaging stations and turbidity sensor installation on the Sumas River, Whatcom County, Washington, 2011–13. (*A*) Sumas River at Massey Road near Nooksack (12214300), February 1, 2011; (*B*) Sumas River at South Pass Road at Nooksack (12214350), May 11, 2011; (*C*) Sumas River near Sumas (12214500), February 1, 2011; and (*D*) turbidity sensor installation, April 20, 2011. Photographs by Steve Sumioka, U.S. Geological Survey.

Suspended-Sediment Concentration

To collect cross-sectional, representative samples of suspended sediment at each of the three USGS gaging stations, the equal-width increment (EWI) method of sampling was used (Edwards and Glysson, 1999. The EWI method uses an **isokinetic sediment sampler**, which is a device that is designed to ensure that the velocity of the water-sediment mixture entering the sampler is equal to the ambient stream velocity, and thus that the sampled SSC accurately represents the in-stream SSC (Edwards and Glysson, 1999). When using the EWI method, 10 equally spaced sampling points were established at each site across the actively flowing stream channel. At each sampling point, the isokinetic sampler was lowered and raised at a uniform rate through the water column. To examine the reproducibility of the measurements, a duplicate sample set (B set) was collected and analyzed independently for each **EWI sample**. When stream conditions were shallow (channel depths less than 1.5 m) and flows were moderate (velocities less than about 0.5 m/s), EWI samples were collected using a handheld DH-59 isokinetic sampler; during high flows (velocities greater than about 0.5 m/s), a D-74AL sampler was used at South Pass and Telegraph (Davis, 2005). All EWI samples were analyzed to determine the concentration of suspended sediment in the water and the percentage of fine material in the sediment (that is, silt and clay particles having diameters less than 0.063 mm) at the USGS sediment laboratory at the Cascade Volcano Observatory (CVO) in Vancouver, Washington. Selected EWI samples from South Pass and Telegraph (that is, samples that appeared to have enough sediment for additional analysis) also were used to obtain detailed measurements of particle-size distribution at the CVO laboratory. Laboratory methods for determining the percentage of fine sediment and particle-size distribution required the use of a chemical dispersant (sodium hexametaphosphate) and physical agitation to separate aggregated particles prior to gravimetric size analysis.

To provide redundancy in the sediment monitoring network, and to increase the number of suspended-sediment samples available for additional types of analyses, automated pump samplers (Isco-6712 portable sampler; Teledyne Technologies Incorporated, 2013) were installed at the South Pass and Telegraph gaging stations. At both gaging stations, the pump samplers initially were programmed to collect 200-mL subsamples at 6-hour intervals, which were composited into a single daily 800-mL sample. At South Pass, an additional pump sampler was used to collect 800-mL storm samples at hourly intervals during high-flow conditions. Because pump samplers collect non-isokinetic point samples of water-sediment mixtures, the location of the sampler intake can substantially affect the measured suspended-sediment concentration. To account for this potential bias, the SSC values measured using the pumped samples were multiplied by a **cross-section coefficient**, which was computed as the ratio between the SSC measured in the EWI samples and the SSC measured in concurrent pumped samples (Edwards and Glysson, 1999). The concentration of suspended sediment was determined for all daily composite pumped samples and for some hourly pumped samples at the CVO laboratory. Most hourly storm samples were analyzed for suspended-sediment concentration and asbestiform-related properties in the field services unit at the USGS Washington Water Science Center in Tacoma, Washington.

Turbidity

Turbidity, a measurement of water clarity, is commonly used as a surrogate measurement for suspended-sediment concentration because it has sample-frequency and cost-saving advantages over traditional water-sediment sampling methods (Pruitt, 2003; Anderson, 2005; Gray and Gartner, 2009). Continuous turbidity monitoring has been successfully used in many studies as a means for computing a continuous record of suspended-sediment concentration and for calculating suspended-sediment load (Lewis, 1996; Uhrich and Bragg, 2003; Rasmussen and others, 2005; Lee and others, 2009; Curran and others, 2014). At each USGS gaging station on the Sumas River, a DTS-12 nephelometric turbidity sensor (Forest Technology Systems, Limited, 2014) was installed in an actively flowing part of the stream and enclosed in a steel pipe for physical protection (fig. 6*D*). For redundancy in turbidity monitoring at South Pass, an additional turbidity sensor (Analite NEP180 [McVan Instruments PTY Limited, 2000]) was installed to measure high turbidity levels using optical backscatter (Anderson, 2005). Turbidity sensors were interfaced with the data-collection platform at each site and 15-minute turbidity data were transmitted hourly. The data were made publicly available through the NWIS Web site (http://waterdata.usgs.gov/wa/nwis).

Results from Continuous Monitoring and Discrete Sampling

All USGS streamflow-gaging stations on the Sumas River began operation during January 1–14, 2011. Massey was operated through September 30, 2012 (1.75 years); South Pass and Telegraph were operated through September 30, 2013 (2.75 years). Daily mean streamflow at each of the USGS gaging stations and at Huntingdon (the long-term reference gaging station operated by EC) is shown in figure 7; for additional reference, the daily precipitation measured at the U.S. streamflow gaging station Nooksack River near North Cedarville (#12210700) is also shown. In 2012, the mean annual streamflow for the Sumas River was 0.30 m^3/s (10.6 ft^3/s) at Massey, 0.78 m^3/s (27.5 ft^3/s) at South Pass, and 1.81 m^3/s (63.9 ft^3/s) at Telegraph. In 2013, it was 0.94 m^3/s (33.2 ft^3/s) at South Pass (+20.6 percent) and 2.10 m^3/s (74.1 ft^3/s) at Telegraph (+16 percent). The largest recorded peak flow at Massey was 1.61 m^3/s (56.8 ft^3/s) on November 23, 2011. During the 2011–13 study, the largest recorded peak flow at South Pass was 7.48 m^3/s (264 ft^3/s) on January 9, 2013, and the largest recorded peak flow at Telegraph was 11.7 m^3/s (413 ft^3/s) on January 10, 2013.

Field observations indicated that the Sumas River overflowed its banks and inundated part of the flood plain near Lindsay Road during the January 9–10, 2013 peak-flow (fig. 8). This overbank inundation occurred in limited sections between RKMs 12–18. The inundation was not spatially extensive and, where it was observed, deposition extended only a few meters onto the flood plain, with no direct effect on structures or agricultural fields. The inundation, however, did leave sandy sediment deposits as thick as 15 cm (fig. 8*C*). Although these observations were not made systematically throughout the study area or at set time intervals throughout the study period, it appeared that the Sumas River left its banks and inundated the flood plain only during this January 2013 peak-flow period. The peak flow measured at Huntingdon on January 10, 2013 was 28.0 m^3/s, the second highest recorded during the study period and for which a recurrence interval of 2.2 years is estimated (Veilleux and others, 2014).

Suspended-Sediment Samples

Fifty-one EWI samples were collected on the Sumas River with a substantial range of suspended-sediment concentrations and streamflow conditions at each of the three USGS gaging stations. A summary of the EWI sample results is shown in table 1, and a complete list of these results is provided in appendix A.

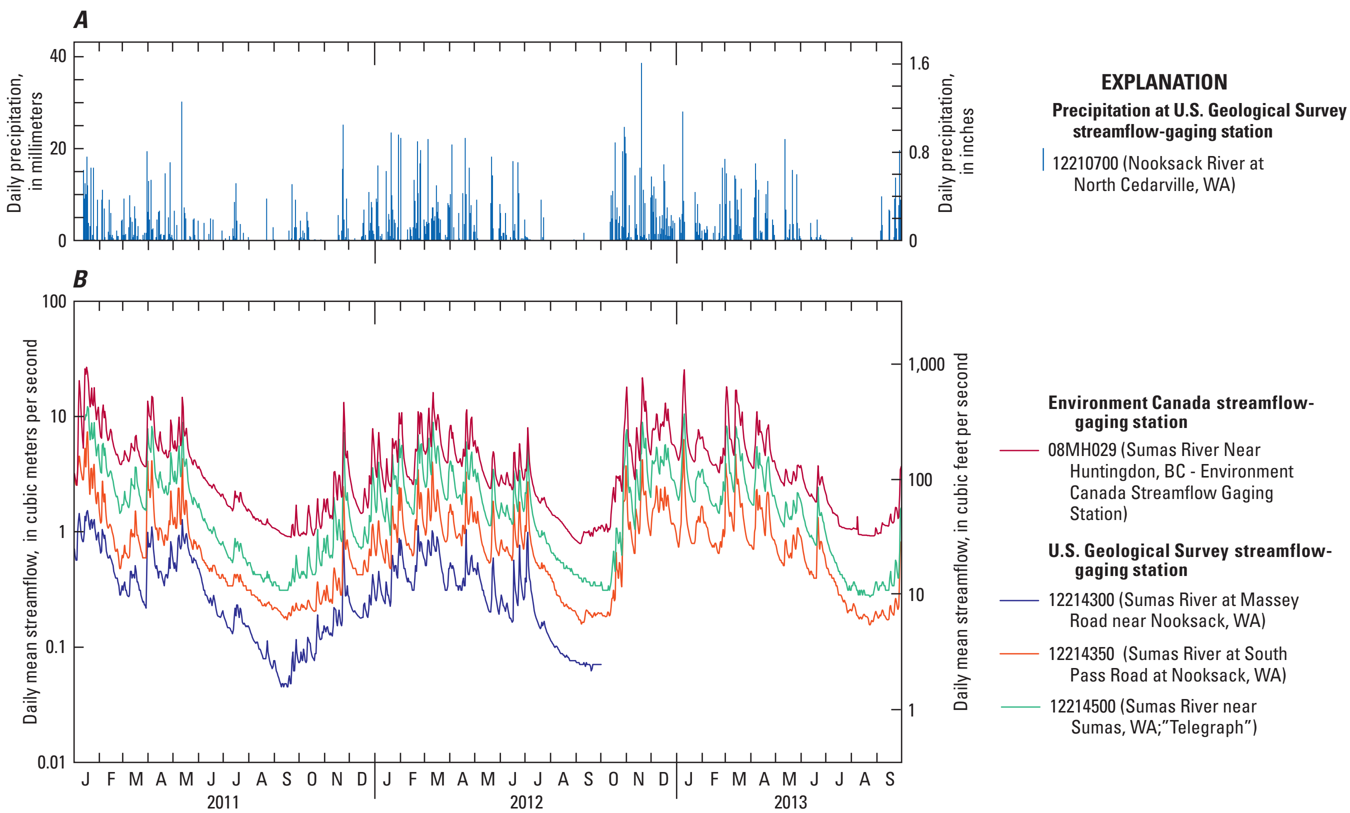

Figure 7. Daily precipitation recorded at Nooksack River at North Cedarville, Washington (12210700), 2011–13 and daily mean streamflow at streamflow-gaging stations on the Sumas River at Massy Road near Nooksack (12214300), at South Pass Road at Nooksack (12214350), Sumas River near Sumas (12214500), Washington, and near Huntingdon, British Columbia (08MH029), 2011–13 (*B*).

Particle-Size Distribution

The particle-size distributions of the suspended sediment were measured for EWI samples collected at South Pass and Telegraph during a storm on March 1, 2013, for which SSC was 11,400 and 4,390 mg/L, respectively (fig. 9). These samples had the largest SSC of any EWI samples collected during the study at each site. The EWI sample collected at South Pass was collected at the peak of the storm hydrograph, and the sample collected at Telegraph was collected on the rising limb (fig. 9).

Pumped Samples

At South Pass, 249 daily composite samples were collected with the automated pump sampler between April 2011 and January 2013. At Telegraph, 154 daily composite samples were collected with the automated pump sampler between June 2011 and January 2013. Hourly pumped samples were collected over 24-hour periods during four individual storms at each of the two sites. Cross-section coefficients for each intake location were developed at both sites from the SSC data obtained using the concurrent EWI and pumped samples. At South Pass, the coefficient value was 1.6 for SSC less than 5,000 mg/L, otherwise 1.0 was used. At Telegraph, the coefficient value was 0.5 for SSC less than 5,000 mg/L; otherwise 1.0 was used (table 2). At high SSC concentrations (that is, greater than 5,000 mg/L), suspended-sediment was assumed to be uniformly mixed throughout the channel and any bias introduced by the sampler intake location was assumed negligible. The suspended-sediment data obtained from the pumped samples collected for this study, as well as the data used to calculate the cross-section coefficients, are provided in appendix B.

Figure 8. Overbank sediments deposited onto the Sumas River flood plain near Nooksack, Washington, during January 8–9, 2013. (*A*) Sumas River near Breckenridge Road and (*B–D*) at several locations near Lindsay Road. Peak flow during the storm was 7.48 m^3/s on January 9, 2013, at the U.S. Geological Survey streamflow-gaging station Sumas River at South Pass Road near Nooksack (12214350), Washington. (*C*) Shovel shows 15-centimeter-thick sediment. (Photographs by Christopher Magirl, U.S. Geological Survey, February 7, 2013.)

Table 1. Summary of suspended-sediment data for samples collected using the equal-width increment method of sampling at selected sites on the Sumas River, Whatcom County, Washington.

[**Station name:** All stations are USGS streamflow gages in Washington, U.S.A. **Number of EWI samples:** Each EWI sample is composed of 6–20 subsamples. **Abbreviations:** EWI, equal-width increment method; SSC, suspended-sediment concentration; mg/L, milligram per liter; mm, millimeter]

Streamflow-gaging station name and No.		Dates of EWI sediment sample collection	Number of EWI samples	Range of SSC (mg/L)	Median SSC (mg/L)	Mean SSC finer than 0.063 mm (percent)
Sumas River at Massey Road near Nooksack	12214300	04-28-11 – 04-20-12	11	2 – 138	8	56
Sumas River at South Pass Road at Nooksack	12214350	04-28-11 – 04-05-13	21	5 – 11,400	515	49
Sumas River near Sumas[1]	12214500	04-28-11 – 04-05-13	19	17 – 4,390	333	58

[1]Also referred to as “Telegraph” because of its location on Telegraph Road.

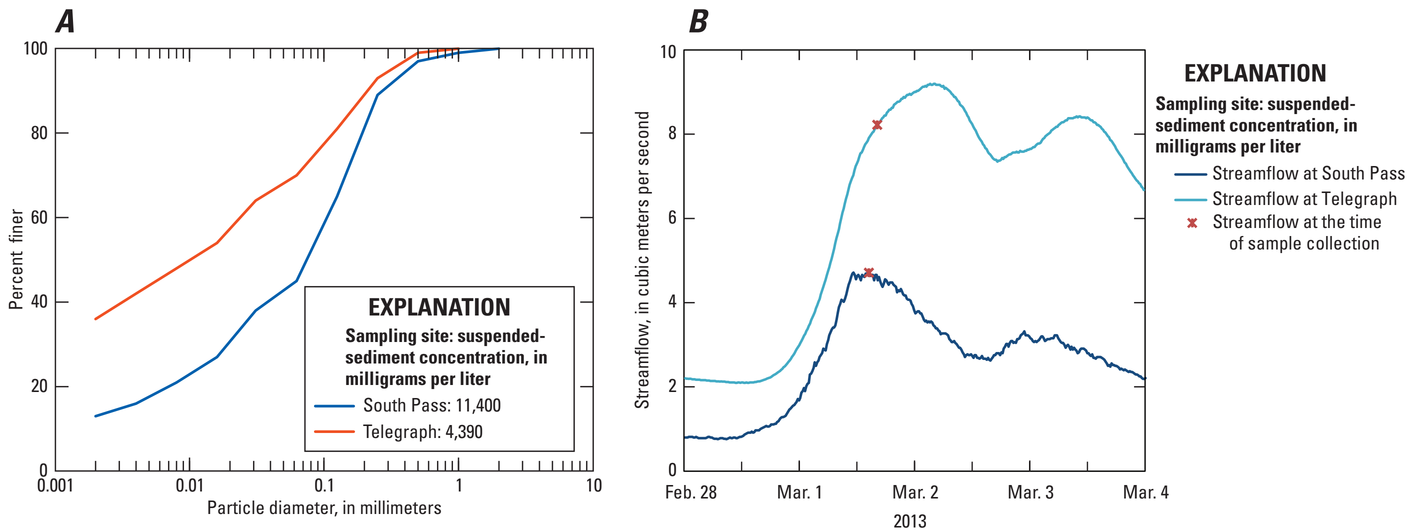

Figure 9. Particle-size distributions of suspended-sediment samples collected during a storm on March 1, 2013, at Sumas River at South Pass Road (12214350; South Pass) during the peak streamflow and at Sumas River near Sumas (12214500; Telegraph) during rising streamflow, Whatcom County, Washington. (*A*) Particle-size distribution of suspended-sediment samples and (*B*) hydrograph showing streamflow at the time of sample collection.

Table 2. Summary of suspended-sediment data for samples collected with an automated pump sampler at selected streamflow-gaging stations on the Sumas River, Washington, April 2011–January 2013.

[**Station name:** All stations are USGS streamflow gages in Washington, U.S.A. **Suspended-sediment concentration range:** Values adjusted with a cross-section coefficient. **Cross-section coefficient:** A multiplier applied to pump sample SSC to adjust for the measured bias due to sampler intake location. SSC, suspended-sediment concentration; mg/L, milligram per liter; < less than; ≥ greater than or equal to]

Streamflow-gaging station name and No.		Sample type	Number of pumped samples	Suspended-sediment concentration		Cross-section coefficient	
				Range (mg/L)	Median (mg/L)	SSC < 5,000 (mg/L)	SSC ≥ 5,000 (mg/L)
Sumas River at South Pass Road at Nooksack	12214350	Daily composite[1]	249	21–4,560	90	1.6	1.0
		Hourly storm	142	83–25,830	1,501	1.6	1.0
Sumas River near Sumas[2]	12214500	Daily composite[1]	154	4–1,985	168	0.5	1.0
		Hourly storm	48	52–4,577	1,403	0.5	1.0

[1]Daily composite samples were a mixture of subsamples collected at 0400, 1000, 1600, 2200 for each day.

[2]Also referred to as “Telegraph” because of its location on Telegraph Road.

Turbidity Monitoring

Continuous, 15-minute turbidity data were recorded at Massey from April 2011 through September 2012 (appendix C), and at South Pass (appendix D) and Telegraph (appendix E) from April 2011 through September 2013. Valid 15-minute turbidity data were measured 97.3 percent of the time at Massey Road, 96.3 percent of the time at South Pass, and 87.7 percent of the time at Telegraph (table 3). Data were missing at all sites, either because of sensor fouling or malfunction or because a sensor was out of the water during low-flow periods in summer (fig. 10**)**. Upstream of the Swift Creek confluence, turbidity recorded at Massey exceeded 200 Formazin Nephelometric Units (FNUs) once during a spring storm on May 11, 2011 (210 FNU) and once during summer low-flow conditions on August 3, 2011 (230 FNU). On several occasions, mostly during winter storms, the turbidity recorded at South Pass and Telegraph exceeded 1,600 FNU, the manufacturer's reported upper limit for the sensor (Forest Technology Systems, Limited, 2014). During these periods, turbidity values were censored and reported as being greater than 1,600 FNU. Turbidity data recorded at all the streamflow-gaging stations are summarized in table 3.

Turbidity-Suspended-Sediment Concentration Models

Several regression models were developed to estimate SSC as a function of turbidity at each gaging station using concurrent measurements of SSC and turbidity (figs. 11*A*, 11*C*, and 11*E*). Models also were developed to estimate the fine fraction of SSC (particle size smaller than 0.063 mm) from turbidity (figs. 11*B*, 11*D*, and 11*F*) and to estimate both SSC and the fine fraction of SSC using streamflow when turbidity data were not available. All turbidity-SSC models developed for South Pass and Telegraph improved in performance after log-transformations were used, which required the calculation of a bias correction factor (bcf) (Duan, 1983; Rasmussen and others, 2009) to re-transform model simulation results into original units. To evaluate model performance and allow comparison between turbidity-SSC and streamflow-SSC models, the Model Standard Percentage Error (MSPE; Rasmussen and others, 2009) and coefficient of determination (R^2) were determined for each model. Model residuals (that is, the magnitude of the prediction errors) were examined over the full range of simulated values to assess the degree to which the distributions of model residuals approximated a normal distribution (in applying linear regression models, it is assumed that residuals are normally distributed). Following the guidance of Rasmussen and others (2009), the confidence intervals for all regression models were determined with 90-percent certainty, and the prediction intervals were determined for estimating individual SSC estimates with 90-percent certainty. The regression models used for estimating SSC from turbidity, as well as associated model performance metrics, are summarized in table 4.
In all cases, the MSPE values were lower in turbidity-SSC models than those for the streamflow-SSC models. Consequently, the turbidity-SSC models were used to estimate SSC whenever the measured turbidity data were available (see "percent utilization" in table 3). At South Pass, if 15-minute turbidity data from the DTS-12 sensor (FNU) were either not available or had sensor limitations that were exceeded, the turbidity data from the Analite sensor (Formazin Backscatter Units [FBUs]) and the associated turbidity-SSC model were used (table 4). For all sites, when measured turbidity data were not available, the streamflow-SSC models from table 4 were used to estimate site specific SSC for each 15 minute flow interval. Estimated 15-minute SSC data and its corresponding streamflow, turbidity, and calculated suspended-sediment load are provided for each of the three sites in appendixes C, D, and E. Summary statistics for the 15-minute SSC values estimated for each site using the regression models during the 2011–13 study period are provided in table 5.

Table 3. Summary of continuous (15-minute) turbidity data measured at U.S. Geological Survey streamflow-gaging stations on the Sumas River, Whatcom County, Washington, 2011–13.

[**Station name:** All stations are USGS streamflow gages in Washington, U.S.A. **Turbidity units:** FNU, Formazin Nephelometric Units; FBU, Formazin Backscatter Units. **Percent utilization:** A ratio of the number of valid recorded values to the total number of possible 15-minute values during the sensor deployment period. **Symbol:** >, greater than]

Streamflow-gaging station name	No.	Turbidity sensor	Turbidity units	Period of data collection	Percent utilization	Range of turbidity	Median turbidity	Mean turbidity
Sumas River at Massey Road near Nooksack	12214300	DTS-12	FNU	04-22-11 – 09-30-12	97.3	0.1 – 230	2.2	3.5
Sumas River at South Pass Road at Nooksack	12214350	DTS-12	FNU	04-22-11 – 09-30-13	96.3	2 – >1,600	11	28.7
		Analite NEP180	FBU	12-12-11 – 07-06-13	84.5	42 – 10,600	984	1,520
Sumas River near Sumas[1]	12214500	DTS-12	FNU	04-21-11 – 09-30-13	87.7	3 – >1,600	19	46

[1]Also referred to as "Telegraph" because of its location on Telegraph Road.

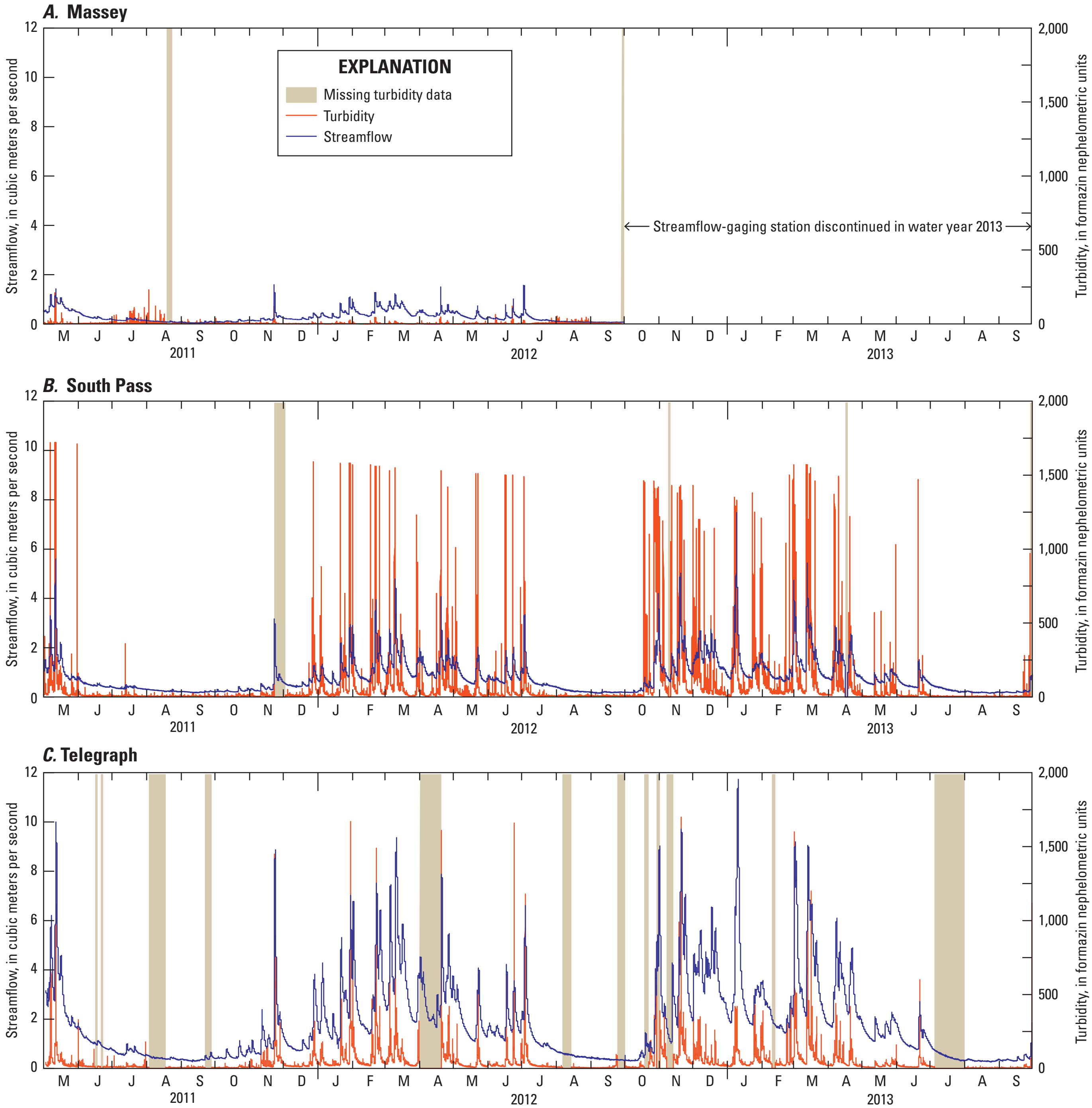

Figure 10. Time-series graphs showing streamflow and turbidity data recorded at U.S. Geological Survey streamflow-gaging stations on the Sumas River, Whatcom County, Washington, 2011–13. (*A*) Sumas River at Massey Road near Nooksack (12214300), referred to as "Massey"; (*B*) Sumas River at South Pass Road at Nooksack (12214350), referred to as "South Pass"; and (*C*) Sumas River near Sumas (12214500), referred to as "Telegraph."

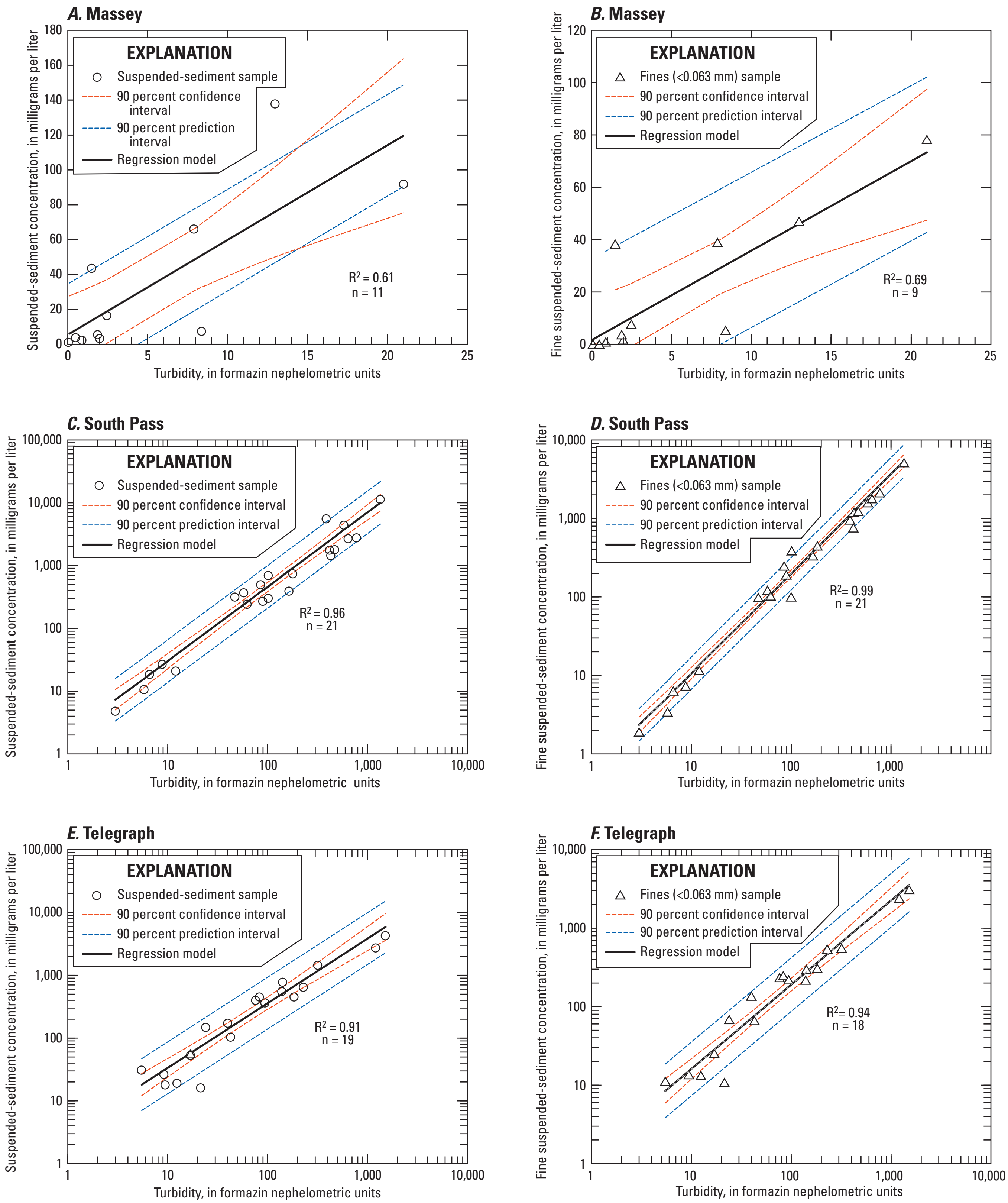

Figure 11. Turbidity suspended-sediment concentration (SSC) models used for the computation of suspended-sediment concentrations at U.S. Geological Survey streamflow-gaging stations on the Sumas River, Washington. (*A*) and (*B*), regressions for Sumas River at Massey Road, near Nooksack (12214300; referred to as "Massey"); (*C*) and (*D*), regressions for Sumas River at South Pass Road at Nooksack (12214350; referred to as "South Pass"); (*E*) and (*F*), regressions for Sumas River at Sumas (12214500; referred to as "Telegraph"); R^2, coefficient of determination; n, number of observations; fines, particles finer than 0.063 millimeters.

Table 4. Models used to estimate suspended-sediment concentration from turbidity and streamflow at U.S. Geological Survey streamflow-gaging stations on the Sumas River, Washington.

[**Station name:** All stations are USGS streamflow gages in Washington, U.S.A. **Model:** bcf, bias correction factor; fine, concentration of suspended sediment of size less than 0.063 mm; SSC, suspended-sediment concentration in milligrams per liter; *Tb*, optical backscatter turbidity (in FBU); *Tn*, turbidity (in FNU); *Q*, streamflow. **R^2:** coefficient of determination. **MSPE:** Model standard percentage error; upper and lower 90-percent confidence limits for MSPE. **Abbreviations:** FBU, Formazin Backscatter Unit; FNU, Formazin Nephelometric Unit; m^3/s, cubic meter per second; –, not used]

Streamflow-gaging station name and No.		Suspended-sediment concentration predictor variable	Model	Bias correction factor	Number of observations	R^2	MSPE (upper/lower)
Sumas River at Massey Road near Nooksack	12214300	Turbidity (FNU)	$SSC = 5.42\,Tn + 5.56$	–	11	0.61	86/-86
			$fine = 3.31\,Tn + 2.93$	–	9	0.69	78/-78
		Streamflow (m^3/s)	$SSC = 87.9\,Q - 10.2$	–	11	0.57	90/-90
			$fine = SSC * 0.56$	–	–	–	–
Sumas River at South Pass Road at Nooksack	12214350	Turbidity (FNU)	$SSC = 1.83\,Tn^{1.18}bcf$	1.10	21	0.96	59/-37
			$fine = 0.552\,Tn^{1.27}bcf$	1.02	21	0.99	32/-24
		Turbidity (FBU)	$SSC = 10\hat{}[-0.338(\log Tb)^2 + 3.16(\log Tb) - 2.79]\,bcf$	1.06	[1]46	0.87	53/-35
			$fine = 0.0351 * Tb^{1.63}bcf$	1.07	13	0.89	42/-30
		Streamflow (m^3/s)	$SSC = 10\hat{}[-0.741(\log Q)^2 + 2.42(\log Q) - 2.56]\,bcf$	1.56	[1]37	0.85	149/-60
			$fine = 115\,Q^{2.26}bcf$	1.88	21	0.69	251/-72
Sumas River near Sumas[2]	12214500	Turbidity (FNU)	$SSC = 2.94\,Tn^{1.03}bcf$	1.07	19	0.91	73/-42
			$fine = 1.34\,Tn^{1.07}bcf$	1.01	18	0.94	57/-36
		Streamflow (m^3/s)	$SSC = 51.1\,Q^{1.65}bcf$	1.52	19	0.75	142/-59
			$fine = 27.1Q^{1.69}bcf$	1.69	18	0.73	155/-61

[1]Number of samples includes both equal-width increment and pumped samples.

[2]Also referred to as "Telegraph" because of its location on Telegraph Road.

Table 5. Summary of estimated, instantaneous (15-minute) suspended-sediment concentration values, in milligrams per liter, at U.S. Geological Survey streamflow-gaging stations on the Sumas River, Washington.

Streamflow-gaging station name and No.		Number of values	Suspended-sediment concentration (mg/L)			
			Minimum	Maximum	Median	Mean
Sumas River at Massey Road near Nooksack	12214300	50,688	0.4	1,250	16.9	24.2
Sumas River at South Pass Road at Nooksack	12214350	85,728	4.0	28,400	38	430
Sumas River near Sumas[1]	12214500	85,728	8.4	6,280	62	164

[1]Also referred to as "Telegraph" because of its location on Telegraph Road.

Computed Suspended-Sediment Loads

The continuous 15-minute records of measured streamflow and estimated SSC were used with equation 1 to compute a continuous 15-minute record of SSL at each of the three USGS streamflow-gaging stations for their respective monitoring periods. Similarly, a record of fine SSL (particle size smaller than 0.063 mm) also was computed for each station. All 15-minute streamflow and turbidity data, with corresponding computed SSC and SSL values and 90-percent confidence intervals, are provided in appendixes C, D, and E for the Massey, South Pass, and Telegraph sites, respectively. Cumulative SSL values at each station for the duration of its monitoring period are shown in figure 12. The SSL computed for the upstream gaging station at Massey for the monitoring period was 400 t (90-percent confidence interval [CI]: 170–790 t)—values that are barely visible in figure 12*A*.

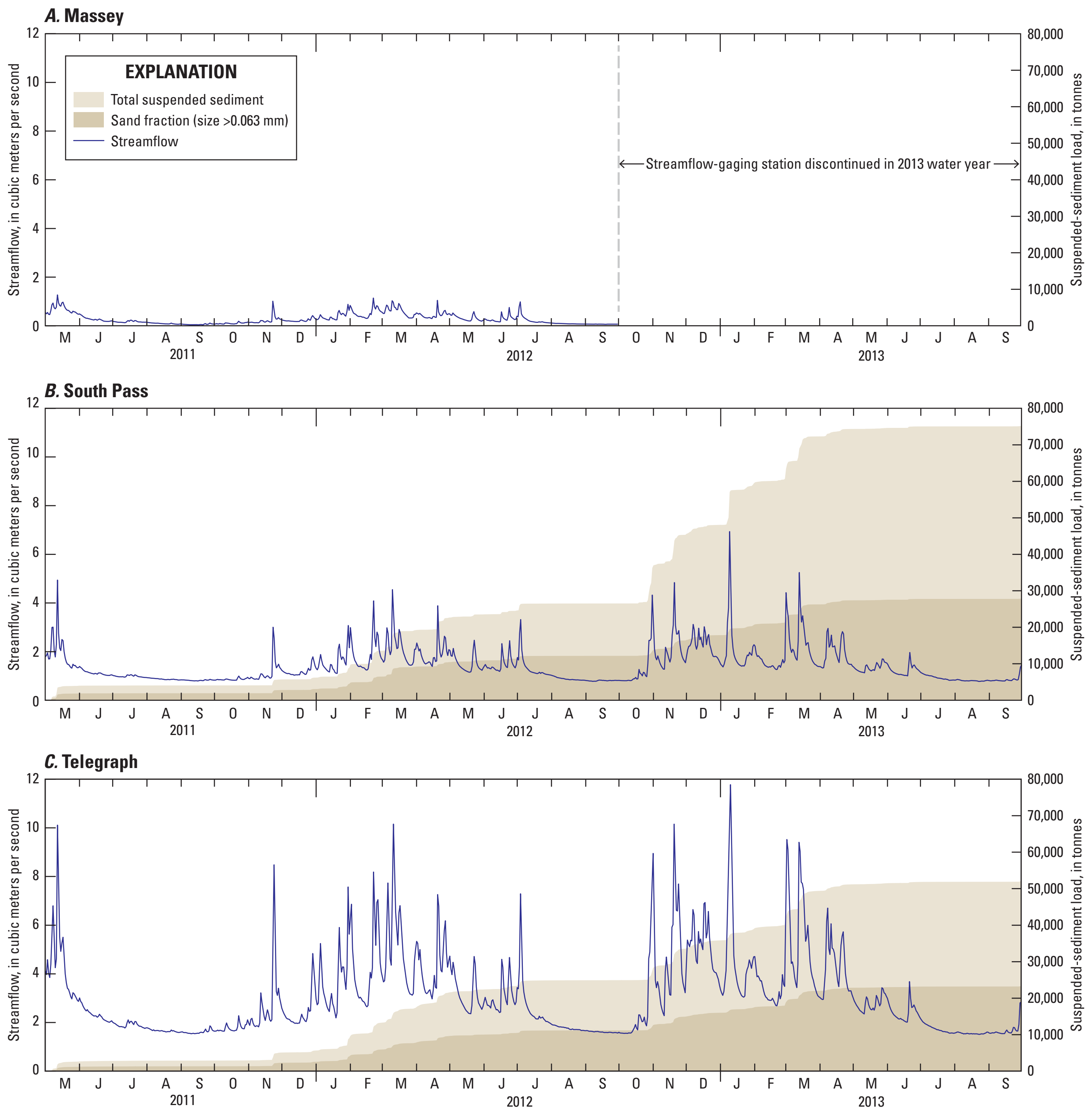

Figure 12. Daily streamflow and cumulative suspended-sediment loads at U.S. Geological Survey streamflow-gaging stations on the Sumas River at (*A*) Massey Road near Nooksack (12214300; referred to as "Massey"); (*B*) South Pass Road at Nooksack (12214350; referred to as "South Pass"); and (*C*) Sumas River near Sumas (12214500; referred to as "Telegraph"), Whatcom County, Washington.

For comparison, the annual SSL computed at South Pass (fig. 12*B*) for 2012 was 22,000 t (90-percent CI: 12,000–46,000 t) and for the same period at Telegraph was 22,000 t (90-percent CI: 8,200–63,000 t). In 2013, the annual SSL computed at South Pass was 49,000 t (90-percent CI: 25,000–110,000 t) and for the same period at Telegraph (fig. 12*C*) was 27,000 t (90-percent CI: 9,800–77,000 t). In 2013, the increases in annual SSL relative to 2012 were 123 and 23 percent at South Pass and Telegraph, respectively, and were consistent with the relative increases in annual peak streamflow recorded at both sites (+56 and +25 percent at South Pass and Telegraph, respectively). The fine (smaller than 0.063 mm) total suspended-sediment load averaged 60 percent at Massey, 63 percent at South Pass, and 55 percent at Telegraph.

The median daily SSL at Massey was 0.33 t, and the maximum daily SSL was 26.9 t on May 12, 2011, during which the peak daily streamflow was 1.44 m^3/s. The median daily SSL at South Pass was 2.3 t and the maximum daily SSL was 7,330 t on January 9, 2013, during which the peak daily streamflow was 7.48 m^3/s. The median daily SSL at Telegraph was 7.8 t and the maximum daily SSL was 1,940 t on March 1, 2013, during which the peak daily streamflow was 8.98 m^3/s.

As expected, the SSL for the Sumas River upstream of the Swift Creek confluence at Massey was small, less than 1 percent of the SSL computed at South Pass in 2012. The upstream gaging station at Massey was discontinued after 2012. Similarly, the relative SSL contribution from the Sumas River upstream of Swift Creek was also small in 2013 (less than 1 percent of the value at South Pass).

Variability in Suspended-Sediment Loads

The monthly SSL values shown in figure 13 for each site indicate the seasonality of sediment transport in the Sumas River, the variability of monthly SSL from year to year, and the differences in SSL between upstream and downstream sites. The largest monthly SSLs generally were measured during the winter storm season (October–March), and are attributed to increased precipitation and streamflow during this period. In 2012, monthly SSLs at South Pass and Telegraph generally were less than SSLs in 2013, reflecting the differences in measured precipitation and streamflow between 2012 and 2013 (fig. 7). The differences in monthly SSLs between South Pass and Telegraph were relatively small in 2012 and indicated that most suspended sediment contributed by Swift Creek was efficiently conveyed through the Sumas River system. However, in 2013, although the seasonal pattern of suspended-sediment transport was similar between sites, large differences in monthly SSL between South Pass and Telegraph were observed throughout the winter storm season, particularly for October 2012 and January 2013, during which seasonally large 24-hour storms occurred (October 30–31, 2012, and January 8–9, 2013). The differences in SSL between South Pass and Telegraph could have been caused by one or more of several processes, including deposition of suspended sediment between sites (transient channel storage or overbank deposition), differences in the mode of sediment transport (for example, suspended load compared with bedload, which was not measured as part of this study), differences in sediment transport capacity between sites, and uncertainty in estimating high SSC values from the SSC-surrogate models used.

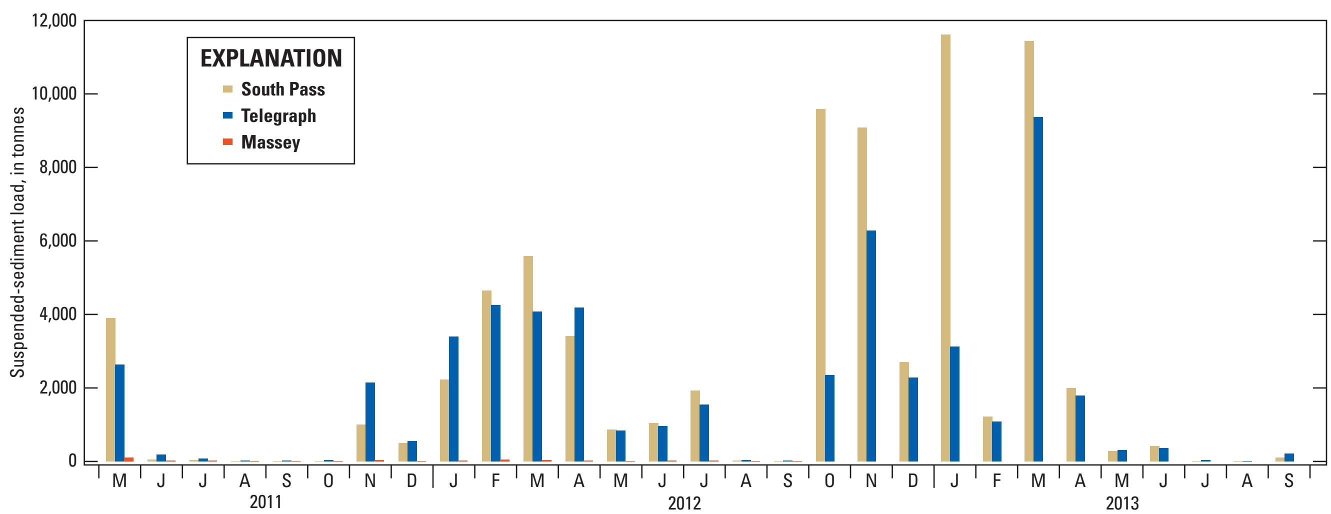

Figure 13. Monthly suspended-sediment loads at U.S. Geological Survey streamflow-gaging stations on the Sumas River at Massey Road near Nooksack (12214300; referred to as “Massey”); South Pass Road at Nooksack (12214350; referred to as “South Pass”); and Sumas River near Sumas (12214500; referred to as “Telegraph”), Whatcom County, Washington.

Weathering and Flocculation of Chrysotile Fibers in Natural Waters

by Jack E. Barbash

Asbestos is a general term used to refer to the fibrous forms of *serpentine* and *amphibole*, two different types of silicate minerals that are detected in some *ultramafic* (manganese- and iron-rich) metamorphic and igneous rocks (Bales and others, 1984). The fibrous form of serpentine is 'asbestiform chrysotile', or *clinochrysotile*, one of the three structural variations of chrysotile (*clinochrysotile*, *orthochrysotile* and *parachrysotile*). The other two forms of serpentine are antigorite and *lizardite*, which have the same chemical composition as chrysotile ($Mg_3Si_2O_5[OH]_4$), but differ in their physical appearance (Wicks and Whittaker, 1975; Klein and Hurlbut, 1993). Lizardite is the most common form of serpentine (Wicks and O'Hanley, 1988). Chrysotile and lizardite are the two serpentine minerals that are present in highest abundance in the materials being eroded from the landslide on Swift Creek (Bayer and Linneman, 2010).

The structure of asbestiform chrysotile consists of approximately 20 pairs of sheets arranged as either a continuous spiral or as concentric rings (Bales and Morgan, 1985). Each pair consists of a sheet of magnesium hydroxide octahedra ($Mg[OH]_6$) attached to a sheet of silica tetrahedra (Si_2O_5). A slight mismatch in the spacing of the points of attachment between the two sheets causes the curvature of the paired sheets, resulting in the formation of the tubular fibers that characterize the macroscopic structure of the mineral (Klein and Hurlbut, 1993). Chrysotile fibers collected from natural waters are commonly 0.5–2.5 µm long and 0.03–0.18 µm thick (McGuire and others, 1982; Bales and others, 1984; Schreier, 1989).

Like other minerals, exposure to air and (or) water at the Earth's surface causes serpentine minerals to undergo weathering through both chemical and physical processes. Laboratory studies indicate that when fresh samples of either chrysotile or lizardite are submerged in water, the pH of the aqueous phase increases substantially (Pundsack, 1955; Choi and Smith, 1971; Luce and others, 1972; Bales, 1984; Bales and Morgan, 1985; Koumantakis and others, 2009). This pH increase is caused by the uptake of protons (H+) by magnesium as $MgOH^+$ and $Mg(OH)_2$ are released into solution (Bales, 1984; Bales and Morgan, 1985). Pundsack (1955) determined that a 0.5 percent suspension of finely divided chrysotile fibers in deionized, CO_2-free water exhibits a pH of 10.33. Following the immersion of unweathered chrysotile fibers in water, the pH increases by as much as 4 pH units within 20 minutes (Koumantakis and others, 2009). As might be expected, the overall magnitude of the observed increase in pH is higher with increasing concentrations of chrysotile in suspension (Choi and Smith, 1971; Koumantakis and others, 2009). Data reported by Schreier (1987) for longitudinal profiles sampled on seven occasions showed overall decreases in pH with increasing distance downstream of the landslide, presumably a result of the relatively alkaline water from the slide being diluted by groundwater and tributary inputs as it moves downstream.

When chrysotile is immersed in water at neutral pH ($7 \le pH \le 9$), the magnesium dissolves more rapidly from the crystal structure than the silicon (Bales and Morgan, 1985). Consequently, as a chrysotile fiber is transported downstream in flowing water, its outer layers become more silica-rich and porous, resulting in more rapid disintegration from physical abrasion. Consistent with this, chrysotile fibers collected immediately downstream of the landslide in Swift Creek had a rougher outer surface than those collected farther downstream in the Sumas River near the International Boundary (Holmes and others, 2012). The ongoing removal of magnesium from chrysotile fibers over time through dissolution appears to be responsible for the observed decrease in magnesium content of Sumas River sediments with increasing distance downstream of the landslide (Schreier, 1987). Other data reported by Schreier (1987) from this area, however, showed no significant correlation between the concentrations of dissolved magnesium and suspended chrysotile fibers within the water column.

The removal of chrysotile, or any other fibers, from the water column of a surface-water body requires that the particles come into sufficiently frequent contact—and that they bind together tightly enough once that contact occurs—to form aggregates large enough to drop out of the water column through sedimentation. This aggregation within the water column occurs as a result of two main processes: (1) the movement of the suspended material in a manner that leads to interparticle contact, and (2) the attachment of the particles to one another once contact has occurred. Within the context of water treatment, the term “flocculation” commonly is used to pertain only to the first process, whereas the word “coagulation” is used to refer to both processes together (Weber, 1972). For natural waters, however, the term flocculation commonly is used to refer to the two processes together (for example, Sholkovitz, 1976; Petticrew and others, 2011).

When a chrysotile fiber is placed in water, its surface is positively charged below a specific pH threshold—known as the *point of zero charge*, or pH_{zpc}—and negatively charged above this pH value. Various studies have observed pH_{zpc} values that range from 8.3 to 11.8 (Choi and Smith, 1971; Jolicoeur and others, 1981; Bales and Morgan, 1985). The flocculation of chrysotile fibers is expected to be negligible at pH values outside of this range, owing to electrostatic repulsion between the fibers less than pH 8.3 (when they are positively charged) or greater than pH 11.8 (when they are negatively charged). Within the pH range between 8.3 and 11.8, however, flocculation is more likely to occur. Jolicoeur and others (1981) observed that the rate of sedimentation of fine chrysotile fibers (that is, those remaining in suspension after more than 2 minutes of settling) increased with the amount of sodium hydroxide (NaOH) added to deionized water, reaching a maximum rate near pH 11.0, well within the range of pH_{zpc} values reported in the literature.

Laboratory studies have indicated that chrysotile fibers immersed in natural waters containing natural organic matter (NOM) acquire a negative surface charge within 1 day (Bales and Morgan, 1985). This observation is presumed to be the combined result of the loss of Mg_{2+} and $MgOH_{+}$ through dissolution, the binding of NOM (which typically exhibits a negative charge in natural waters) to positively charged surface sites on the $Mg(OH)_6$ octahedra, and the sorption of NOM to the crystal surfaces. This explanation is corroborated by the results from field studies indicating that chrysotile fibers sampled from natural streams typically exhibit a negative surface charge—even in locations relatively close to their source—as well as by results from laboratory studies suggesting that the surfaces of chrysotile and other particles become coated with NOM relatively soon after they enter natural waters (Bales and Morgan, 1985). Therefore, the longer chrysotile fibers reside in suspension within the water column, the less likely they are to attach to one another as a result of electrostatic forces alone. This may explain why Bales (1984) observed significant flocculation and sedimentation of chrysotile fibers in the presence of settling particles of silica, but negligible degrees of flocculation of the chrysotile fibers when silica particles were not present. Together, these observations suggest that if particles of other composition are not present in the water column, a substantial percentage of chrysotile fibers—especially the smaller ones—are unlikely to undergo sufficient degrees of flocculation to be removed by sedimentation.

Sediment transported by the Sumas River includes the weathered serpentine minerals chrysotile and lizardite, as indicated by XRD analysis of sediments sampled from the streambed of Swift Creek and from the toe of the landslide (Jed Januch and others, U.S. Environmental Protection Agency, written commun., July 2006; Bayer and Linneman, 2010). In multiple samples of the Swift Creek bed sediments analyzed by Jed Januch and others (U.S. Environmental Protection Agency written commun., 2006), chrysotile was listed as a major constituent (greater than 20 percent by weight), as was lizardite. An exception to this pattern involved a sample of suspended sediment in which lizardite was characterized as a minor constituent. Although the three different forms of chrysotile are indistinguishable by XRD analysis, asbestiform chrysotile (clinocrysotile) may be differentiated from the other two forms with a light microscope. Microscopic examination of sediment from Swift Creek and the Sumas River reveals many of the characteristic physical features of asbestiform chrysotile including (1) individual fibers that are typically on the order of 1–3 μm long, (2) individual floccules that can range in size to those of sand-sized particles, and (3) individual fibers that are disaggregated from sand-sized grains of serpentine (Schreier, 1987; Bayer and Linneman, 2010). The asbestiform chrysotile fibers reported to be present in the Sumas River (Schreier, 1987) generally are smaller than fibers described in documents that summarize the asbestos measurement methods used for assessing environmental or human-health effects. Asbestiform chrysotile fibers typically are characterized as being greater than 5 μm long and less than 0.5 μm thick, with length-to-width ratios of up to 100:1. They are often curved, commonly arranged in parallel, and occur either in bundles displaying splayed ends, or in matted masses of individual fibers (U.S. Environmental Protection Agency, 1993).

Sediment Load Implications

The measured suspended-sediment load at South Pass (figs. 1 and 2) ranged from 22,000 to 49,000 t/yr for the study period. Although not measured as part of this study, a substantial amount of bedload, predominantly sand-sized, likely moves through the Sumas River. Assuming 10–40 percent additional transport resulting from unmeasured bedload, the total load transported at South Pass during this study was likely on the order of 25,000–65,000 t/yr. With a drainage area of 41 km^2, these values correspond to a sediment yield at South Pass during the study that ranged from 600 to 1,600 (t/km^2)/yr. This range is considerably larger than those for other rivers draining into Puget Sound (Czuba and others, 2011), and comparable to those for rivers draining glaciated volcanoes of western Washington (Czuba and others, 2012). Assuming that the bulk density of the suspended sediment was between 1.5 and 1.6 g/cm^3, the volume of suspended-sediment load measured at South Pass ranged from 16,000 to 40,000 m^3. Including the estimated (but unmeasured) bedload, the total sediment load transported at South Pass during this study was on the order of 15,000–38,000 m^3/yr (20,000–50,000 yd^3/yr), which is on the lower end of published estimates of total sediment load in Swift Creek. Substantial bedload accumulates in Swift Creek each year (Whatcom County, 2012); this would explain part of the discrepancy between results from this study and published load estimates. Although flows during the study period were greater than normal, based on hydrologic measurements from the Huntingdon site, peak flows were not exceptionally large, only modestly exceeding the 2-year flood (27.0 m^3/s [953 ft^3/s]) on two occasions. Following the second-largest peak flow observed at Huntingdon during the study (28.0 m^3/s [989 ft^3/s] on January 10, 2013), limited overbank deposits of sediment were observed only in the Sumas River floodplain at several locations near Lindsay Road; extensive overbank flooding did not occur. This indicates that other, lesser peak flows likely remained within the Sumas River banks and suggests that large, geomorphically important flooding did not occur during this study. Mass wasting from the landslide likely increases exponentially with increasing peak flows and it is possible that the limited study period was insufficient to estimate the full range of sediment-producing storms typical within the watershed.

Continued movement and associated sediment erosion of the landslide through mass wasting and runoff are likely to maintain large sediment loads in Swift Creek and the Sumas River for the foreseeable future. In turn, given the current channel morphology of the river system, acute aggradation on the Swift Creek alluvial fan and, to a lesser degree, in the main stem of the Sumas River (at rates comparable to those documented in the latter part of the 20th century) are likely to persist.

Asbestiform Chrysotile Content in Suspended Sediment

Chrysotile has been identified as a major component of suspended and bottom sediments from Swift Creek and the Sumas River (Jed Januch and others, U.S. Environmental Protection Agency, written commun., July 2006; Bayer and Linneman, 2010; Wroble, 2011). Microscopic examination of sediment particles from Swift Creek has revealed chrysotile fibers disaggregating from sand-sized grains of serpentine, individual chrysotile fibers that average about 2 µm in length, and floccules of chrysotile fibers ranging to sand-sized particles (Bayer and Linneman, 2010). Suspended sediment carried by the Sumas River, particularly during high flow, likely contains a larger fraction of flocculated fibrous material than typically is detected in other rivers draining the western slopes of the Cascade Range in Washington. Several different techniques were used to determine some of the physical characteristics of the suspended sediments in the Sumas River, and to measure asbestiform chrysotile content. In addition, pH was measured—in selected discrete samples and on a short-term continuous basis at a single site—to assist in the interpretation of the chrysotile data.

Methods for Measuring Asbestiform Chrysotile Content in Suspended Sediment

Samples of water and suspended sediment were collected using an Isco 6712 automated pumping sampler. During selected runoff events, the sampler was programmed to collect as many as 24 hourly samples of about 900 mL each at the South Pass and Telegraph gaging stations. Because most sediment transport in the Sumas River occurs during periods of high flow, the samples used to measure the asbestiform chrysotile content of suspended sediment were collected during periods of high flow. This approach reduced the amount of sample compositing required to obtain the minimum sample mass of 2 g (dry weight) required for asbestiform chrysotile analysis. For some sampling events, however, multiple hourly sediment samples were combined to obtain a sufficient amount of sediment for analysis. A multi-parameter instrument also was installed at South Pass gaging station from November 1 to December 5, 2011, and from December 16, 2011, to January 7, 2012, to record measurements of water temperature, specific conductance (YSI 6920 water-quality sonde), pH (YSI 6565 pH sensor), and dissolved oxygen (YSI 6150 optical dissolved-oxygen probe) at 15 minute intervals during the sampling periods (appendix F).

Water and suspended-sediment samples were collected to measure the asbestiform chrysotile content of the suspended sediment during five rainfall-runoff periods at South Pass and Telegraph (fig. 14). It was beyond the scope of this

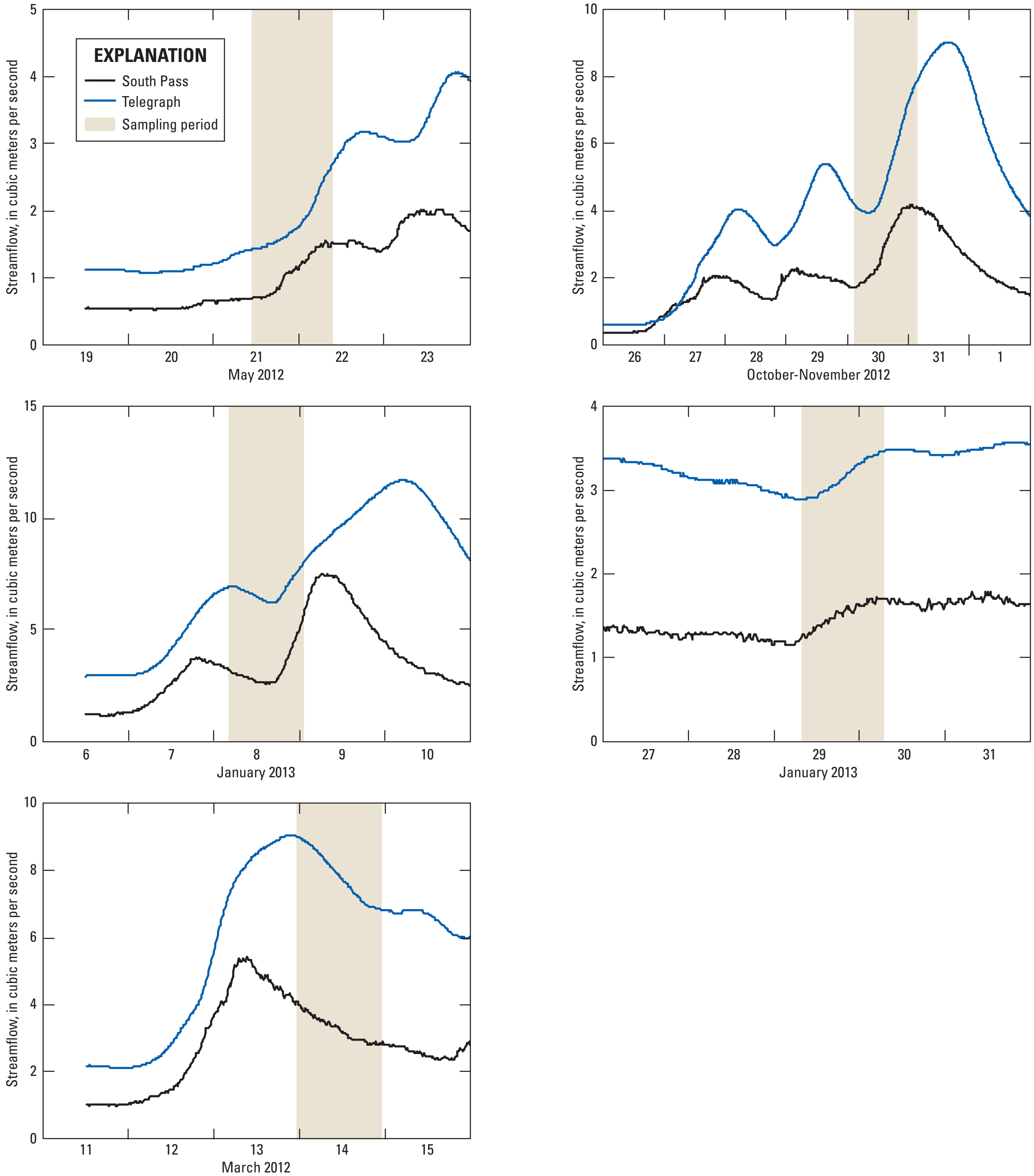

Figure 14. Streamflow during five sampling periods at Sumas River at South Pass Road near Nooksack, Washington (12214350; referred to as “South Pass”) and at Sumas River near Sumas, Washington (12214500; referred to as “Telegraph”), 2012 and 2013. Sampling periods are shaded to indicate when hourly suspended-sediment samples were collected with an automated pump sampler.

investigation to measure the concentrations of non-asbestos forms of chrysotile and other serpentine minerals such as lizardite. Samples of suspended sediment were collected during storms with highly varied hydrologic conditions, which resulted in a wide range of suspended-sediment concentrations, from less than 100 mg/L to greater than 25,000 mg/L. Suspended-sediment concentrations (appendix B) were typically larger on the rising limb of the hydrograph than on the falling limb. Continuous measurements of turbidity were evaluated to identify runoff events that were generating substantial suspended-sediment loads, and presumably substantial asbestiform chrysotile loads, to Swift Creek and the Sumas River. This information was, in turn, used to select specific samples for quantifying the asbestiform chrysotile concentrations in the suspended sediment.

After collection, the samples were returned to the USGS Washington Water Science Center laboratory in Tacoma for dewatering and processing; the dried material was sent to a commercial laboratory (Lab/Cor Inc., Seattle, Washington) for the analysis of asbestiform chrysotile content. The dewatering process consisted of allowing the sediment sample to settle undisturbed for at least 24 hours, and then carefully drawing off the overlying water (hereinafter referred to as **supernatant** water) using a peristaltic pump and a J-tube intake.

The pH and specific conductance of the supernatant water were measured after it was drawn off from the sample. The sediment and its remaining (mostly interstitial) water were transferred to a 300-mL glass storage jar for further processing. A composite of the supernatant water was retained for analysis of chrysotile fibers that were too small to settle out of suspension.

For some runoff periods, the flocculated and non-flocculated fractions of selected samples were qualitatively separated in the laboratory using an Imhoff cone equipped with a pinch clamp installed at the base (fig. 15). Complete separation was not achieved with this process as some silt and clay sized particles remained in the flocculated fraction; therefore, the flocculated and non-flocculated fractions were operationally defined. Partially dewatered suspended-sediment samples in the 300-mL storage jars were agitated, mixed, and transferred to the Imhoff cone containing approximately 300 mL of tap water. Before allowing the suspended sediment to settle, additional tap water was added to bring the settling volume to 800 mL. The Imhoff cone was capped and inverted several times to thoroughly mix the water and suspended sediment, then was allowed to settle for several minutes, allowing the separation of the non-flocculated sediment from the flocculated sediment. As shown in figure 15, the predominantly non-flocculated sediment, which settled rapidly to the bottom of the Imhoff cone, was darker than the overlying predominantly flocculated sediment, although silt- and sand-sized particles regardless of ability to flocculate remained in suspension throughout these measurements. For two samples, the supernatant water in the Imhoff cone was passed through a 0.47 micron filter and the remaining sediment was dried and weighed to determine the mass, which for these samples, was less than 2 mg. For some samples, the volumes of the flocculated and non-flocculated sediment were recorded directly from the graduated scale on the Imhoff cone.

Non-flocculated and flocculated sediment were drawn off separately from the base of the Imhoff cone. The separate fractions were repeatedly washed, decanted, and visually inspected to separate the darker non-flocculated sediment from the predominantly tan-colored flocculated material. The washing process was repeated as many as five times to achieve better separation of the two sediment fractions. On several occasions, the water remaining in the cone was passed through a 5-µm filter to measure the mass of the residual sediment retained in the supernatant water. The dry-weight mass then was determined for the flocculated and non-flocculated components of the suspended sediment. The total SSC was calculated for each individual sample by dividing the dry-weight mass of the sediment by the volume of the whole-water sample. At South Pass, SSC values less than 5,000 mg/L were multiplied by a cross-section coefficient of 1.6 (table 2) to account for sampler intake location and the natural variation in SSC within the cross section (appendix B). Pumped samples from Telegraph for the October 30–31, 2012 storm (appendix B) were used only for the measurement of chrysotile content; the irregular and high SSC values for these samples likely are the result of sloughing of bank material near the sampler intake, which was noted during a field inspection following this storm.

Complementary measurement techniques used to determine the asbestiform chrysotile content of the suspended sediments included polarized light microscopy (PLM) and transmission electron microscopy (TEM); X-ray diffraction (XRD) also was used, but this technique does not differentiate between the asbestiform and non-asbestiform types of chrysotile. Most analyses of asbestiform chrysotile were done using PLM so that the resulting data could be more directly compared with existing information from the Sumas River area (most previous measurements of the concentrations of asbestos in the soils and sediments of the Sumas area have been made using the PLM method [Wroble, 2011]). The fibrous habit, or needle-like morphology, of asbestos is used in both PLM and TEM procedures to identify asbestos particles. Mineralogical properties of asbestos particles, including refractive indices, birefringence, and extinction angle also are used in the PLM method to distinguish between asbestiform and non-asbestiform chrysotile. The high magnification capabilities of TEM allow the resolution of particle size to of 0.01 µm (Millette, 2006); this particle size is more than 100 times smaller than can be resolved by PLM. Prior to the analysis of chrysotile content, the dried sediment samples were ground in a Bico mill to provide a more homogeneous particle-size distribution for analysis.

Figure 15. Two samples of suspended sediment collected from Sumas River at South Pass Road at Nooksack (12213500), Washington during a winter storm on January 8 and 9, 2013. Samples were allowed to settle in a 1-liter Imhoff cone. Sample *A* collected on January 8 at 2215 shown on the left; sample *B* collected on January 9 at 0515 shown on the right.

The PLM quantification procedures include standardized point-counting using 400-point count procedures with plane-polarized light, following the California Air Resources Board (1991) Method 435 and U.S. Environmental Protection Agency (1993) methods for analysis of asbestos in bulk material. The method uses counting rules for distinguishing what should be identified as countable asbestos fibers; these include counting only particles that (1) are longer than 5 µm, (2) have an aspect ratio (that is, a ratio of length to width) greater than 3, and (3) exhibit the physical and optical characteristics of asbestos minerals. Although these counting rules help to provide more consistent results, some particles, particularly shorter chrysotile fibers, may not be counted if they do not meet the minimum length specified by the counting rules. Additionally, small chrysotile particles may be overlooked by quantification methods that use light microscopes because of the practical limitations on the spatial resolution associated with the wavelengths of visible light. Such constraints limit the identification of asbestos fibers to those with a minimum diameter of about 0.2 µm (Kerr, 1977; National Institute of Occupational Safety and Health, 1994; Millette, 2006; National Institute of Occupational Safety and Health, 2011). Consequently, a subset of samples that were analyzed using PLM also were analyzed with TEM. Analysis of selected samples by TEM used visual estimation procedures outlined for analytical electron microscopy methods in U.S. Environmental Protection Agency (1993). For each sample analyzed, visual estimates of fiber concentrations were made at a magnification of 20,000×of 10 grid openings on two separated grid preparations for each sample analyzed. X-ray diffraction procedures using NIOSH method 9000 also were used for a subset of samples (National Institute for Occupational Safety and Health, 1994); although XRD does not distinguish between asbestiform and non-asbestiform chrysotile, it does provide an additional measurement for comparison.

Three samples of supernatant water removed from suspended-sediment samples also were analyzed to check for the presence of asbestiform chrysotile using U.S. Environmental Protection Agency method 100.2 (U.S. Environmental Protection Agency, 1994). Quantification of asbestiform chrysotile in samples of suspended sediment and water were carried out by Lab/Cor, Incorporated (Seattle, Washington). The estimated analytical error associated with the PLM measurements (as reported by Lab/Cor) was ±20 percent.

Physical Characteristics of the Suspended Sediment

The suspended sediment carried by the Sumas River, downstream of the confluence of Swift Creek, often consisted of a combination of flocculated and non-flocculated sediment particles particularly at high flows. Floccules as much as 2 mm in size often were visible (fig. 16). Samples of suspended sediment that were collected at South Pass during a storm on January 8 and 9, 2013 were allowed to settle in a 1-L Imhoff cone for 24 hours. Sample *A* (fig. 15) contained 2–3 mL of non-flocculated sediment and about 33 mL of flocculated material; sample *B* (fig. 15) contained 3–4 mL of non-flocculated sediment and about 34 mL of flocculated material. The average bulk density of the non-flocculated sediment was between 1.5 and 1.6 g/cm^3, a value within the typical range for fluvial sediment. The bulk density of the flocculated material was much smaller and more variable. After settling for about 1 hour, the volume of the flocculated material in the two samples was approximately 68–72 mL, yielding an equivalent bulk density of about 0.08 g/cm^3. However, self-compaction of the floccules continued for some time after the initial settling, resulting in an increase in the bulk density of the flocculated fraction to about 0.16 g/cm^3 after the samples were allowed to settle for 24 hours. Further self-compaction likely occurred but was not measured.

Use of pH as an Indicator of Chrysotile Concentrations in Suspended Sediment

Measured values of pH and turbidity were used to select specific samples for quantifying the chrysotile concentrations in the suspended sediments. The chrysotile concentration in suspended sediment was determined from samples collected during storms when increased runoff and higher concentrations of suspended-sediment in samples were expected to provide a sufficient amount of material for analysis. For example, at South Pass during the October 30–31, 2012 storm, the measured suspended-sediment concentrations (flocculated and non-flocculated) and pH from samples followed the general trend of turbidity and streamflow recorded for that site (fig. 17); however, the pumping sampler (on an hourly sampling interval) likely missed the period of greatest suspended-sediment concentration that presumably occurred during the turbidity maximum on the morning of October 31, 2012. The increasing trend in the concentration of flocculated suspended sediment during the storm at South Pass indicate a substantial input of freshly weathered chrysotile and other serpentine minerals occurred, perhaps as a results of erosion in the Swift Creek landslide area. A direct relation between sample pH and the concentration of flocculated suspended sediment was observed during the October 30–31, 2012, and the January 8–9, 2013 storms (fig. 18). These measurements are consistent with the results from laboratory studies by Choi and Smith (1971) and Koumantakis and others (2009), indicating that the pH of chrysotile suspensions in distilled water increases with increasing concentrations of suspended chrysotile.

The correlations, calculated as the Pearson's correlation coefficient, between the pH measured from samples at South Pass and various measures (log-transformed) of suspended sediment, turbidity, and streamflow for the October 30–31, 2012, and the January 8–9, 2013 sampling periods are shown in table 6. The strongest correlations with pH were observed for the concentration of the flocculated suspended-sediment in the samples from the two sampling periods ($r=0.92$ and 0.89 for the October 2012 and January 2013 storms, respectively).

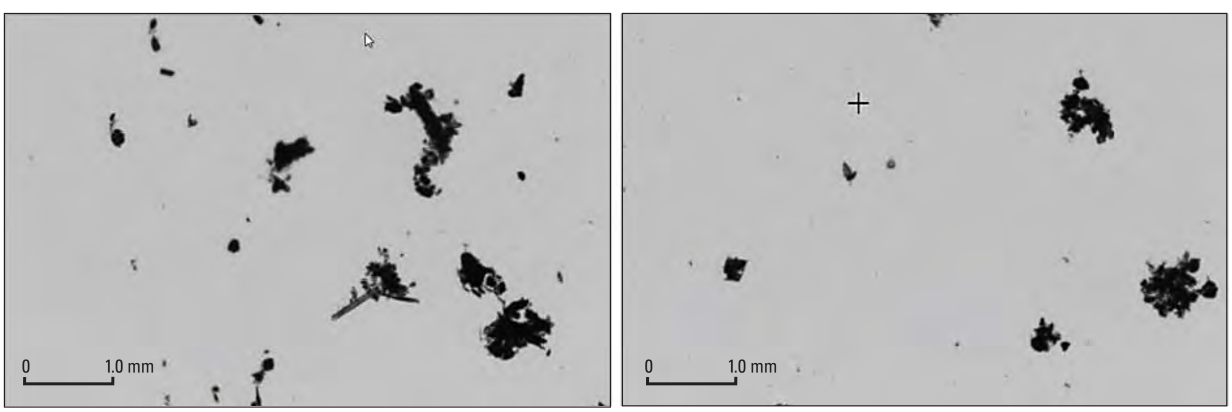

Figure 16. Flocculated particles falling in a column of native water during the laboratory measurement of settling velocity. Scale bars are 1 millimeters in length. Photographs by Kate Norton, U.S. Geological Survey, Vancouver, Washington, March 2013.

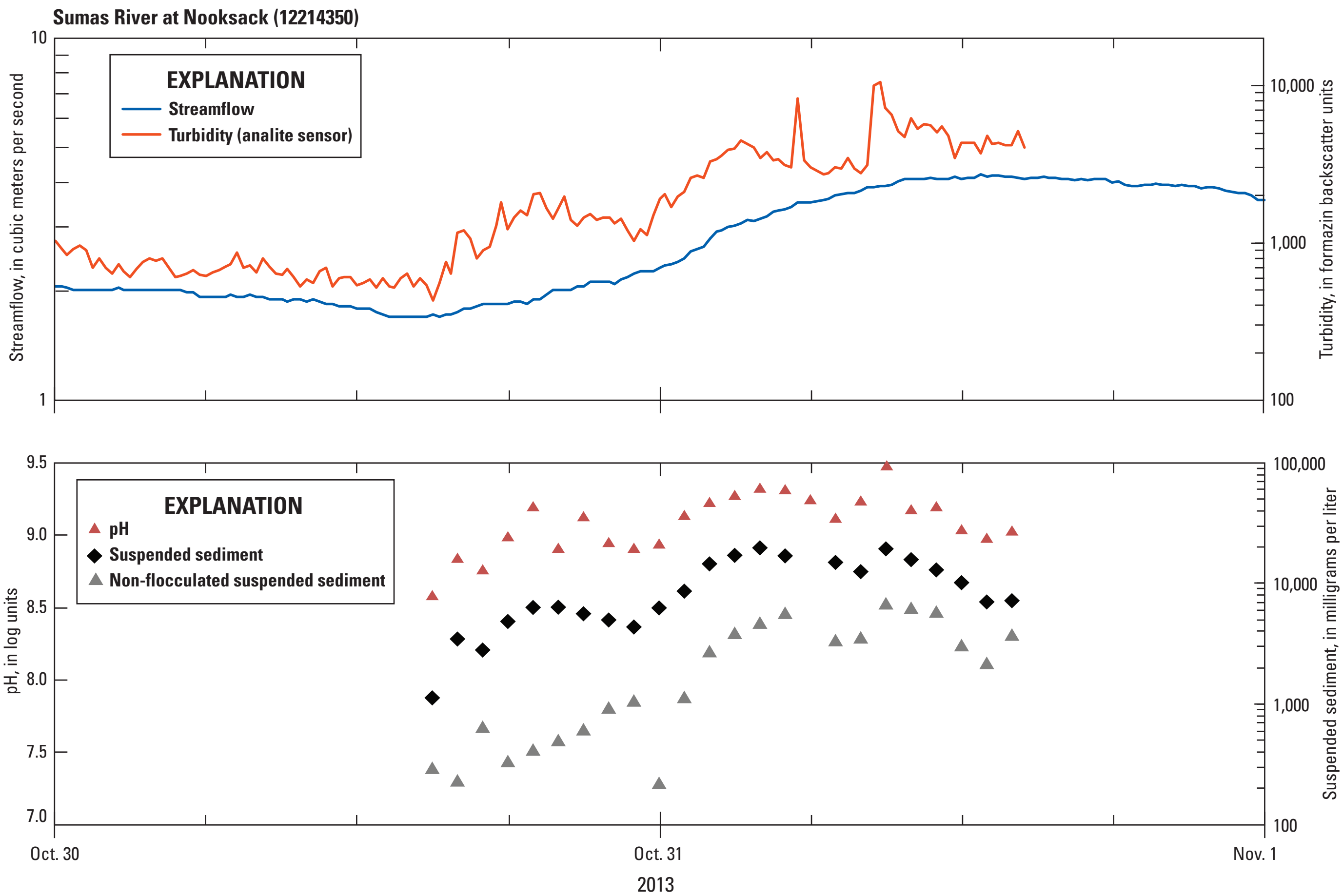

Figure 17. Streamflow, turbidity, pH, and the mass of flocculated and non-flocculated suspended sediment at Sumas River at South Pass Road at Nooksack, Washington (12214350) during storm on October 30–31, 2012. Streamflow and turbidity are continuous 15-minute data. The concentration of suspended sediment and corresponding pH measurements were determined in the laboratory from samples collected with an automated sampler.

Table 6. Correlations between pH and various measures of suspended-sediment concentration from samples collected at the Sumas River at South Pass Road streamgage (12214350) during storms on October 30–31, 2012, and January 8–9, 2013, Washington.

[Turbidity and streamflow values based on recorded values at the streamflow-gaging station at the time of sample collection. The data used for these calculations are displayed in appendix B. **r**: Pearson's correlation coefficient. **Abbreviations:** SSC, suspended-sediment concentration; mg/L, milligrams per liter; FBU, Formazin Backscatter Units; m³/s, cubic meters per second]

Sampling dates	Parameter	Number of samples	r
October 30–31, 2012	$\log_{10}$ (SSC, mg/L)	23	0.90
	$\log_{10}$ (flocculated SSC, mg/L)	23	0.92
	$\log_{10}$ (non-flocculated SSC, mg/L)	23	0.73
	$\log_{10}$ (turbidity, in FBU)	23	0.79
	$\log_{10}$ (streamflow, m^3/s)	23	0.60
January 8–9, 2013	$\log_{10}$ (SSC, mg/L)	16	0.84
	$\log_{10}$ (flocculated SSC, mg/L)	16	0.89
	$\log_{10}$ (non-flocculated SSC, mg/L)	16	0.69
	$\log_{10}$ (streamflow, m^3/s)	16	0.47

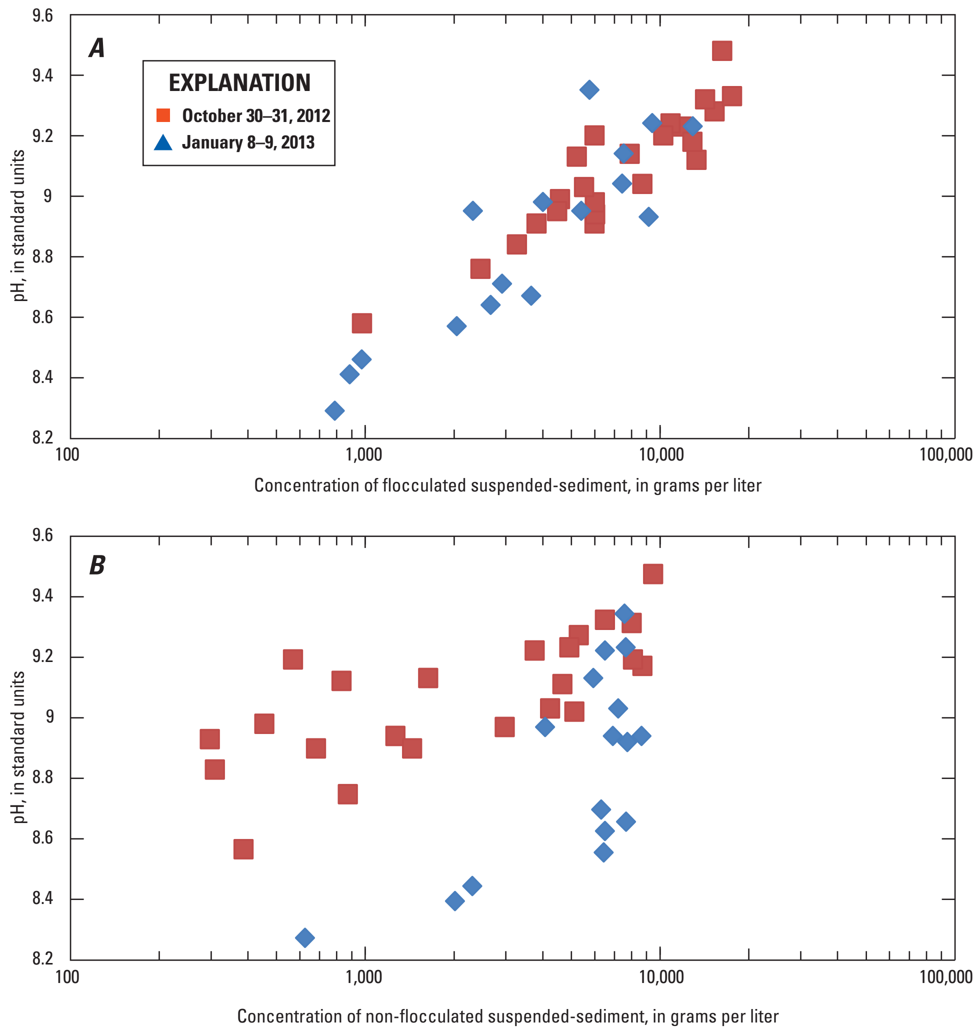

Figure 18. pH and the concentration of flocculated suspended sediment (*A*) and pH and the concentration of non-flocculated suspended sediment (*B*), in 900-milliliter pumped samples collected from the Sumas River at South Pass Road at Nooksack, Washington (12214350), during storms on October 30–31, 2012, and January 8–9, 2013.

Weaker correlations were noted between pH and turbidity (r=0.79), and between pH and the concentration of non-flocculated material (r=0.73 and 0.69). These results suggest that pH may be a useful indicator of the concentration of fresh asbestiform chrysotile and associated serpentine minerals in suspension, even in the presence of other suspended material. This finding is of particular interest because the concentrations of suspended chrysotile fibers in surface waters have generally been determined to be only poorly correlated—if at all—with turbidity (McGuire and others, 1982; Hayward, 1984).

The utility of pH as a potential indicator of fresh chrysotile concentration is also illustrated by the continuous pH data measured at 15-minute intervals at South Pass from November 1 to December 5, 2011, and from December 16, 2011 to January 7, 2012 (fig. 19), when streamflow, turbidity, and suspended-sediment data also were available. Several pH peaks were measured, although most were less than 0.5 pH units. A substantially larger peak was measured over the November 24–25 period, during which the pH increased more than 1.5 pH units and corresponded to a peak in the daily composite suspended-sediment concentration. Although pH was not continuously measured at Telegraph, a pH variation of about 0.3 pH units was measured in samples collected at Telegraph during a storm on January 29–30, 2013 (see data in appendix B). Other water-quality factors such as organic matter and agricultural drainage may also influence pH measurements.

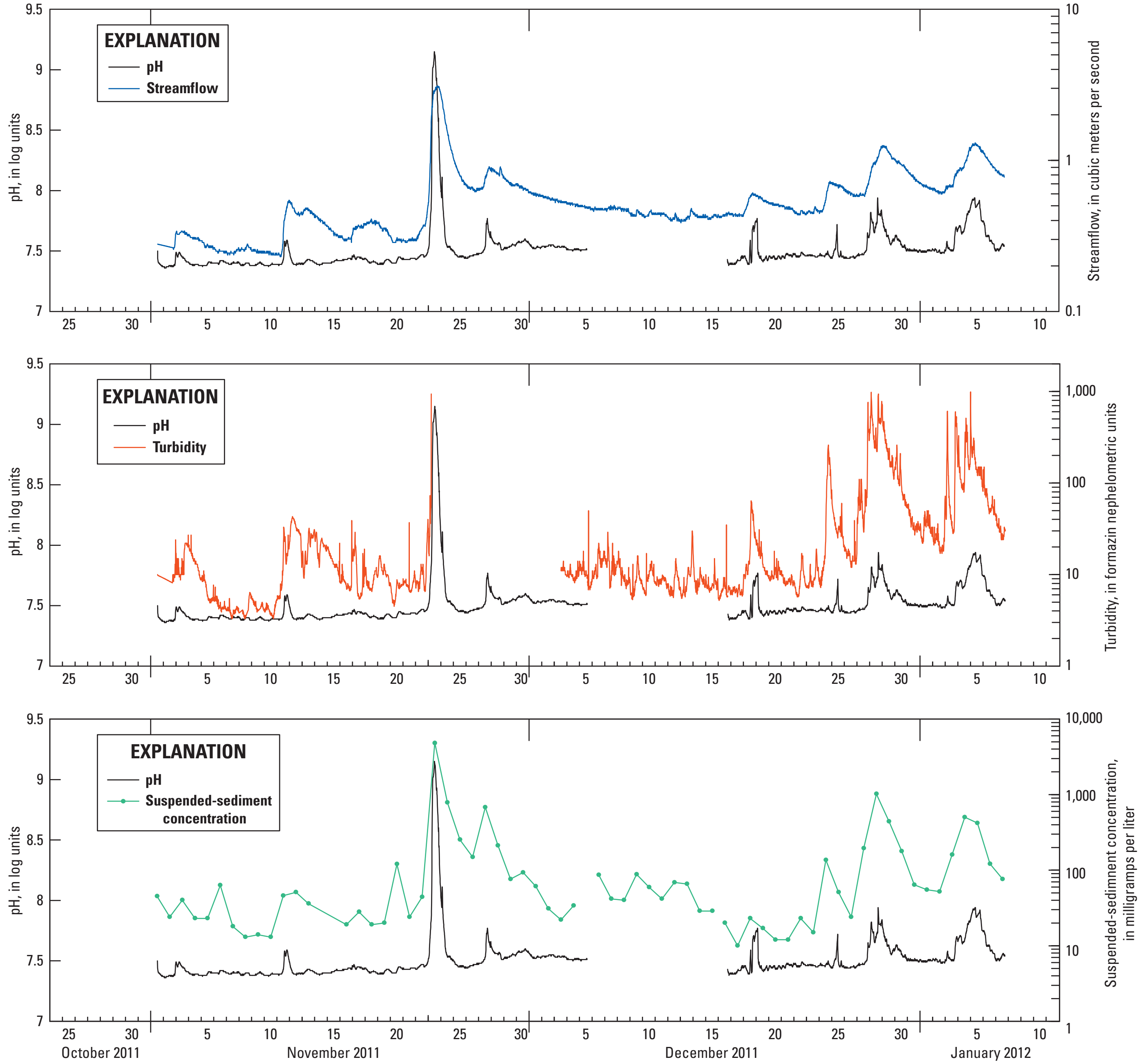

Figure 19. Measured values (15-minute) of pH, streamflow, and turbidity, and suspended-sediment concentration of daily samples at Sumas River at South Pass Road at Nooksack (12214350), Washington, November 1, 2011–January 7, 2012. The pH sensor was removed for servicing December 6–16, 2011. The 15-minute record of turbidity is discontinuous. Daily composited samples of suspended sediment were collected with an Isco-6712 automated pump sampler.

Measured Asbestiform Chrysotile Content in Suspended Sediment

The asbestiform chrysotile content of the samples analyzed using the PLM and TEM methods ranged from 0.5 to 77 percent by mass; the total chrysotile content (asbestiform and non-asbestiform) as measured by XRD ranged from 2.07 to 9.31 percent by mass. Variations in chrysotile content were evident in the measured values between split samples using the three methods (table 7**)**. For each method, replicate analyses of blind duplicate samples showed good agreement. The large range in measured asbestiform chrysotile content was in large part dependent on the method of quantification. The values obtained using the TEM analyses typically were at least twice as high as corresponding PLM values. This discrepancy is reasonable given that the average length of chrysotile fibers from the Swift Creek landslide is about 2 microns, which is near the resolution limits of PLM and well within the measuring range of TEM. Similar differences in results among methods were reported by Wagner (2015) as part of an assessment of naturally occurring asbestos in serpentinite rocks from northern California. Wagner (2015) concluded that because of differences in sample preparation and microscope resolution, the different analyses assess two distinct populations of particle sizes. The TEM method focuses on particles with dimensions in the range of 0.01 to 10 µm, which is mostly the clay size fraction of sediment. In contrast, the PLM analysis focuses on particles in the range of 10–100 µm, which is predominantly the silt- and fine-sand-size fraction. Results from the two methods are thus complimentary, providing a more complete assessment of asbestiform chrysotile content than would be available from either of the methods alone.

The PLM method requires 400 point counts per analysis and is a well-developed approach for the analysis of asbestos in building materials, however, the method could underestimate asbestos in materials that contain asbestos fibers too small to be observed with a light microscope (National Institute for Occupational Safety and Health, 2011). The chrysotile fibers observed in suspended sediment from Swift Creek and the Sumas River samples are about 2 µm long, which is near the lower limit of particle size observable by the visible light used in the PLM method. Therefore, chrysotile likely was present in suspension that could not be detected by the PLM method, but could have been detected by the TEM method. The TEM method, although having greater resolution for smaller particle sizes, also involves a greater degree of visual estimation than PLM and therefore may yield more variable results. However, in this study, duplicate TEM measurements of a single blind split of bulk sediment sample differed by less than 5 percent (table 7).

The PLM method was used to measure asbestiform chrysotile content in samples of bulk sediment, as well as in the flocculated and non-flocculated fractions separately. In total, asbestiform chrysotile concentrations were measured in 22 samples using PLM, including three duplicate samples,

Table 7. Chrysotile composition as a percentage by mass of suspended-sediment samples collected at selected streamflow-gaging stations at the Sumas River, Whatcom County, Washington.

[**Station name:** All stations are USGS streamflow gages in Washington, U.S.A. **Sample media:** F, flocculated sediment; NF, non-flocculated sediment; B, bulk sediment. **Percent chrysotile, by analysis method:** Only asbestiform chrysotile is reported for PLM and TEM methods. PLM, Polarized Light Microscopy; TEM, Transmission Electron Microscopy; XRD, X-Ray diffraction. –, not tested]

Streamflow-gaging station name	No.	Date of sample collection	Time of sample collection	Sample media	Chrysotile, by analysis method (percent)		
					PLM	TEM	XRD
Sumas River at South Pass Road at Nooksack	12214350	10-30-12	1200	F	19.5	69	2.13
		10-30-12	[1]1201	F	19.5	–	–
		10-30-12	1200	NF	2.25	77	4.42
		01-29-13	0800	NF	22.5	50	9.31
		01-29-13	0800	F	23.5	73	4.84
Sumas River near Sumas[2]	12214500	05-21-12	2340	B	1.25	–	–
		05-21-12	[1]2341	B	3.25	–	–
		10-30-12	1200	NF	0.5	75	2.07
		03-14-13	1300	B	25.5	61	6.56
		03-14-13	[1]1301	B	29	64	6.72

[1]Duplicate sample.

[2]Also referred to as "Telegraph" because of its location on Telegraph Road.

(table 8) and content ranged from 0.25 to 37.5 percent of the sediment fraction examined. The bulk sediment contained 14±4 percent asbestiform chrysotile, and exhibited the greatest range in asbestiform chrysotile content, from 1.25 to 37.5 percent. Substantial differences in asbestiform chrysotile content were observed among the flocculated, non-flocculated, and bulk-sediment fractions (fig. 20). These data show that the flocculated sediments typically contained substantially more asbestiform chrysotile than either the bulk sediment or the non-flocculated fraction and are consistent with the hypothesis (supported by the data in table 6) that pH may be an indicator of the concentration of fresh asbestiform chrysotile as well as non-asbestiform chrysotile and other serpentine minerals suspended in the water column. Whereas the measured asbestiform chrysotile content of the flocculated material was relatively consistent (22±3 percent [mean ±95 percent confidence limit]), the asbestiform chrysotile content of the non-flocculated sediments (5.2 ± 5.4 percent) was substantially more variable and lower than the flocculated fraction.

The amounts of non-settling asbestiform chrysotile measured in the supernatant water ranged from 2.4 to 19.5 million fibers per liter. Using this procedure, only fibers longer than 10 µm were counted. Although it is likely that many shorter fibers also were present, the operational definition used in the method of analysis does not count shorter fibers that exhibit the properties of chrysotile. Assuming a fiber length of 15 µm, a diameter of 0.1 µm, and a density of chrysotile of 2.55 g/cm^3, the additional mass of material transported as non-settling chrysotile was calculated to be less than 1 mg/L.

Table 8. Suspended-sediment concentrations and the flocculated fraction, and the asbestiform chrysotile content of bulk, flocculated, and non-flocculated fractions of suspended sediment at selected streamflow-gaging stations at the Sumas River, Whatcom County, Washington.

[Includes data from table 7. **Station name:** All stations are USGS streamflow gages in Washington, U.S.A. **Flocculated SSC:** Weight percentage of flocculated (lighter colored) material in sediment collected after settling in an Imhoff cone. **Asbestiform chrysotile:** Percentage of each fraction that was estimated to be asbestiform chrysotile using Polarized Light Microscopy. F, flocculated sediment; NF, non-flocculated sediment; B, bulk sediment. **Boldface** values are calculated values, based on mass balance for the flocculated fraction. *Italic* values are derived from the analysis of split samples to assess laboratory reproducibility. **Abbreviations:** SSC, suspended-sediment concentration; mg/L; milligram per liter; –, not tested]

Streamflow-gaging station name	No.	Date of sample collection	Time of sample collection	Suspended-sediment concentration (mg/L)	Flocculated SSC (percent)	Abestiform chrysotile (percent)		
						B	NF	F
Sumas River at South Pass Road at Nooksack	12214350	05-21-12	0300	397	–	11.2	–	–
		05-22-12	1700	80	–	9.25	–	–
		10-30-12	1600	3,580	91	**17.1**	2.3	18.5
		10-31-12	0000	6,330	95	–	–	18.8
		10-31-12	1200	13,000	67	**13.8**	2.25	*19.5*
		10-31-12	[1]1201	–	–	–	–	*19.5*
		01-29-13	2100	20,700	4	**6.2**	5.25	29
		01-30-13	0800	4,670	7	**23.4**	23.5	22.5
		03-13-13	1200	3,300	29	**7.38**	1	23
		03-14-13	1000	8,550	24	**11.8**	6.5	28.5
Sumas River near Sumas[2]	12214500	05-21-12	2340	517	–	*1.25*	–	–
		05-21-12	[1]2341	–	–	*3.25*	–	–
		05-22-12	0440	282	–	7.75	–	–
		05-22-12	1740	808	–	10.5	–	–
		10-30-12	1700	19,700	13	**2.43**	0.25	17
		10-31-12	1200	14,400	14	**3.44**	0.5	21.5
		01-30-13	0300	180	–	22.5	–	–
		01-30-13	1400	387	–	37.5	–	–
		03-13-13	1300	4,580	–	*25.5*	–	–
		03-13-13	[1]1301	–	–	*29*	–	–
		03-13-13	2230	1,460	–	20.5	–	–
		03-14-13	0730	1,300	–	22	–	–

[1]Duplicate (split) sample.

[2]Also referred to as "Telegraph" because of its location on Telegraph Road.

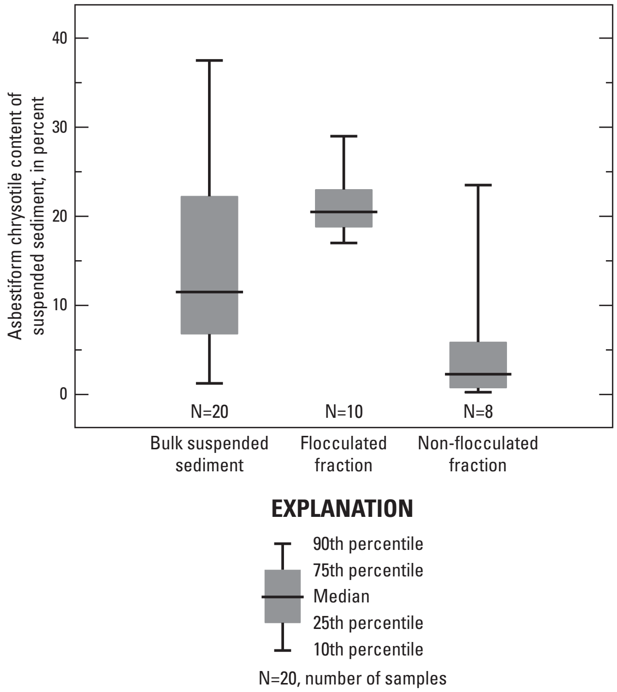

Figure 20. Asbestiform chrysotile content of suspended sediment in bulk, flocculated, and non-flocculated sediment fractions at selected streamflow-gaging stations at the Sumas River, Whatcom County, Washington. Data from table 8.

Fluvial Transport of Chrysotile Sediment

In still water, a particle denser than water will accelerate downward under the influence of gravity. The acceleration will continue until the opposing velocity-dependent drag force equals the gravitational force, at which point the particle will stop accelerating and fall at a constant velocity. This particle-dependent velocity is often referred to as the particle's "*terminal velocity*" or "*settling velocity*." For simple spherical particles of a given size and density, the settling velocity can be computed directly using Stokes' Law (Lamb, 1993); all else being equal, larger particles fall faster than smaller particles. However, particles of natural sediments are rarely perfect spheres, and settling velocity is strongly influenced by variations in particle shape, structure and density (Dietrich, 1982). In the Sumas River, the distribution of particle settling velocities must be known in order to design an effective settling basin—an option that is under consideration as a means of reducing the risk of public exposure to asbestos within the study area (Whatcom County, 2012). Knowledge of the distribution of settling velocities also is required to understand the transport dynamics of suspended sediment through the study area.

Streamflow in all natural rivers is turbulent, resulting in vertical flow velocities that vary substantially in time and space (Reynolds, 1883; 1895). Comparing the settling velocity of a given particle with the turbulent mixing velocities of a stream system offers insight into the transport potential of suspended sediments. Particles with relatively small settling velocities will be well distributed throughout the water column, comprising the suspended-sediment load. Particles with larger settling velocities will remain close to the streambed, remaining as bed material or transporting as *bedload*.

In the Sumas River downstream of the Swift creek confluence, floccules can comprise a large percentage of the suspended-sediment concentration, up to 95 percent by mass (table 8). The complex shapes and structures of these floccules, however, preclude the use of empirical equations to simulate settling velocities. Consequently, the settling-velocity distributions of the Sumas River sediment samples were measured directly, using a custom-built apparatus. The complex and potentially fragile nature of flocculated sediment presents a challenge for analysis of its physical characteristics. Changes in environmental conditions, physical agitation, or weathering may alter the shapes, sizes, and other properties of floccules. In the laboratory, such disturbances may lead to measured settling-velocity distributions that are systematically offset from distributions in natural settings. Although a complete exploration of flocculation dynamics in the Sumas River system was beyond the scope of this study, the methods for this investigation were used to minimize the storage and handling of samples, and included analyses to examine the effects of storage and handling on the settling-velocity measurements.

Measuring Settling Velocity

The settling velocity was analyzed for suspendedsediment samples collected from three sites: Swift Creek at Goodwin Road (referred to herein as Goodwin), South Pass, and Telegraph (see data in appendix G). In each instance, a grab sample was collected by hand along the channel edge within a zone of active flow using a 500-mL graduated cylinder. Fourteen samples were collected from the three sites during three separate storms, including several duplicate samples. Samples collected on February 22, 2013, were collected during a minor increase in streamflow, with moderately high levels of turbidity (fig. 21). Samples were collected on March 1 and 13, 2013, during streamflow peaks, when measured turbidity was near the upper end of the observed range for the study period.

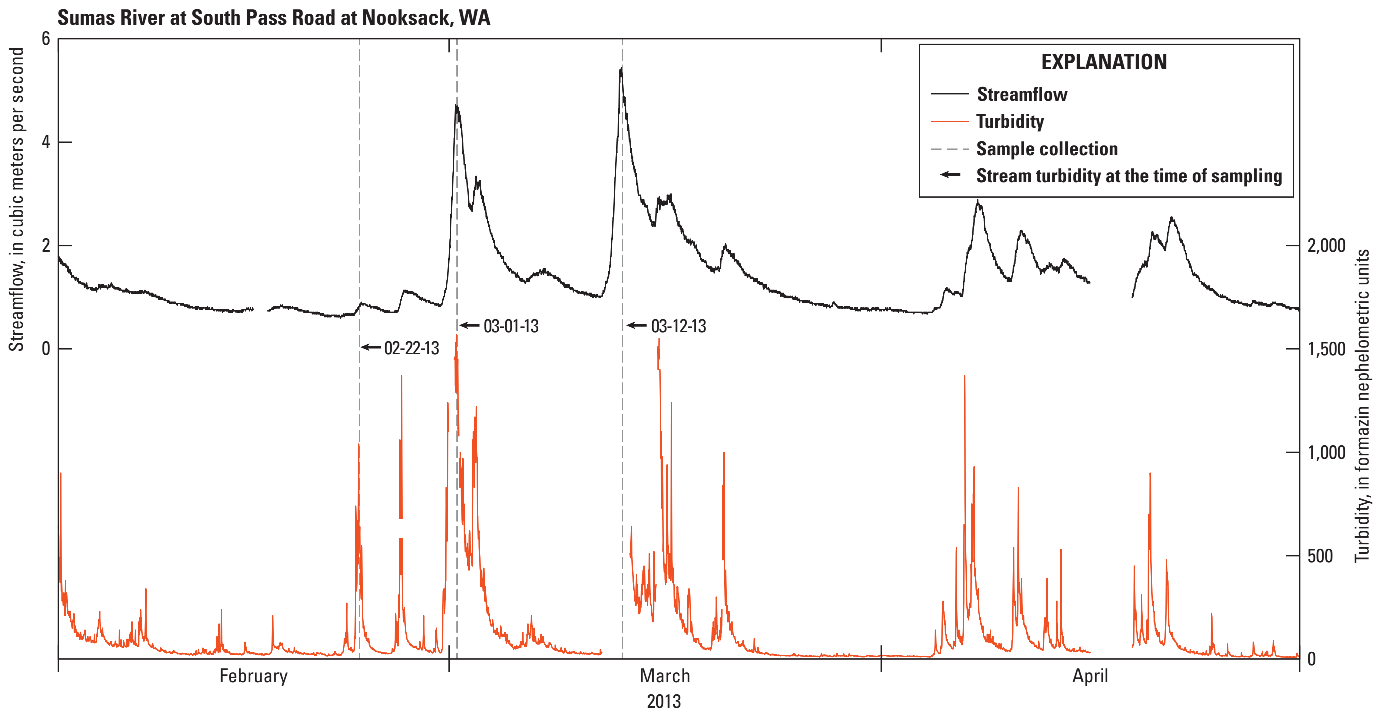

Figure 21. Discharge and turbidity for the Sumas River at South Pass Road at Nooksack (12214350), Washington, and sample collection times. Grab samples were collected from Swift Creek at Goodwin Road and Sumas River near Sumas (12214500), Washington, within 1 hour of the samples collected at South Pass.

Methods for Measuring Settling Velocity

Settling velocities were measured using a custom-built apparatus that combined elements of a visual accumulation (VA) tube and a custom valve assembly (fig. 22). The apparatus consisted of a 1.61 m VA tube (labeled "B" in fig. 22), with the outlet attached to a three-way valve (C). The straight-through axis of the three-way valve was connected to a sediment reservoir that consisted of a length of acrylic tubing (D) closed off at the bottom by a stopcock (E). The 90-degree axis of the three-way valve was connected to a deionized-water reservoir (G) that was constructed from a length of 2.54-cm diameter PVC tubing and used to flush the sediment reservoir without allowing air bubbles to enter the system.

In preparation for the settling-velocity measurements, each whole-water suspended-sediment sample was settled for at least 48-hours until the overlying water, or "*supernatant*," was clear. After the pH and temperature of the sample were measured, the supernatant was drawn off, passed through a 0.45-µm membrane filter to remove any remaining sediment, and poured into the settling tube so that the settling velocity of the sediment could be measured in its native water. If the volume of the supernatant was insufficient to fill the settling tube, additional filtered native water was added from concurrent supplemental samples that were collected to provide water for this purpose, if needed. To keep the sediment concentration low enough to permit unhindered settling during the measurement of settling velocities, after the supernatant was removed from each sample the remaining sediment was subsampled by coring with a small section of rigid tubing attached to a rubber bulb to provide gentle suction. After the settling tube was cleared of all bubbles, the subsample was introduced into the funnel at the top of the VA tube, from which it was separated by a closed valve ("A" in fig. 22). Before commencing the settling-velocity measurements, the stopcock (E) at the base of the sediment reservoir was closed and the three-way valve (C) set in the straight-through position, to allow sediment to pass from the VA tube directly into the reservoir.

At a noted time, the upper valve below the funnel was opened, allowing the sediment to enter and settle through the column. At predetermined intervals, the three-way valve was moved to the 90-degree configuration, switching the sediment reservoir input from the VA tube to the deionized-water reservoir. The stopcock on the sediment reservoir was then opened, allowing deionized water to flush the accumulated sediment out of the sediment reservoir and into a sediment dish ("F" in fig. 22) at the outlet. Once all of the sediment was flushed out from the sediment reservoir, the stopcock at the bottom of the reservoir was re-closed and the three-way valve returned to the straight-through position, once again allowing sediment to collect in the sediment reservoir.

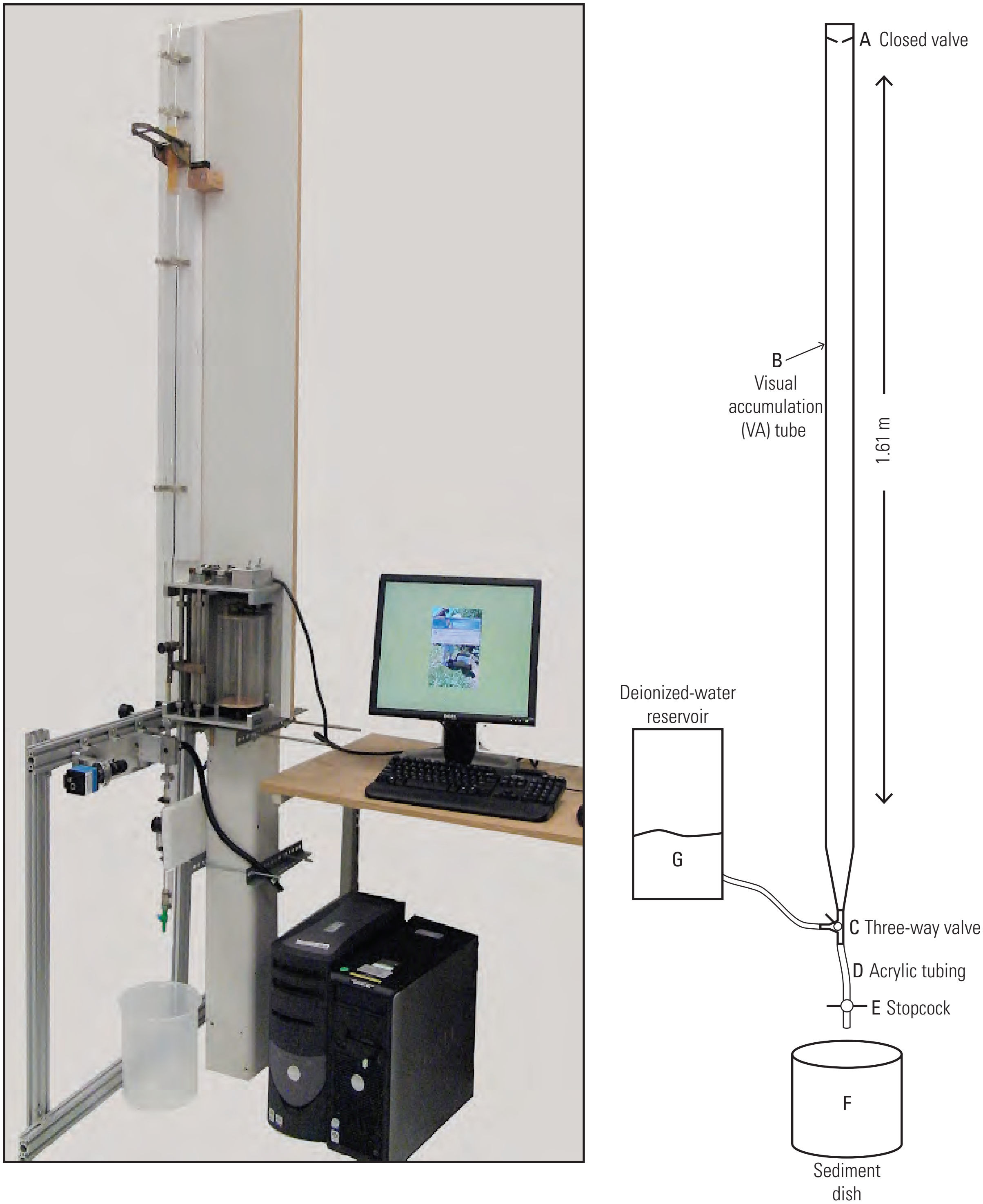

Figure 22. Laboratory apparatus used to measure the settling velocity of sediment samples collected from the Sumas River, Whatcom County, Washington. Measurements were done at the U.S. Geological Survey sediment laboratory at the Cascade Volcano Observatory, Vancouver, Washington.

Using this approach, the sediment collected in each sediment dish contained all particles with settling velocities greater than a specific value for each collection time, $V_{min,t}$, which was computed as follows:

$$V_{\min,t} = \frac{d_{app}}{t}\ , \qquad (2)$$

where

d_{app} is the distance from the air-water interface at the top of the sample in the apparatus to the center of the three-way valve, and

t is the time interval elapsed between the start of the settling and the collection time.

By repeating this collection process and measuring the mass of sediment in each dish at known intervals, a mass-based settling velocity distribution ($V_{min,t}$ for a range of t) was obtained for each sample.

Settling velocities are commonly expressed in terms of a “*fall diameter*” or a “*hydraulic diameter*,” defined as the diameter of a spherical quartz grain with a density (ρ_s) of 2.65 g/cm^3 that would have the same settling velocity in 24 °C water as that of the particle(s) of interest (Subcommittee on Sedimentation, 1957). For this work, the empirical relation presented by Gibbs and others (1971) to calculate the radius of a quartz sphere from its settling velocity and density—as well as from the density and dynamic viscosity of the fluid—was used to convert the measured settling velocities to hydraulic diameters.

Assessing Effects of Temperature and Hold Time

To determine whether temperature changes or hold times may have had significant effects on settling velocity of the floccules, the speed of the **settling front** between the floccule phase and overlying supernatant water was recorded in the field and in the laboratory across a range of temperatures and hold times. To measure the speed of the settling front, each sample was agitated until all sediment was in suspension and allowed to settle while being filmed. The resulting videos were reviewed in the laboratory to determine the location of the settling front through time. This process was repeated in the laboratory on multiple occasions for hold times that ranged from 0 to 32 days. These measurements were also made over a range of temperatures between 4.8 and 24 °C, encompassing most of the measured Sumas River water temperatures (3.5–8.9 °C), as well as the full range of room temperatures over which the settling velocities were measured (21.7–22.4 °C). In addition, the measurements were carried out after reaching the desired temperatures by either cooling from higher temperatures or heating from lower temperatures, to account for the possibility that any effects of temperature on floccule characteristics—and, by extension, settling velocities—may have been hysteretic.

Particle Transport Mode

The Rouse number (Rouse, 1937), Z_R, is a non-dimensional parameter that represents the ratio between the settling velocity of a particle and the turbulent mixing that acts to keep it in suspension and is defined as follows:

$$Z_R = \frac{\omega_p}{k u_*} \qquad (3)$$

where

ω_p is the settling velocity of a particle in meters per second,

k is the dimensionless von Kármán constant (typically assumed to have a value of 0.41), and

u_* is the shear velocity in meters per second, defined as

$$u_* = \sqrt{\frac{\tau_b}{\rho_w}} \qquad (4)$$

where

ρ_w is the density of water kilograms per cubic meter, and

τ_b is the shear stress at the bed kilograms per meter per square second, calculated as

$$\tau_b = \rho_w g H s \qquad (5)$$

where

g is the acceleration due to gravity meters per square second,

H is the flow depth in meters, and

s is the slope of the water surface (dimensionless).

Thus, the Rouse number uses information regarding the settling velocity of a particle and local hydraulic conditions to quantify the relative importance of settling and turbulent mixing in the transport of that particle. Rouse numbers greater than 2.5 generally indicate that the transport of the sediment of interest occurs primarily as bed load, values between 0.8 and 2.5 indicate transport as suspended load, and values less than 0.8 indicate “*wash load*” (that is, sediment that remains in suspension without deposition). Between 0.8 and 2.5, higher Rouse number values indicate that a particle is likely to spend a higher fraction of the time at or near the bed. As Rouse numbers decrease through this range, the particles become increasingly well-mixed in the vertical dimension, leading to higher relative concentrations near the top of the water column.

In this study, Rouse numbers were computed by combining the measured settling velocities (ω_p) with field measurements of flow depth (H) and surface slopes (s). Mean flow depths were computed from numerous streamflow measurements made at South Pass and Telegraph, and surface slopes were estimated using light detection and ranging (lidar) data obtained in 2006. These measurements were combined (using equation 5) to obtain cross-section-averaged values of bed shear stress (τ_b) which, in turn, were used with equation 4 to compute shear velocities (u_*) for the range of flows over which the streamflow measurements were made. Rouse numbers were calculated (eq. 3) for three settling velocities, representing the median, 84th, and 95th percentile values of the averaged settling velocity distribution of all samples collected at South Pass and Telegraph.

Settling Velocity Results and Transport Implications

Effects of Temperature and Hold Time on Settling Rates

Of the original samples collected in the field, only those from Goodwin had sediment concentrations high enough to consistently produce an identifiable settling front in the graduated cylinders. Multiple linear regression analysis indicated that for these samples, both temperature and hold time were significantly related to the relative height of the settling front (referred to hereinafter as the **fractional settling height**) at the specified time for every time interval investigated ($p < 0.05$), the regression coefficients exhibiting the same sign for every time interval (fig. 23). The adjusted R^2 values for the models ranged from 0.70 to 0.92, indicating that most of the variability in the observed rate of descent of the settling front among the samples examined could be explained by variations in temperature and hold time. The results for the 120-second time interval are shown in figure 23 because that was the time interval for which the highest adjusted R^2 was observed (0.92), a value with an associated probability (p-value) of 6.1×10^{-9}.

Warm temperatures caused the settling front to drop rapidly, resulting in a 0.3–1 percent decrease in fractional settling height per degree Celsius, depending on the time interval examined (fig. 23). The direction of this relation is consistent with the expected effect of temperature variations on the dynamic viscosity of water, and thus on settling velocity (Lamb, 1993). Similar results at individual temperatures were observed whether the sample was warmed to the desired temperature from a lower temperature or cooled from a higher temperature. This indicated that the effects of temperature changes on floccule properties—and, by extension, settling velocities—were not hysteretic within the range of temperatures examined. In light of these results, the primary settling-velocity measurements carried out for this study (using the apparatus shown in fig. 22) were conducted at the same temperature for all samples (22.0 ± 0.1 °C).

Increasing hold times resulted in a statistically significant but relatively minor decrease in the rate of descent of the settling front, with each day of holding time leading to a 0.04–0.3 percent increase in the fractional settling height at the specified time of measurement, depending on the time interval examined. Given that the settling-velocity measurements were carried out over an 11-day period, variations in hold time among different samples were likely to have been responsible for no more than 4 percent of the overall variability in settling velocities—and could therefore be neglected.

These tests did not cover the full range of possible environmental variations that could influence the distribution of floccule sizes of the Sumas River suspended sediments. However, the results suggest that neither the 6- to 10-day hold times, the physical agitation during transport, nor the temperature variations of the samples were likely to have altered the size distributions of the floccules in the Sumas River samples substantially—or, by extension, to have introduced a significant bias to the measured distributions of settling velocity.

Comparison of Settling Velocities among Sites and Events

Settling-velocity distributions were similar among the three sites (Goodwin, South Pass, and Telegraph) and across all three sampling periods (fig. 24), with most of the particles (including floccules) exhibiting settling velocities between those for coarse silts and fine sands (0.001–0.03 m/s). Using the empirical formula of Gibbs and others (1971), this range of settling velocities corresponded to hydraulic diameters between 30 and 250 µm. To determine whether the distributions of settling velocities were significantly different among samples obtained from different sites (fig. 24*A*) or at different times (fig. 24*B*), a three-factor analysis of variance (ANOVA) was used. This analysis used the mass-based percentage of sediment in each size class for each sample as the response variable, and sampling location, sampling date, and the settling velocity as the three factors of interest. The ANOVA results indicate that variations in the weight percent of individual sediment fractions among samples, although significantly related to settling velocity, were not significantly related to either sampling location or sampling time ($p > 0.05$). A more detailed presentation of the ANOVA results is provided in appendix H.

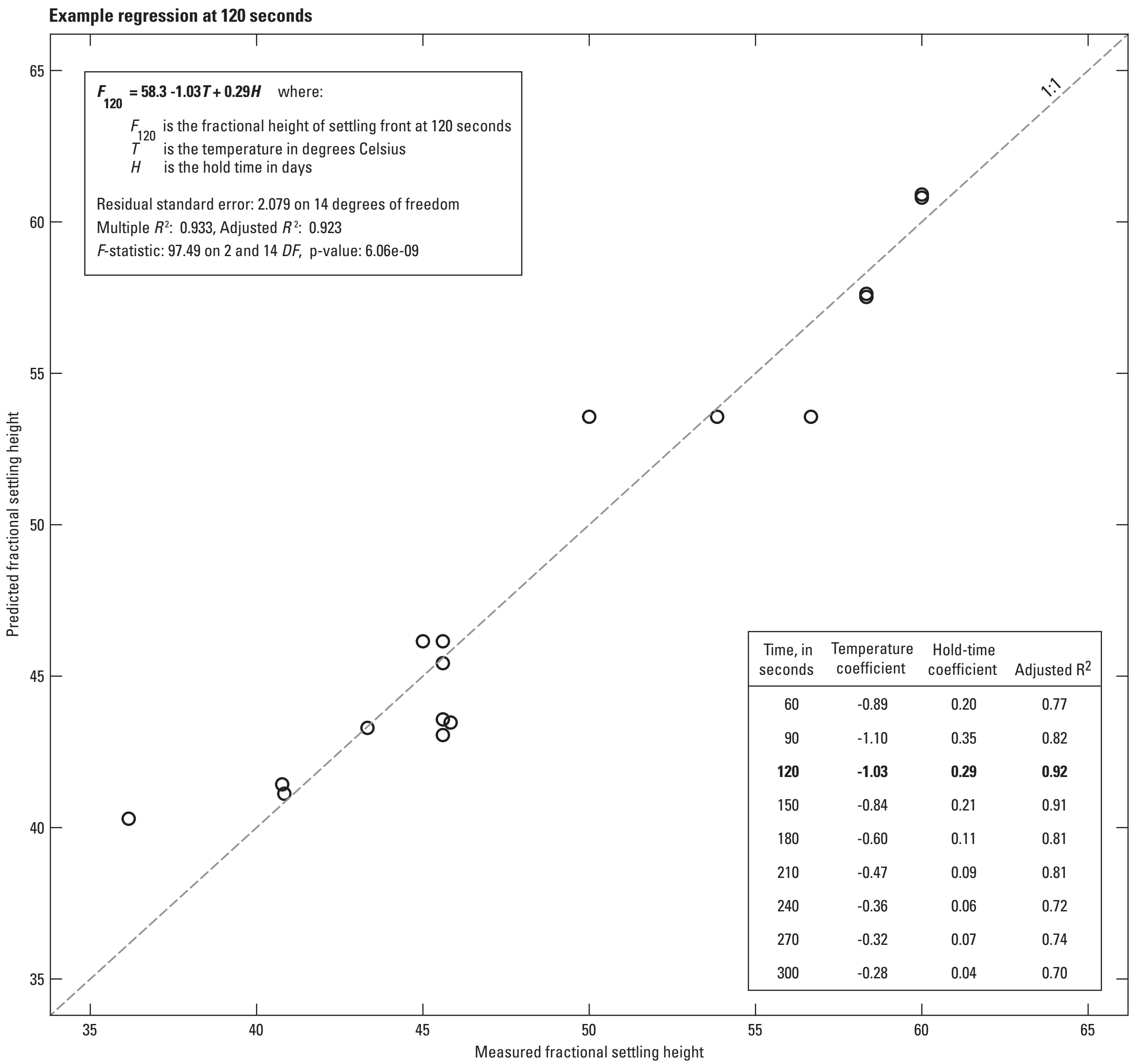

Time, in seconds	Temperature coefficient	Hold-time coefficient	Adjusted R^2
60	-0.89	0.20	0.77
90	-1.10	0.35	0.82
120	**-1.03**	**0.29**	**0.92**
150	-0.84	0.21	0.91
180	-0.60	0.11	0.81
210	-0.47	0.09	0.81
240	-0.36	0.06	0.72
270	-0.32	0.07	0.74
300	-0.28	0.04	0.70

Figure 23. Model-predicted and measured fractional settling height (ranging from 0 to 100 percent) of the clear-water front at 120 seconds, as recorded in settling videos for the sediment sample collected from Swift Creek at Goodwin Road, Whatcom County, Washington. Regression coefficients (R^2) and adjusted R^2 values for all time steps examined are listed in the inset table. Settling temperatures (T) ranged from 4.8 to 22 °C and hold times (H) ranged from 0 to 32 days.

The measured settling velocities of Sumas River sediment were 22.0±0.1 °C. In contrast, water temperatures in the Sumas River during the winter flood season are typically between 5 and 10 °C. The colder water in the natural system would result in slower settling velocities as the dynamic viscosity of the water and (to a lesser degree) its density increased. The empirical formula provided by Gibbs and others (1971) is valid across the full range of water temperatures expected in natural systems, and thus provides a way to estimate how a given temperature change would affect settling velocities. From the equation of Gibbs and others (1971), a change in water temperature from 24 to 7 °C would decrease settling velocities by 10–37 percent, the magnitude of the difference increasing monotonically with decreasing hydraulic diameter (table 9).

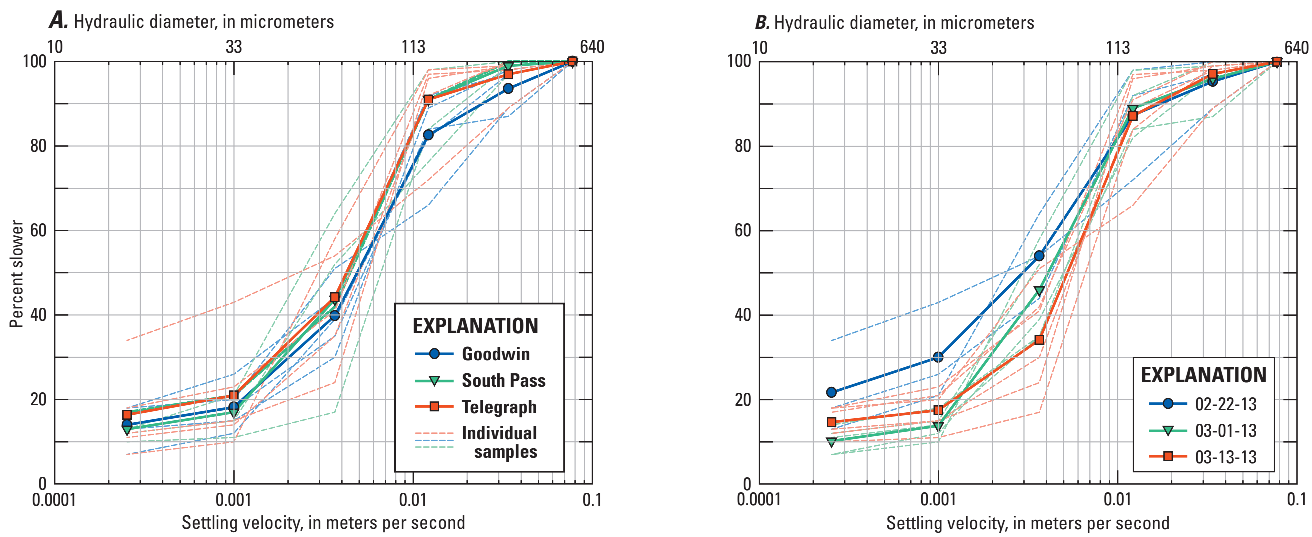

Figure 24. Settling-velocity distributions of suspended sediments averaged by sample location (*A*) and collection date (*B*) for samples collected at Swift Creek at Goodwin Road (referred to as "Goodwin"), Sumas River at South Pass Road (referred to as "South Pass"), and Telegraph Road (referred to as "Telegraph"), Whatcom County, Washington. Individual samples are shown as dimmed dashed lines; averages are shown as darker solid lines. Hydraulic diameters are expressed as measured settling velocities, based on the empirical formula of Gibbs and others (1971).

Table 9. Estimated effect of temperature on settling velocity as a function of hydraulic diameter.

[**Particles with slower settling velocities:** Average of all samples. **Estimated settling velocity at 7 °C:** Computed using the equation introduced by Gibbs and others (1971). **Abbreviations:** µm, micrometer; °C, degrees Celsius; m/s, meter per second]

Hydraulic diameter (µm)	Particles with slower settling velocities (percent)	Measured settling velocity at 24 °C (m/s)	Estimated settling velocity at 7 °C (m/s)	Reduction in settling velocity from 24 to 7 °C (percent)
500	100	0.077	0.070	10
250	96	0.034	0.027	19
125	88	0.0122	0.0087	29
63	42	0.0037	0.0024	34
32	19	0.00100	0.00064	36
16	15	0.00025	0.00016	37

Rouse Numbers

Settling-velocity distributions for the sediments sampled at South Pass and Telegraph were not significantly different from one another, thus, the settling velocities for the two locations were averaged, and the same values were used to calculate Rouse numbers (eq. 3) for both sites. At South Pass, the Rouse numbers indicate that all particles would remain suspended at all but the lowest flows, with only the fastest-falling fraction potentially coming into contact with the bed at the lowest flows (fig. 25). At Telegraph, the Rouse numbers indicate that all particles would be fully mixed throughout the water column at all flows. Rouse numbers are generally lower at Telegraph than at South Pass, as flow depths at Telegraph are generally deeper, but slopes are the two sites are almost identical.

Implications for Fluvial Transport

The ANOVA results (appendix H) indicate that the settling-velocity distributions of the suspended sediments from the Sumas River system were statistically indistinguishable among the three sites examined between 3 and 25 km downstream of the toe of the Swift Creek landslide (figs. 2 and 3) and across a range of flows. This consistency, combined with the large floccules observed at Goodwin and at the toe of the landslide, indicates that the flocculation of the chrysotile occurs during the initial stages of transport in Swift Creek downstream of the landslide, and that the size distribution of floccules in suspension reaches a steady state by the time the material reaches Goodwin, remaining relatively consistent along the length of the study reach. To explain this, three different floccule-transport scenarios are considered.

The simplest, or first scenario is that the floccules form rapidly downstream of the landslide source—as a result of the combined influence of electrostatic attraction between positively and negatively charged sites on the fiber surfaces, interactions with natural organic matter (NOM), and physical entanglement—stabilize, and then cease to form or disaggregate as they are carried downstream. In a second scenario, as floccules travel in suspension downstream,

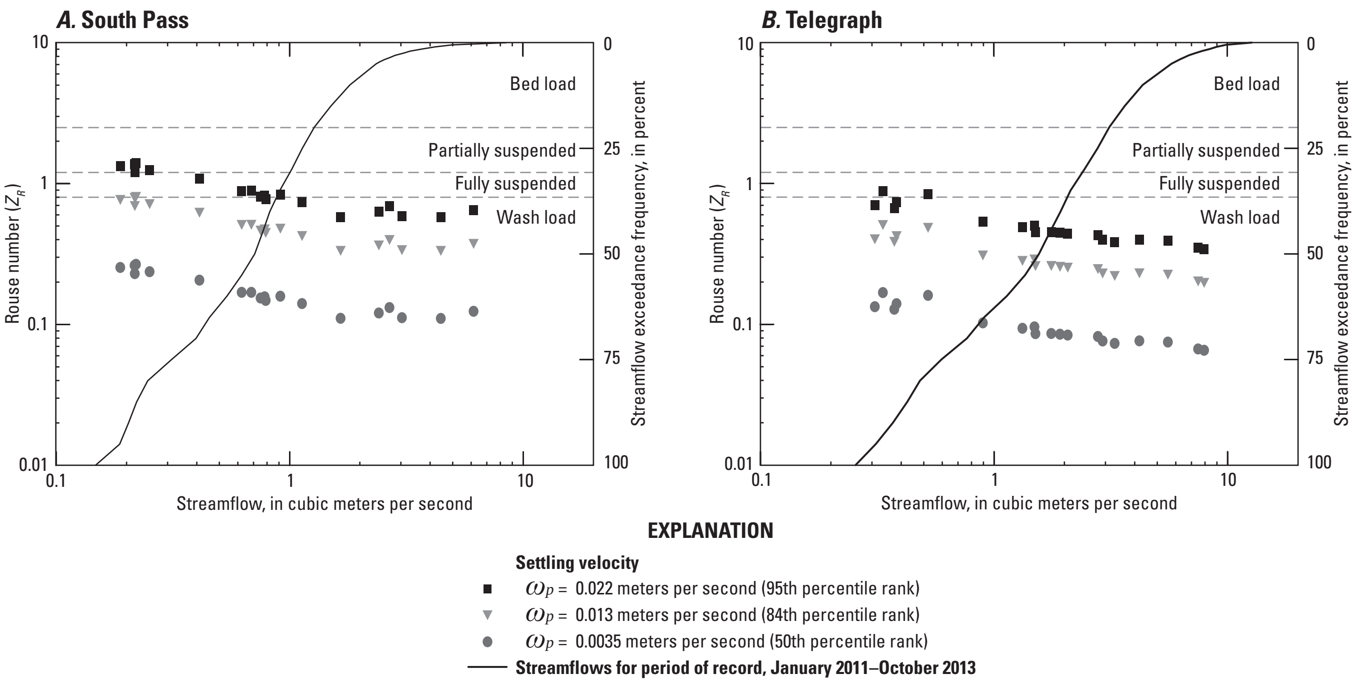

Figure 25. Rouse numbers (Z_R) calculated for a range of measured streamflows using the settling velocities measured for sediment samples collected from the Sumas River at (*A*) South Pass Road, referred to as "South Pass" and at (*B*) Telegraph Road, referred to as "Telegraph" Dashed lines indicate thresholds in Z_R (that is, Z_R values of 0.8, 1.2, and 2.5) that are generally considered to represent boundaries between different modes of sediment transport.

they continue to aggregate and disaggregate at equal rates, producing a steady-state size distribution. In a third scenario, floccules continue to aggregate during transport and, after reaching a critical density, fall out of suspension while smaller floccules continuously aggregate to replace them at a rate equal to that of the deposition of the large floccules.

Of the three scenarios, the first is the most strongly supported by previous studies of the surface chemistry of chrysotile fibers in aqueous environments. Data from this study, from Schreier (1987), and from Greg Dipple (Professor of Geology, University of British Columbia, oral commun., May 8, 2015) provide measured pH values in Swift Creek ranging from 7.5 to 10.0, with an average of 8.9±0.3 (N = 26) among the combined results from the three investigations. Comparing these data with the range of pH_{zpc} values of 8.9 to 11.8 from previous investigations indicates that soon after their entry into Swift Creek, the surfaces of the chrysotile fibers derived from the landslide are likely to be dominated by regions of positive charge, along with some regions of negative charge. Electrostatic attraction between negatively and positively charged regions on the fiber surfaces—aided by the physical turbulence of the flowing water—would facilitate some initial attachment among the fibers, which also may become physically entangled, leading to floccule formation. As the floccules and unattached fibers enter the Sumas River, they come in contact with higher concentrations of NOM (Schreier and Lavkulich, 2015) which, given its predominant negative charge, is likely to bind to many of the positively charged sites on the chrysotile surfaces. Electrostatic attraction between the attached NOM and any remaining positively charged regions of the chrysotile surfaces would lead, in turn, to additional binding among chrysotile fibers. As with other types of sediments, neutrally charged regions of the chrysotile fibers also are likely to become coated with NOM (Bales and Morgan, 1985). At all points along this process, the physical entanglement of fibers that are initially held together by electrostatic attraction is likely to lead to additional stabilization of the floccules.

The second scenario is supported because following physical agitation in the laboratory, floccules disaggregated and then rapidly reformed, suggesting that the consistency of settling-velocity distributions observed in the field may be the result of a dynamic equilibrium between formation and disaggregation. Additional analyses would be needed to distinguish between the relative likelihood of the first and second scenarios. Observations from this study provide the least amount of evidence for the third proposed scenario. The absence of a significant change in the predominance of the coarsest fraction of the settling-velocity distributions across a six-fold increase in streamflow provides little indication of an accumulation of large floccules near or within the stream bed, and the Rouse numbers indicate that little, if any, of the sampled suspended sediment is likely to settle to the bed over the range of natural flows.

Fisheries and Asbestos in the Sumas River

by Patrick W. Moran

The Sumas River joins the Fraser River as a tributary in southern British Columbia, Canada, near Barrowton, about 90 kilometers upstream of the mouth of the Fraser River at Stevenson. This proximity to the Fraser River provides migratory access and both habitat and population refugia for Sumas River fish. Fish species in the Sumas River also are found in the Fraser River, and anadromous stocks must migrate through the Fraser River when accessing the Sumas River. Although five native stocks of salmonids (Coho salmon [*Oncorhynchus kisutch*], Fall Chinook salmon [*O. tshawytsch*)], fall chum salmon [*O. keta*], winter steelhead [*O. mykiss*] and Dolly Varden/bull trout [*Salvelinus confluentus*]) persist in the Sumas River, some "straying" of Fraser River stocks into the lower Sumas River and the historical release of hatchery fish also have been documented (Smith, 2002). A review of coastal cutthroat trout (*O. clarki clarki*) (Blakley and others, 2000) noted a distinct stock complex based in the Sumas River Basin with both anadromous and resident forms considered to be native and sustained by wild production. Non-game fish, such as prickly sculpin (*Cottus asper*), northern pikeminnow (*Ptychocheilus oregonensis*), redside shiner (*Richardsonius balteatus*), and threespine stickleback (*Gasterosteus aculeatus*) were documented by Schreier and others (1987). Black crappie (*Pomoxis nigromaculatus*) also have been reported (Shead, 2004) downstream, in the Sumas River in southern British Columbia.

The headwaters of the Sumas River drain west off predominately forested Sumas Mountain. Except for Swift Creek, these headwaters are good fish habitat. The flood plain and main stem reaches, however, are affected by degraded water quality, excess nutrients, diminished riparian vegetation, and low dissolved oxygen. Smith (2002, p. 220) notes, "*Levels of nitrogen (including ammonia) and phosphorous in the Sumas River are among the highest levels in the Puget Sound region, and low dissolved oxygen levels have been documented in several Sumas River tributaries*."

Studies on the effects of asbestos fibers on aquatic life are limited. The gills, kidneys, and lateral line appear to be the primary susceptible tissues when fish and aquatic life are exposed to asbestos (Batterman and Cook, 1981; Woodhead and others, 1983; Belanger and others, 1986a). Behavioral effects such as loss of orientation in Coho salmon and green sunfish (*Lepomis cyanellus*), reduced stress test performance, and tumorous swellings in the gill of Coho salmon have been reported at concentrations between 1.5 and 3.0 million fibers per liter (Belanger and others, 1986b). Uptake and accumulation of asbestos fibers in the tissue of fish (Batterman and Cook, 1981) and Asiatic clams (*Corbicula manilenis*; Belanger, 1986a) showed tissue concentrations as high as 1,247 and 181 fibers per milligram wet weight, respectively (Converted using 80 percent moisture content for Asiatic clams; Dauble and others, 1985). Following 6-month exposures to doses between 0.1 and 1 mg asbestos per liter, Woodhead and others (1983) showed increased incidence of kidney and gill damage. A study by Schreier and others (1987) points out the heavy metal load that accompanies Sumas River chrysotile asbestos fibers can result in significant accumulation of nickel and manganese is certain tissues. The increased cancer risk of asbestos following decades of exposure considered for humans is generally considered not applicable to freshwater fish, particularly those in the Sumas River, because of their short life spans (Sutter and others, 2005).

Summary

Large volumes of landslide-derived sediment, on the order of 23,000–94,000 m^3/yr (30,000–120,000 yd^3/yr) (Van Gosen, 2010; Whatcom County, 2012), are transported down Swift Creek on an annual basis. The coarser-grained part of this sediment load falls out of transport on the Swift Creek alluvial fan as bed material, historically leading to acute aggradation and requisite sediment management by Whatcom County (2012) to maintain flood-conveyance capacity. Sand- and smaller-sized sediment continues downstream into the main stem of the Sumas River where fine sand, silts, clays, and flocculated sediments are transported in suspension from the South Pass Road crossing downstream to Telegraph Road. Although it is less acute than the rates documented in Swift Creek, aggradation also occurs in the main stem of the Sumas River downstream of South Pass Road, and requires occasional manual sediment removal (Whatcom County, 2012).

In 2012 and 2013 water years (WYs), the measured suspended-sediment load (SSL) in the Sumas River at South Pass Road (referred to as “South Pass”), 0.6 km downstream from the Swift Creek confluence, ranged from 22,000 to 49,000 t/yr; at Telegraph Road (referred to as “Telegraph”), 18.8 km downstream from the Swift Creek confluence, SSL ranged from 22,000 to 27,000 t/yr. Upstream from the Swift Creek confluence, background SSL measured in the Sumas River at Massey Road was less than 1 percent of the SSL measured downstream in WY 2012. The largest monthly SSLs generally occurred during the winter storm season (October–March). The differences observed in monthly SSLs between South Pass and Telegraph were relatively small in WY 2012, indicating that most suspended sediment contributed by Swift Creek was efficiently conveyed through the Sumas River. However, in 2013 WY, although the seasonal pattern of suspended-sediment transport was similar between sites, large differences in monthly SSL between South Pass Road and Telegraph were observed in October 2012 and January 2013, during which seasonally large 24-hour storms occurred (October 30–31, 2012 and January 8–9, 2013). The observed differences in SSL between South Pass Road and Telegraph could have been caused by one or more of several factors: deposition of suspended-sediment between sites (transient channel storage or overbank deposition), differences in the mode of sediment transport (for example, suspended load versus bedload; bedload was not measured as part of this study), differences in sediment transport capacity between sites, and (or) uncertainty in estimating high SSC values from the SSC-surrogate models that were used.

Although not measured as part of this study, a substantial amount of bedload, predominantly sand-sized, likely moves through the Sumas River. Assuming 10–40 percent additional transport resulting from unmeasured bedload, the total load transported at South Pass during this study was likely on the order of 25,000–65,000 t/yr. With a drainage area of 41 km^2 at South Pass, these values correspond to a sediment yield for the Sumas River that ranged from 600 to 1,600 (t/km^2)/yr during the study . This range is considerably larger than those for other rivers draining into Puget Sound (Czuba and others, 2011), and comparable to those for rivers draining glaciated volcanoes of western Washington (Czuba and others, 2012). Assuming that the bulk density of the suspended sediment was between 1.5 and 1.6 g/cm^3, the volume of suspended-sediment load measured at South Pass ranged from 16,000 to 40,000 m^3. Including the estimated (but unmeasured) bedload, the total sediment load transported at South Pass during this study was on the order of 15,000–38,000 m^3/yr (20,000–50,000 yd^3/yr), which is on the lower end of published estimates of total sediment load in Swift Creek. Substantial bedload accumulates in Swift Creek each year (Whatcom County, 2012); this would explain part of the discrepancy between results from this study and published load estimates. Although annual mean streamflow during the study period was greater than normal (based on the long-term streamflow record at the Huntingdon, B.C. gaging station [#08MH029; Environment Canada, 2013b]), peak flows were not exceptionally large and only modestly exceeded the 2-year flood (27.0 m^3/s [953 ft^3/s]) on two occasions. Following the second-largest peak flow measured during the study period at the Huntingdon, B.C. gage (28.0 m^3/s [989 ft^3/s] on January 10, 2013), limited overbank deposits of sediment were observed only in the Sumas River floodplain at several locations near Lindsay Road; extensive overbank flooding did not occur. This indicates that other, lesser peak flows likely remained within the Sumas River banks and suggests that large, geomorphically important flooding did not occur during this study. Mass wasting from the landslide likely increases exponentially with increasing peak flows and it is possible that the limited study period was insufficient to estimate the full range of sediment-producing storms typical within the watershed. Continued movement and associated sediment erosion of the landslide through mass wasting and runoff are likely to maintain large sediment loads in Swift Creek and the Sumas River for the foreseeable future. In turn, given the current channel morphology of the river system, acute aggradation on the Swift Creek alluvial fan and, to a lesser degree, in the main stem of the Sumas River (at rates comparable to those documented in the latter part of the 20th century) are likely to persist.

The suspended sediment carried by the Sumas River consisted of three major components: (1) a relatively dense, largely non-flocculated material that settled rapidly out of suspension; (2) a lighter component containing relatively high proportions of flocculated material; and (3) individual chrysotile fibers that were too small to flocculate or settle out, and that therefore remained suspended in the wash load. Whereas the bulk density of the first (heaviest) component was between 1.5 and 1.6 g/cm^3 (within the expected range for fluvial sediments), the bulk density of the flocculated material was an order of magnitude lower (0.16 g/cm^3), even after 24 hours of settling. The concentrations of the non-flocculated chrysotile fibers that remained in suspension were estimated to range from 2.4 to 19.5 million fibers per liter, corresponding to estimated mass-based concentrations of less than 1 mg/L. Hydrologic conditions varied among sites and samples collected after storms, resulting in total suspended-sediment concentrations in individual samples that ranged from less than 100 mg/L to greater than 25,000 mg/L.

Asbestiform chrysotile concentrations ranged from 0.25 to 37.5 percent with a particular sediment fraction examined, which included substantial differences in asbestiform chrysotile content among the flocculated, non-flocculated, and bulk sediment fractions. As expected, the non-flocculated sediments contained substantially less asbestiform chrysotile than either the bulk sediment or the flocculated fraction. Whereas the measured asbestiform chrysotile content of the flocculated material was relatively consistent among samples (22 ± 3 percent), the asbestiform chrysotile content of the non-flocculated sediments was 5.2 ± 5.4 percent, substantially more variable than that of the flocculated fraction. The bulk sediment contained 14 ± 4 percent asbestiform chrysotile, and exhibited the greatest range in chrysotile content, from 1.25 to 37.5 percent.

Upon immersion in water, chrysotile fibers are known to cause a rapid increase in pH. In light of the challenges associated with the direct measurement of chrysotile concentrations in suspension, pH was examined as a potential indicator of chrysotile concentrations in the water column downstream of the Swift Creek landslide. Significant, positive correlations were observed between pH and the mass of flocculated suspended sediment in the water column during each of two major runoff events at South Pass. Temporal changes in pH at this site also followed changes in turbidity and suspended-sediment concentration at this site. The patterns of correlation noted at South Pass are hypothesized to result from the ongoing input of freshly weathered chrysotile—and perhaps other serpentine minerals present in the sediment—from mass-wasting events at the Swift Creek landslide, and suggest that pH might serve as a reliable indicator of the concentration of asbestiform chrysotile (and, potentially other serpentine minerals) in suspension if pH is measured in a downstream location close to where fresh sediment from the landslide is released into the water column.

In the Sumas River, knowledge of the distribution of particle settling velocities is essential for understanding the transport dynamics of suspended sediment through the river, and for assessing remediation alternatives. Because the complex shapes and structures of the chrysotile floccules precluded the use of empirical equations to estimate their settling velocities, the settling-velocity distributions of the Sumas River sediment samples were measured directly in the laboratory using a custom-built apparatus. Analyses of settling-velocity were done on grab samples collected during three separate hydrologic events (including winter storms) from three sites: Swift Creek at Goodwin Road, and Sumas River at South Pass and Telegraph. Settling-velocity distributions were similar among the three sites and across all three sampling periods, with most sediments having settling velocities between 0.001 and 0.03 m/s. Most of the sediment from these sites had hydraulic diameters between 30 and 250 µm, indicating that they had settling velocities similar to those of coarse silts and fine sands. The spatial and temporal consistency of settling velocities for the suspended sediments in the Sumas River indicates a relatively consistent distribution of floccule sizes in suspension along the length of the study reach. This fact, combined with the observation of large floccules in Swift Creek at Goodwin Road and at the toe of the landslide, indicates that the flocculation of the chrysotile occurs during the initial stages of transport in Swift Creek at the landslide, and that the size distribution of floccules reaches a steady state by the time the material reaches the Goodwin Road site.

Acknowledgments

The study was completed with data and technical insight provided by Scott Linneman and Ben Ferreira of Western Washington University and Paul Pittman of Element Solutions, a division of Pacific Surveying and Engineering, Incorporated, in Bellingham, Washington. Dr. Hans Schreier and Dr. Les Lavkulich of the University of British Columbia provided important data, insight, and background for the project. Additional technical support was provided by individuals at the Environmental Protection Agency, Whatcom County, the Washington State Department of Ecology, and Environment Canada. Jeffrey Kamps of the Washington Department of Fish and Wildlife provided insight on the aquatic ecology of the Sumas River network. Brad Van Gosen and Chris Sherwood (U.S. Geological Survey), Tim Milligan (Fisheries and Oceans Canada), Julie Wroble (U.S. Environmental Protection Agency) and others provided technical support. The study also benefitted greatly from technical exchanges at several Swift Creek/Sumas River Workshops hosted by the University of British Columbia and Western Washington University. Funding for the study was provided by the U.S. Environmental Protection Agency.

References Cited

Anderson, C.A., 2005, Turbidity, *in* National field manual for the collection of water-quality data: U.S. Geological Survey Techniques of Water Resource Investigations, book 9, chap. A6.7, accessed May 17, 2011, at http://water.usgs.gov/owq/FieldManual/Chapter6/6.7_contents.html.

Armstrong, J.E., Crandell, D.R., Easterbrook, D.J., and Noble, J.B., 1965, Late Pleistocene stratigraphy and chronology in southwestern British Columbia and northwestern Washington: Geological Society of America Bulletin, v. 76, p. 321–330.

Bales, R.C., 1984, Surface chemical and physical behavior of chrysotile asbestos in natural waters and water treatment: California Institute of Technology Division of Engineering and Applied Science, Report No. AC-8-84, 275 p.

Bales, R.C., and Morgan, J.J., 1985, Dissolution kinetics of chrysotile at pH 7 to 10: Geochimica et Cosmochimica Acta, v. 49, p. 2,281–2,288.

Bales, R.C., Newkirk, D.D., and Hayward, S.B., 1984, Chrysotile asbestos in California surface waters—From upstream rivers through water treatment: Journal of the American Water-Works Association, v.76, no. 5, p. 66–74.

Batterman, A.L., and Cook, P.M., 1981, Determination of mineral fiber concentrations in fish tissues: Canadian Journal of Fisheries and Aquatic Sciences, v. 38, p. 952–959.

Bayer, T.M., and Linneman, S., 2010, The nature and transport of the fine-grained component of Swift Creek Landslide, Northwest Washington: Earth Surface Processes and Landforms, v. 36, p. 624–640, doi:10.1002/esp.2081.

Belanger, S.E., Cherry, D.S., and Cairns, J., Jr., 1986b, Uptake of chrysotile asbestos fibers alters growth and reproduction of Asiatic clams: Canadian Journal of Fisheries and Aquatic Sciences, v. 43, p. 43–52.

Belanger, S.E., Schurr, K., Allen, D.A., and Gohara, A.F., 1986a, Effects of chrysotile asbestos on Coho salmon and green sunfish—Evidence of pathological stress: Environmental Research, v. 39, p. 74–85.

Blakley, A., Leland, B., and Ames, J., eds., 2000, Salmonid stock inventory (SaSI) coastal cutthroat trout volume: Washington Department of Fish and Wildlife, Publication 00192, 271 p., accessed April 2, 2015, at http://wdfw.wa.gov/publications/00192.

Booth, D.B., 1994, Glaciofluvial infilling and scour of the Puget lowlands, Washington, during ice-sheet glaciation: Geology, v. 22, no. 8, p. 695–698.

California Air Resources Board, 1991, Method 435 determination of asbestos content of serpentine aggregate: California Air Resources Board, 19 p., accessed June 2012, at http://www.arb.ca.gov/testmeth/vol3/M_435.pdf.

Choi, I., and Smith, R.W., 1971, Kinetic study of dissolution of asbestos fibers in water: Journal of Colloid and Interface Science, v. 40, no. 2, p. 253–262.

Clague, J.J., 1986, The Quaternary stratigraphic record of British Columbia—Evidence for episodic sedimentation and erosion controlled by glaciation: Canadian Journal of Earth Sciences, v. 23, no. 6, p. 885–894, doi:10.1139/e86-090.

Clement, C.R., 2014, Estimating sediment yield from the Swift Creek landslide, Whatcom County, Washington State: Bellingham, Western Washington University, master's thesis, 124 p.

Collins, B.D., and Montgomery, D.R., 2011, The legacy of Pleistocene glaciation and the organization of lowland alluvial process domains in the Puget Sound region: Geomorphology, v. 126, nos. 1–2, p. 174–185, doi:10.1016/j.geomorph.2010.11.002.

Converse Davis Dixon Associates, 1976, Swift Creek tributaries, Sumas River watershed, Whatcom County, Washington: Final geotechnical report prepared for the Soil Conservation Service, Contract AG53-scs-0041, W-75-332, 47 p.

Curran, C.A., Magirl, C.S., and Duda, J.J., 2014, Suspended-sediment concentration during dam decommissioning in the Elwha River, Washington, September 2011 to September 2013: U.S. Geological Survey Data Set, accessed April, 16, 2014, at http://wa.water.usgs.gov/pubs/misc/elwha/ssc/pdf/elwhasscV2_2014.pdf, doi:10.5066/F7T43R31.

Czuba, J.A., Magirl, C.S., Czuba, C.R., Curran, C.A., Johnson, K.H., Olsen, T.D., Kimball, H.K., and Gish, C.C., 2012, Geomorphic analysis of the river response to sedimentation downstream of Mount Rainier, Washington: U.S. Geological Survey Open-File Report 2012-1242, 134 p., accessed January 10, 2013, at http://pubs.usgs.gov/of/2012/1242/.

Czuba, J.A., Magirl, C.S., Czuba, C.R., Grossman, E.E., Curran, C.A., Gendaszek, A.S., and Dinicola, R.S., 2011, Sediment load from major rivers into Puget Sound and its adjacent waters: U.S. Geological Survey Fact Sheet 2011–3083, 4 p., accessed March, 15, 2012, at http://pubs.er.usgs.gov/publication/fs20113083.

Dauble, D.D., Daly, D.S., and Abernethy, C.S., 1985, Factors affecting growth and survival of Asiatic Clam, Corbicula sp., under controlled laboratory conditions, *in* Cardwell, R.D., Purdy, R., and Bahner, R.C., eds., Aquatic toxicology and hazard assessment—Seventh symposium, ASTM STP 854: Philadelphia, American Society for Testing and Materials, p. 134–144.

Davis, B.E., 2005, A guide to the proper selection and use of federally approved sediment and water-quality samplers: U.S. Geological Survey Open-File Report 2005-1087, 26 p., accessed October 10, 2012, at http://water.usgs.gov/osw/pubs/OFR_2005_1087/OFR_2005-1087.pdf.

Dietrich, W.A., 1982, Settling velocity of natural particles: Water Resources Research, v. 18, p. 1615–1626.

Dragovich, J.D., Norman, D.K., Haugerud, R.A., and Pringle, P.T., 1997, Geologic map and interpreted geologic history of the Kendall and Deming 7·5 minute Quadrangles, Western Whatcom County, Washington: Washington Division of Geology and Earth Resources Open File Report 97-2.

Duan, N., 1983, Smearing estimate—A nonparametric retransformation method: Journal of the American Statistical Association, v. 78, no. 383, p. 605–610.

Easterbrook, D.J., 1963, Late Pleistocene glacial events and relative sea-level changes in the northern Puget lowland, Washington: Geological Society of America Bulletin, v. 74, no. 12, p. 1,465–1,483.

Edwards, T.K., and Glysson, D.G., 1999, Field methods for measurement of fluvial sediment: U.S. Geological Survey Techniques of Water-Resources Investigations, book 3, chap. C2, 89 p., accessed October 10, 2012, at http://pubs.usgs.gov/twri/twri3-c2/pdf/TWRI_3-C2.pdf.

Environment Canada, 2013a, National climate data and information archive: Environment Canada database, accessed May 22, 2014, at http://climate.weather.gc.ca/.

Environment Canada, 2013b, Water survey of Canada: Environment Canada data products and services Web site, accessed December 10, 2013, at http://www.ec.gc.ca/rhc-wsc/default.asp?lang=En&n=894E91BE-1.

Forest Technology Systems, Limited, 2014, DTS-12 Technical specifications: Forest Technology Systems, Limited Web site, accessed September 1, 2014, at http://www.ftsenvironmental.com/products/sensors/dts12/specs/.

Gibbs, R.L., Matthews, M.D., and Link, M.D., 1971, The relationship between sphere size and settling velocity: Journal of Sedimentary Petrology, v. 41, no. 1, p. 7–18.

Gray, J.R., and Gartner, J.W., 2009, Technological advances in suspended-sediment surrogate monitoring: Water Resources Research, v. 45, no. 4, doi:10.1029/2008WR007063.

Guy, H.P., 1970, Field methods for measurement of fluvial sediment: Techniques of Water-Resources Investigations, book 3, chap. C2, 59 p., accessed October 10, 2012, at http://pubs.er.usgs.gov/publication/twri03C2_1970.

Hayward, S.B., 1984, Field monitoring of chrysotile asbestos in California waters: Journal of the American Water Works Association, v. 76, no. 3, p. 66–73.

Holmes, E.P., Wilson, J., Schreier, H., and Lavkulich, L.M., 2012, Processes affecting surface and chemical properties of chrysotile—Implications for reclamation of asbestos in the natural environment: Canadian Journal of Soil Science, v. 92, p. 229–242.

Jolicoeur, C., Roberge, P., and Fortier, J.-L., 1981, Separation of short fibers from bulk chrysotile asbestos fiber materials—Analysis and physic-chemical characterization: Canadian Journal of Chemistry, v. 59, p. 1,140–1,148.

Kerr, P.F., 1977, Optical mineralogy (4th ed.): New York, McGraw-Hill, 492 p.

Kerr Wood Leidal Associates, Limited, 2005, Swift Creek management Plan: Report prepared by Kerr Wood Leidal Associates, Limited, for Whatcom County, 87 p.

Klein, C., and Hurlbut, C.S., Jr., 1993, Manual of mineralogy (21st ed.): New York, Wiley, 681 p.

Knighton, D., 1998, Fluvial forms and processes—A new perspective: New York, Oxford University Press, 383 p.

Koumantakis, E., Kalliopi, A., Dimitrios, K., and Evangelos, G., 2009, Asbestos pollution in an inactive mine—Determination of asbestos fibers in the deposit tailings and water: Journal of .Hazardous Materials, v. 167, p. 1,080–1,088.

Kovanen, D.J., and Easterbrook, D.J., 2001, Late Pleistocene, post-Vashon, alpine glaciation of the Nooksack drainage, North Cascades, Washington: Geological Society of America Bulletin, v. 113, no. 2, p. 274–288, doi:10.1130/0016-7606(2001)113<0274:lppvag>2.0.co;2.

Kovanen, D., and Slaymaker, O., 2015, The paraglacial geomorphology of the Fraser lowland, southwest British Columbia and northwest Washington: Geomorphology v. 232, p. 78–93.

Lamb, H., 1993, Hydrodynamics (6th ed.): Cambridge University Press, ISBN 9780521458689.

Lee, C.J., Rasmussen, P.P., Ziegler, A.C., and Fuller, C.C, 2009, Transport and sources of suspended sediment in the Mill Creek watershed, Johnson County, northeast Kansas, 2006-07: U.S. Geological Survey Scientific Investigations Report 2009-5001, 52 p.

Lewis, Jack, 1996, Turbidity controlled suspended-sediment sampling for runoff event load estimation: Water Resources Research, v. 32, no. 7, p. 2,299–2,310.

Linneman, S.R., Pittman, P.D., and Bayer, T., 2009, The source of asbestiform chrysotile at Swift Creek WA—Geology, mineralogy and sediment transport [abs.]: Geological Society of America Abstracts with Programs, Paper No. 274-6, v. 41, no. 7, p. 704.

Luce, R.W., Bartlett, R.W., and Parks, G.A, 1972, Dissolution kinetics of magnesium silicates: Geochemica et Cosmoschemica Acta, v. 36, p. 35–50.

McGuire, M.J., Bowers, A.E. and Bowers, D.A., 1982, Asbestos analysis case history—Surface water supplies in Southern California: Journal of the American Water Works Association, v. 74, no. 9, p. 470–478.

McKenzie-Johnson, A.S., 2004, Kinematics of the Swift Creek landslide, northwest Washington: Bellingham, Western Washington University, Master’s thesis, 51 p.

McVan Instruments Pty Limited, 2000, Analite NEP 180 and 190 series manual: Victoria, Australia, McVan Instruments Pty Limited, accessed September 1, 2014, at http://www.observatormeteohydro.com/cms/uploads/documenten/licentie_1/document_59.pdf.

Millette, J.R., 2006, Asbestos analysis methods, chap. 2 *of* Dodson, R.G., and Hammar, S.P., eds., Asbestos—Risk assessment epidemiology and health effects (2d ed.): Boca Raton, Florida, CRC Press, p. 23–48.

Mueller, D.S., Wagner, C.R., Rehmel, M.S., Oberg, K.A., and Rainville, Francois, 2013, Measuring discharge with acoustic Doppler current profilers from a moving boat (ver. 2.0): U.S. Geological Survey Techniques and Methods, book 3, chap. A22, 95 p., accessed August 23, 2013, at http://dx.doi.org/10.3133/tm3A22.

National Institute of Occupational Safety and Health, 1994, Method 9000, asbestos, chrysotile by XRD: National Institute for Occupational Safety and Health Manual of Analytical Methods (NMAM) (4th ed.), 6 p., accessed December 12, 2013, at http://www.cdc.gov/niosh/docs/2003-154/pdfs/9000.pdf.

National Institute of Occupational Safety and Health, 2011, Asbestos fibers and other elongate mineral particles—State of the science and roadmap for research: National Institute for Occupational Safety and Health, Current Intelligence Bulletin 62, NIOSH publication number 2011-159, 153 p., accessed May 20, 2013, at http://www.cdc.gov/niosh/docs/2011-159/.

Neiman, P.J., Schick, L.J., Ralph, F.M., Hughes, M., and Wick, G.A., 2011, Flooding in western Washington—The connection to atmospheric rivers: Journal of Hydrometeorology, v. 12, p. 1,337–1,358.

Petticrew, E.L., Rex, J.F., and Albers, S.J., 2011, Bidirectional delivery of organic matter between freshwater and marine systems—The role of flocculation in Pacific salmon streams, Journal of the North American Benthological Society, v. 30, no. 3, p. 779–786.

Pittman, P.D., Maudlin, M.R., and Collins, B.D., 2003, Evidence of a major late Holocene river avulsion [abs.]: Geological Society of America Abstracts with Programs, v. 35, no. 6, p. 334.

Porterfield, G., 1972, Computation of fluvial sediment discharge: U.S. Geological Survey Techniques of Water-Resources Investigations, book 3, chap. C3, 66 p.

Pruitt, B.A., 2003, Uses of turbidity by States and Tribes, *in* Gray, J.R., and Glysson, G.D., eds., Proceedings of the Federal interagency workshop on turbidity and other sediment surrogates, April 30–May 2, 2002, Reno, Nevada: U.S. Geological Survey Circular 1250, p. 31–46.

Pundsack, F.L., 1955, The properties of asbestos—I, The colloidal and surface chemistry of chrysotile: Journal of Physical Chemistry, v. 59, p. 892–895.

Rantz, S.E. and others, 1982, Measurements and computation of streamflow—Volume 1, Measurements of discharge: U.S. Geological Survey Water Supply Paper 2175, 631 p.

Rasmussen, P.P., Gray, J.R., Glysson, G.D., and Ziegler, A.C., 2009, Guidelines and procedures for computing time-series suspended-sediment concentrations and loads from in-stream turbidity-sensor and streamflow data: U.S. Geological Survey Techniques and Methods, book 3, chap. C4, 53 p.

Rasmussen, T.J., Ziegler, A.C., and Rasmussen P.P., 2005, Estimation of constituent concentrations, densities, loads, and yields on lower Kansas River, northeast Kansas, using regression models and continuous water-quality modeling, January 2000 through December 2003: U.S. Geological Survey Scientific Investigations Report 2005-5165, 117 p., accessed March 2015, at http://pubs.usgs.gov/sir/2005/5165/.

Reynolds, O., 1883, An experimental investigation of the circumstances which determine whether the motion of water in parallel channels shall be direct or sinuous and of the law of resistance in parallel channels: Philosophical Transactions of the Royal Society, v. 174, p. 935–982.

Reynolds, O., 1895, On the dynamical theory of incompressible viscous fluids and the determination of the criterion: Philosophical Transactions of the Royal Society, v. 186, p. 123–164.

Rouse, H., 1937, Modern conceptions of the mechanics of fluid turbulence: Transactions of American Society of Civil Engineers, v. 102, p. 463–543.

Schreier, H., 1987, Asbestos fibres introduce trace metals into streamwater and sediments: Environmental Pollution, v. 43, p. 229–242.

Schreier, H., 1989, Asbestos in the natural environment—Studies in environmental science, volume 37: New York, Elsevier, 159 p.

Schreier, H., and Lavkulich, L., 2015, Cumulative effects of the transport of asbestos-rich serpentine sediments in the trans-boundary Sumas watershed in Washington State and British Columbia: Canadian Water Resources Journal, v. 40, iss. 3, p. 262–271, accessed May 8, 2015, at http://dx.doi.org/10.1080/07011784.2015.1051495.

Schreier, H., Northcote, T.G., and Hall, K., 1987, Trace metals in fish exposed to asbestos rich sediments: Water Air and Soil Pollution, v. 35, no. 3, p. 279–291.

Shead, R., 2004, Summary of surface water quality sampling on Sumas River and tributaries, Abbotsford, British Columbia: Surrey, British Columbia, Canada, Ministry of Water, Land and Air Protection, Environmental Quality Section.

Sholkovitz, E.R., 1976, Flocculation of dissolved organic and inorganic matter during the mixing of river water and seawater: Geochimica et Cosmochimica Acta, v. 40, p. 831–845.

Smith, C.J., 2002, Salmon and steelhead habitat limiting factors in WRIA 1, the Nooksack Basin: Lacey, Washington, Washington State Conservation Commission, 325 p.

Subcommittee on Sedimentation, 1957, Report No. 12—Some fundamentals of particle size analysis—A study of methods and analysis of sediment loads in streams: Interagency Committee on Water Resources, accessed March 10, 2015, at http://water.usgs.gov/fisp/docs/Report_12.pdf.

Sutter, G.W., Norton, S.B., and Fairbrother, A., 2005, Individuals versus organisms versus populations in the definition of ecological assessment endpoints: Integrated Environmental Assessment and Management, v. 1, no. 4, p. 397–400.

Teledyne Technologies Incorporated, 2013, Isco model 6712: Teledyne Technologies Incorporated product Web site, accessed March 26, 2015, at http://www.isco.com/products/products3.asp?PL=201101010.

Uhrich, M.A., and Bragg, H.M., 2003, Monitoring in-stream turbidity to estimate continuous suspended-sediment loads and yields and clay-water volumes in the upper North Santiam River Basin, Oregon, 1998–2000: U.S. Geological Survey Water-Resources Investigations Report 2003-4098, 43 p., accessed October 12, 2012, at http://pubs.er.usgs.gov/publication/wri034098.

U.S. Geological Survey, 2014a, National Water Information System—USGS water-quality data for Washington: U.S. Geological Survey database, accessed August 24, 2014, at http://waterdata.usgs.gov/wa/nwis/qw.

U.S. Geological Survey, 2014b, StreamStats: U.S. Geological Survey database, accessed August 24, 2014, at http://water.usgs.gov/osw/streamstats/Washington.html.

U.S. Environmental Protection Agency, 1993, Method for determination of asbestos in bulk building materials: U.S. Environmental Protection Agency Office of Research and Development, EPA-600/R-93/116, NTIS number PB 93-218576, 99 p.

U.S. Environmental Protection Agency, 1994, Determination of asbestos structures over 10 µm in length in drinking water: U.S. Environmental Protection Agency Office of Research and Development, EPA-600/R-94/134, NTIS number PB 93-218576, 20 p.

Van Gosen, B.S, 2010, Reported historic asbestos mines, historic asbestos prospects, and other natural occurrences of asbestos in Oregon and Washington: U.S. Geological Survey Open-File Report 2010-1041, 1 p., accessed December 12, 2013, at http://pubs.usgs.gov/of/2010/1041/.

Varnes, D.J., 1978, Slope movement types and processes, *in* Schuster, R.L., and Krizek, R.J., eds., Landslides—Analysis and control: Washington, D.C., National Research Council, Transportation Research Board, Special Report, v. 176, p. 11–33.

Veilleux, A.G., Cohn, T.A., Flynn, K.M., Mason, R.R., Jr., and Hummel, P.R., 2014, Estimating magnitude and frequency of floods using the PeakFQ 7.0 program: U.S. Geological Survey Fact Sheet 2013–3108, 2 p., accessed January 6, 2015, at http://dx.doi.org/10.3133/fs20133108.

Wagner, Jeff, 2015, Analysis of serpentine polymorphs in investigations of natural occurrences of asbestos: Environmental Science—Processes and Impacts, v. 17, p. 985–996.

Wagner, R.J., Boulger, R.W., Jr., Oblinger, C.J., and Smith, B.A., 2006, Guidelines and standard procedures for continuous water-quality monitors—Station operation, record computation, and data reporting: U.S. Geological Survey Techniques and Methods, book 1, chap. D3, 51 p.

Weber, W.J., Jr., 1972, Physiochemical processes for water quality control: New York, : Wiley, 640 p.

Whatcom County, 2012, Swift Creek sediment management action plan (SCSMAP): Whatcom County Public Works Department, accessed March 24, 2013, at: http://www.whatcomcounty.us/documentcenter/view/1079.

Wicks, F.J., and O'Hanley, D.S., 1988, Serpentine minerals: structures and petrology, Reviews in Mineralogy and Geochemistry, v. 19, p. 91–167.

Wicks, F.J., and Whittaker, E.J.W., 1975, A reappraisal of the structures of the serpentine minerals: Canadian Mineralogist, v. 13, p. 227–243.

Woodhead, A.D., Setlow, R.B., and Pond, V., 1983, The effects of chronic exposure to asbestos fibers in the Amazon *moly Poecilia Formosa*; Environment International, v. 9, p. 173–176.

Wroble, J.T., 2009, Investigation of the Sumas Mountain landslide—A case study of EPA's framework applied to a naturally occurring asbestos site [abs.]: Geological Society of America Abstracts with Programs, Paper No. 274-5, v. 41, no. 7, p. 703–704.

Wroble, J.T., 2011, Environmental monitoring for asbestos—Sumas Mountain asbestos site selected residential properties—Bulk sampling analysis, activity based sampling, surface water sampling: U.S. Environmental Protection Agency, Region X, Seattle, Washington, Office of Environmental Assessment, 133 p.

This page left intentionally blank

Glossary

Cross-section coefficient A correction factor used to account for differences between the SSC measured using a pumped sample and the SSC measured using the EWI method.

Earthflow A type of slope movement characterized by an hour-glass shape and an elongated flow path, and generally occurring in saturated, fine-grained material , in which 80 percent or more of the particles are sand-size or finer.

EWI sample A composite of suspended-sediment samples collected on a single occasion at a specific site using the equal-width increment (EWI) sampling method.

Floccule An aggregation of particles formed by flocculation in water.

Fractional settling height The height of the settling front in the water column, after an elapsed time, as a percentage of the initial height.

Isokinetic sediment sampler A suspended-sediment sampling device designed to ensure that the velocity of the water-sediment mixture entering the sampler is equal to the ambient stream velocity, and thus that the sample SSC accurately represents in-stream SSC.

pH_{zpc} pH threshold, known as the point of zero charge, for which particle surfaces are positively charged at pH below this threshold, and negatively charged above this pH.

Settling front The visual interface in the water column between clear water and flocculated suspended sediment

Supernatant The clear-water phase that lies above the sediment-water interface following the settling of suspended sediment in a sample.

This page left intentionally blank

Appendixes

The appendixes are Microsoft© Excel files and can be downloaded at http://dx.doi.org/10.3133/sir20155177.

Appendix A. Suspended-Sediment Data for Samples Collected Using the Equal-Width Increment Method of Sampling

Appendix B. Methods and Data for Suspended-Sediment Samples Collected Using an Automated Pump Sampler

Appendix C. Continuous 15-Minute Data Collected at Sumas River at Massey Road near Nooksack, Washington (12214300)

Appendix D. Continuous 15-Minute Data Collected at Sumas River at South Pass Road at Nooksack, Washington (12214350)

Appendix E. Continuous 15-Minute Data Collected at Sumas River near Sumas, Washington (12214500)

Appendix F. Continuous 15-Minute pH, Temperature, Specific Conductance, and Dissolved Oxygen Data Collected from November 1 to December 5, 2015, and December 16, 2015 to January 7, 2016, at Sumas River at South Pass Road at Nooksack, Washington (12214350)

Appendix G. Results of Settling Velocity Measurements

Appendix H. Results from Analysis of Variance (ANOVA) in Suspended-Sediment Mass Percentages Among Particle Sizes, Sampling Locations, and Sampling Events

Publishing support provided by the U.S. Geological Survey
Science Publishing Network, Tacoma Publishing Service Center

For more information concerning the research in this report, contact the
Director, Washington Water Science Center
U.S. Geological Survey
934 Broadway, Suite 300
Tacoma, Washington 98402
http://wa.water.usgs.gov

USGS

Curran and others—**Transport and Deposition of Asbestos-Rich Sediment in the Sumas River, Whatcom County, Washington**—Scientific Investigations Report 2015–5177

ISSN 2328-0328 (online)
http://dx.doi.org/10.3133/sir20155177